Department of Imaging and Applied Physics

Diagnostic Value of Nuclear Cardiology in Coronary Artery Disease

Mansour Z Al Moudi

This thesis is presented for the Degree of
Doctor of Philosophy
of
Curtin University

January 2014

Contents

Declaration

To the best of my knowledge and belief this thesis contains no material previously published by any other person except where due acknowledgment has been made.

This thesis contains no material which has been accepted for the award of any other degree or diploma in any university.

Signature:

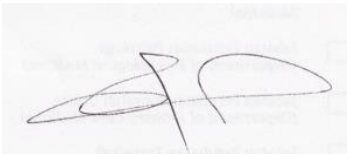

Date: January 2014

Dedicated to my mother Sarah Al Dafiyan and my wife Dalal Al Dawood

Acknowledgement

Firstly, I would like to express my deep gratitude to Professor Zhonghua Sun, my research supervisor, for his patient guidance, enthusiastic encouragement and useful critiques of this research work. His willingness to give his time so generously has been very much appreciated.

I would also like to thank Ministry of Health and King Saud Medical City for financial support of my PhD study. Furthermore, I would like to express my appreciation to Saudi Cultural Mission in Canberra.

I would also like to extend my thanks to the medical imaging staff for their assistance throughout my study. In particular, the administration staff in the general office are so helpful dealing with issues related to my research study as well as assistance with many conference travels.

Finally, I wish to thank my mother and wife for their support and encouragement throughout my study.

List of Publications

List of Publications included as part of this thesis

1. **Al Moudi M**, Sun Z. Myocardial perfusion imaging using 99Tc-sestamibi SPECT: a cardiac phantom study. J Med Imaging Health Inf 2013; 3: 480-486.
2. **Al Moudi M**, Sun Z. A head-to-head comparison of the coronary calcium score by computed tomography with myocardial perfusion imaging in predicting coronary artery disease. J Geriatr Cardiol 2012; 9: 349-354.
3. **Al Moudi M**, Sun Z, Lenz N. Diagnostic value of SPECT, PET and PET/CT in the diagnosis of coronary artery disease: A systematic review. Biomed Imaging Interv J 2011; 7(2):e1-9.

List of additional publications relevant to the thesis but not forming part of it

1. **Al Moudi M**, Sun Z. Coronary artery calcium score: Re-evaluation of its predictive value for coronary artery disease. World J Cardiol 2012; 4: 284-287.
2. Sun Z, **Al Moudi M**. Coronary computed tomography angiography: an overview of clinical applications. Interv Cardiol 2013; 5: 89-100.

List of conferences

International conferences

1. **Al Moudi M**, Sun Z. Myocardial perfusion imaging using 99Tc-sestamibi SPECT: a cardiac phantom study. 81st European Atherosclerosis Society, 2-5, June, 2013, Lyon, France.

2. **Almoudi M**, **Sun Z**, Ng KH. Coronary CT virtual intravascular endoscopy: Assessment of coronary artery plaques. World Congress of Medical Physics and Biomedical Engineering, 26-31 May, 2012, Beijing, China.
3. **Al Moudi M**, Ng Kh, Sun Z. Coronary CT Angiography in Diagnosis of Coronary Artery Disease. World Congress of Medical Physics and Biomedical Engineering, 26-31 May, 2012, Beijing, China.
4. **Al Moudi M,** Sun Z. A head to head comparison of coronary calcium score at coronary computed tomography with myocardial perfusion imaging. 9th International Congress on coronary artery disease, 23-26, October, 2011, Venice, Italy.

National conferences

1. **Al Moudi M,** Sun Z, Lenz N. Diagnostic value of SPECT, PET and PET/CT in the diagnosis of coronary artery disease: A systematic review. RANZCR/AIR/FRO/ACPSEM Combined Scientific Meeting, 22-25 October, 2009. Brisbane, Queensland, Australia.

List of Abbreviations

AMI	Acute myocardial infarction
ANOVA	Analysis of variance
CA	Coronary angiography
CAC	Coronary artery calcium
CAD	Coronary artery disease
CFR	Coronary flow reserve
CHD	Coronary heart disease
CT	Computed tomography
CMRI	Cardiac magnetic resonance imaging
DE-MRI	Delayed enhancement magnetic resonance imaging
DPV	Diastolic peak velocity
DSCT	Dual source computed tomography
ECG	Electrocardiogram
^{18}F-FDG	^{18}F-fluorodeoxyglucose
LA	Left atrium
LAD	Left anterior descending
LCA	Left coronary artery
LCX	Left circumflex
LM	Left main
LV	Left ventricle
MBQ	Mega becquerel
MBV	Myocardial blood volume
MCE	Myocardial contrast echocardiography
MDCT	Multidetector computed tomography
MPI	Myocardial perfusion imaging
MRA	Magnetic resonance angiography
MRI	Magnetic resonance imaging
MVI	Myocardial viability imaging
^{13}N-NH_3	^{13}N-Ammonia
NPV	Negative predictive value
OM	Obtuse marginal
PDA	Posterior descending artery
PPV	Positive predictive value
PET	Positron emission tomography
PET/CT	Positron emission tomography/computed tomography
RA	Right atrium
^{82}Rb	Rubidium-82
RCA	Right coronary artery
RF	Radiofrequency
RV	Right ventricle
SDS	Summed difference score
SPECT	Single photon emission computed tomography
SPV	Systolic peak velocity
SPECT/CT	Single photon emission computed tomography/computed tomography
SSS	Summed stress score
SRS	Summed rest score
^{99m}Tc-MIBI	Technetium (^{99m}Tc) Sestamibi
2D	Two-dimensional

3D	Three-dimensional

Abstract

Increasing evidence shows that cardiac nuclear imaging with use of SPECT, PET or hybrid imaging plays an important role in providing valuable information about myocardial viability, perfusion and function. This study was conducted to investigate the diagnostic value of cardiac nuclear imaging techniques, cardiac SPECT and PET with regard to their clinical value in the diagnostic assessment of patients with suspected or known coronary artery disease. The research was performed in four stages, with stage 1 covering a comprehensive systematic literature review of diagnostic performance of SPECT, PET and SPECT/CT and PET/CT in the diagnosis of coronary artery disease; stage 2 is a retrospective analysis of head to head comparison of cardiac SPECT with coronary calcium scores in coronary artery disease; stage 3 is a phantom study with experiments conducted on an anthropomorphic cardiac phantom, while stage 4 involves a prospective study of comparing cardiac PET with SPECT, echocardiography and invasive angiography in terms of the diagnostic value in myocardial viability.

A systematic literature review was first conducted with the aim of identifying the current research direction with regard to the diagnostic value of SPECT, PET and integrated PET/CT in coronary artery disease. Our analysis consisting of 25 studies shows that PET has high diagnostic value with mean sensitivity and specificity of 91% and 89% in diagnosing coronary artery disease, when compared with SPECT or integrated SPECT/CT imaging modality.

Coronary artery calcium (CAC) score has been regarded as a reliable marker to predict future cardiac events. However, the extent to which the added value of CAC score to the diagnostic performance of myocardial perfusion imaging (MPI) by SPECT remains unclear. In this stage of the study, a retrospective review of the CAC scores and cardiac SPECT was conducted in 48 patients with suspected coronary artery disease. Results showed that there is a lack of correlation between the CAC scores and MPI-SPECT assessments with a significant difference observed between these two techniques, especially in patients with zero or mild calcification (CAC scores 0-100). Of 48% of the patients with CAC scores more than 100, only 44% of these patients demonstrated abnormal, or probably abnormal SPECT imaging. Of the 25% of patients with a zero CAC score, only 6% had normal MPI-SPECT findings.

This study further highlights the suggestion that CAC score should be combined with myocardial perfusion imaging in low-to-intermediate risk patients to improve the diagnostic performance.

In the phantom experiments, we have developed a thorax-heart phantom with insertion of infarcted areas in the left ventricular wall, and tested SPECT myocardial perfusion imaging. Both normal myocardium and simulated abnormal areas are clearly visualized on SPECT images. The phantom can be used for further studies; in particular, optimization of nuclear cardiac imaging protocols for radiation dose reduction.

The last part of this research project is a prospective multi-centre study involving recruitment of 30 patients with known or proven coronary artery disease. Although only 10 patients met our strict selection criteria, all of these patients underwent ^{18}F-FDG PET, ^{99m}Tc-tetrofosmin SPECT, echocardiography and invasive coronary angiography. This study concludes that ^{18}FDG PET has the highest diagnostic value in the assessment of myocardial viability, with 100% sensitivity compared to other imaging modalities. ^{18}F-FDG PET is superior to SPECT in the accurate assessment of myocardial changes, with excellent inter-observer agreement.

In summary, the results of this project show that ^{18}F-FDG PET has high diagnostic value for diagnosing coronary artery disease. Furthermore, FDG-PET is a valuable technique for assessment of myocardial viability when compared to other functional imaging modalities such as SPECT and echocardiography. More prospective studies based on a large cohort are needed to confirm the diagnostic performance of cardiac PET in coronary artery disease, especially in guiding patient management.

Chapter 1 Introduction and literature review

1.1 Coronary artery

1.1.1 Normal anatomy

Coronary artery system consists of left and right coronary arteries arising from ostia in the left and right sinuses of Valsalva.[1,2] Left main coronary artery (LM) gives rise to the left anterior descending coronary artery (LAD) and left circumflex coronary artery (LCX). The LAD courses in the anterior epicardial ventricular septum and is further divided into proximal, mild, and distal segments. The LCX runs in the left atrial ventricular sulcus and gives rise to obtuse marginal branches (OM). The length of left main coronary artery varies from 1 to 2.5 cm before bifurcating into the LAD and LCX branches. The length of LAD is around 10-13 cm. Usually, length of LCX ranges from 6-8 cm and the right coronary artery is about 12-14 cm in length before giving arise to the posterior descending artery.[3,4]

The right artery (RCA) originates from right coronary sinus and is further divided into proximal, mild, and distal segments. The proximal segment of the RCA is form the ostuim to the origin of first acute marginal artery. The sinoatrial artery originates from the proximal RCA and is the second artery to be visualised. RCA is protected by fat and runs deep in the right arteriole-ventricular sulcus with the right atrium (RA) cephalad and the right ventricle (RV) caudad. It continues to pass around the AM of the heart and then posteriorly, remaining in the AV sulcus until reaches the inter-ventricular sulcus at the crux. It gives a number of branches during its course surrounding the myocardium.

The posterior descending artery (PDA) originates from the RCA, LCX, or both dominances. Approximately 80% of humans are RCA dominance. In RCA dominance, the distal RCA at the level of crux of the heart typically bifurcates into the PDA and a posterior-lateral branch. The PDA courses in the posterior ventricular septum giving origin to the SA nodal artery and posterior ventricular branch while, in LCX dominance, the PDA originates from the distal LCX. In both dominances, there are right and left PDAs originating from the RCA and LCX.[5,6]

1.1.2 Coronary artery disease

Coronary artery disease (CAD), also known as coronary heart disease (CHD), is a condition of the coronary arteries with supply of oxygen and nutrients to the heart muscle being interrupted. When the regional arteries are insufficient to carry the oxygen to the heart muscle, this may lead to cause of death as result of CAD. CAD is the leading cause of mortality and morbidity in developed countries, despite recent advances in diagnostic techniques and treatments. In 2008, one in six Australians had coronary artery disease and it is estimated to be 3.4 million people of the total population. One in three Australians die of CAD and estimated around 46,000 people from the total CAD patients.[7,8] In America more than 16 million people have CAD and about 385,000 die every year from CAD.[9]

Coronary artery wall is composed of three layers, namely intima, media and adventitia and the major element of the atherosclerotic plaque is deposition of plaque consisting of lipid, fibrous connective tissue and calcium in the artery wall.[10-12] As the plaque accumulates in the coronary arteries, blood supply to the heart muscle is decreased which results in ischemia, a local and temporary impairment of circulatory and myocardial damage as an infarction (an area of ischemic necrosis). Atherosclerosis is an active, different stage of disease process which develops in the arterial wall. There are diverse factors contributing to the growth and advancement of atherosclerosis. The earliest sign of atherosclerosis is endothelium dysfunction causing change to the vascular homeostasis by regulating vascular tone, smooth muscle cell proliferation and thrombogenicity.[13]

Thus, the change of homeostasis leads to destabilisation of vascular regulatory mechanisms and leads to destruction to the arterial wall. Furthermore, inflammation, macrophage infiltration, extracellular medium digestion, oxidative stress, lipid deposition, calcification, cell apoptosis and thrombosis are almost futures of molecular mechanisms giving to plaque growth and movement.[14] The total direct and indirect cost of cardiovascular disease and stroke in the United States for 2010 is estimated to be $503.2 billion. In comparison, in 2008, the estimated cost of all cancer and benign neoplasms was $228 billion. Due to the current global focus on healthcare utilization, costs, and quality, it is essential to monitor and understand the magnitude of healthcare delivery and costs, as well as the quality of healthcare delivery in relation to the cardiovascular disease. There are several imaging modalities that can be used to detect the CAD with variable diagnostic value.

1.2 Imaging modalities in the diagnosis of coronary artery disease

1.2.1 Invasive coronary angiography

1.2.1.1 Imaging Principles

The diagnostic evaluation of coronary artery disease is important for inspection of function, perfusion and viability of heart muscle in addition to the assessment of the morphology and function of the coronary arteries. Coronary angiography (CA) is currently regarded as the gold standard to determine the degree of stenosis in coronary artery disease.[15-18] Coronary angiography is a safe invasive technique but it is associated with harmful risks. Therefore, the need arises for exploring non-invasive techniques such as coronary computed tomography, echocardiography, cardiac magnetic resonance imaging and cardiac nuclear medicine imaging.

CA offers the most consistent evidence responsible for applying treatment in patients with CAD. CA has been established as a routine procedure on a daily clinical practice. The necessity of clinical practice to do the invasive CA in catheterization laboratory involves radiographic system, equipment for physiologic data, nursing and acquisition console, and kit for emergency patients care. Modern x-ray imaging is essential for optimal visualisation of the coronary arteries. CA is performed under local anaesthesia with small diameter catheters inserted through a trans-arterial sheath.[19]

Patients with suspected CAD who have severe symptoms and those with definited high risk for CAD should be recommended for CA. Low ejection fraction and poor exercise volume on an exercise test are included in the high risk criteria. Acute coronary syndromes refer to unstable angina, myocardial infarction and high risk features for developing ongoing ischemia and heart failure.[20]

1.2.1.2 Diagnostic accuracy

CAD is defined as more than 50% angiographic diameter stenosis in one or more of the coronary arteries. CAD is classified as single, double or triple vessel disease. When stenosis is less than 50% it is reflected as non-symptom producing, excluding cases with active obstruction. Recent studies have examined the case of acute coronary syndromes which

mostly commonly occur at the location of coronary stenosis with < 50% diameter stenosis, and it is probably associated with thin cap fibro-atheroma.[21,22] Recording systems have been established to precisely characterise the coronary vasculature with regard to the amount of lesions and their functional influence, locality, and density.[23,24]

According to a recent study for invasive coronary angiography accuracy of coronary in-stent restenosis illustration that sensitivity, specificity and positive predictive value, and negative were 92%, 81% and 98%.[25] Moreover, another study demonstrated that invasive coronary angiography with <50% diameter stenosis had a sensitivity of 67%, specificity 75%, positive average likelihood ratio of 2.6 and negative average likelihood ratio of 0.4 predictive values. [26]

CA advances in the consideration of pathophysiology of atherosclerotic plaque validate that in encouraging stages of plaque development, the plaque is vulnerable to rapture. Also, CA option is to use the diagnostic examination tool with other invasive devices with patient still in the characterisation workroom. Both anatomy and physiology of coronary arteries can be simply evaluated with these additional procedures. [27,28]

The choice of imaging method should be exclusive to all individuals on the medical decision of patient risk, clinical history, and local knowledge. CA will continue to be the technique of high-quality with great possibility for an invasive supportive procedure, particularly in acute coronary conditions. [29]

1.2.1.3 Limitations

The major complications are infrequent occurrence during diagnostic procedures; vascular complications related to the arterial puncture site are the most common complication, allergic to contrast reactions, deteriorating kidney function, cerebrovascular accidents, iatrogenic coronary artery dissection are potential life threatening and mortality risk is 0.1%. Usually, CA is performed by emergent coronary artery stenting or bypass surgery. [30]

Coronary angiography is a safe invasive procedure, but it is still as associated with potential harmful risks. Therefore, the need arises for exploring non-invasive techniques as a substitute for the study of coronary artery. [31-33]

Although, repetitive invasive coronary artery was linked with higher early mortality and the trend towards a mortality reduction at follow up. Future approaches should investigate methods to minimise the primary hazard and increase advanced benefits by concentrating on higher risk patients and improving effectiveness of intervention.[34]

1.2.2 Echocardiography

1.2.2.1 Imaging Principles

Ultrasound waves are sound waves with higher than perceptible frequency. The perceptible frequency ranges from 20 hertz (Hz) to 20,000Hz (20 kHz). Ultrasound frequency range used in cardiac imaging applications of 1-10MHz (megahertz). The sound wave is longitudinal wave, consisting of cyclic pressure deviation with explorations counting movement of encountered media particles in trend of wave transmission. The imaging resolution is controlled by wavelength. [35]

The wavelength less than 1mm is obtained to get adequate resolution in echocardiography. The higher frequency corresponds to a shorter wavelength, and vice versa.. Echocardiography imaging characterises the demonstration of incoming ultrasound waves from studied structures, with location determined by their travel time. The electrical signal with radiofrequency (RF) is generated by incoming echo.[35-37]

Plus-Wave Doppler technology is used in colour flow Doppler but with the calculation of multiple regions of interest within the pathway of the sound beam. A flow velocity approximation is covered on the two dimensional (2D) image with a colour scale created on flow course, mean velocity and occasionally velocity variance, in all of multiple regions.[38-40]

The affected structure in this situation is tissue, such as myocardium, which has higher degree of backscatter ultrasound and an inferior velocity than the red blood cells. The three dimensional (3D) systems suggest the opportunity of quantifying distances and area straight in the images. [41-44]

The 3D echocardiography could demonstrate lesions such as an atrial septal defect very well. The precise location of the defect, its relation to adjacent valves, vena cava, and pulmonary veins, are also easily located. In addition, measurements of the size, length of pathological lesions, volume and function of cardiac chambers which may influence management decisions can be obtained. [45-48]

The ability to reconstruct the chamber in all its dimensions and slice it three-dimensionally could aid in measuring left ventricular volume and ejection fraction accurately without any geometric assumptions. This could be especially helpful in ventricles with distorted shape.[48-51]

1.2.2.2 Diagnostic accuracy

A recent study indicated that, using the diastolic and systolic peak velocities DPV /SPV at rest after stress of <0.6 cm/s had sensitivity of 83%, a specificity of 94% and an accuracy of 92% for identifying abnormal segments.[52, 53] On the other hand, all these three diagnostic performance values increased to 100% when using the diastolic and systolic peak velocities (DPV/SPV) at rest after stress of <1.5 cm/s. [54]

Assessment of the myocardial microcirculation by myocardial contrast echocardiography (MCE) is a perfect imaging tool. MCE notices contrast MB at the vessel level within the myocardium. Thus, it is possible to measure tissue viability. [55]

At baseline, about 8% of left ventricular mass is established by blood current in the microcirculation named myocardial blood volume (MBV), 90% of which is included of blood in the capillaries. In normally perfused myocardium, the rate of capillary blood flow is 1 mm/s. Saturation of the coronary microvasculature by MB then incomes about 5 s. When there is no flow controlling stenosis, MBV increases 5 times during hyperemia (stress testing), and so the myocardium refills in 1s. [55]

While, these approaches enhanced the signal-to-noise ratio, off-line image processing is frequently required to evaluate myocardial perfusion, because tissue signals is still present. Harmonic imaging also used high acoustic powers that destroyed MB. Thus, the imaging surround rate had to be concentrated significantly with electrocardiographic starting to tolerate MB to replace the myocardial microcirculation between pulses. [56-57]

Also, it is not evaluated whether the echocardiogram created new, clinically unsuspected evidence or it just confirmed the results from clinical valuation. There is substantial consideration as to the quantity of training essential in order to achieve and understand echocardiograms in critically ill patients and a requirement of skills has been recommended. One of the recommendations is operators with exact training. They are able to achieve

concentrated echocardiography in the peri-resuscitation location to distinguish gross pathology such as a large pericardial effusion, severe left ventricular damage, right ventricular dilatation, and gross hypo-volaemia, trusting on two-dimensional imaging only.[58-65]

1.2.2.3 Limitations

Several limitations exist in 3D echocardiography imaging. First, system sensitivity is still limited to some extent. The definition of the endocardia borders is a crucial issue in quantitative echocardiography, and the determination of right ventricular volume requires saline contrast enhancement to adequately locate right ventricular endocardium for the purpose of measurement. Second, the frame rate of echocardiography is 22 frames/seconds. This relatively slow frame rate may provide sufficient samples at slow heart rates but could be quite problematic for the determination of volumes in small children and infants or in adults with high heart rates.. Third, there is a lack of evidence supporting the overview of echocardiography for the intensive care units.[63] When accurate RF function assessment is required, traditional echocardiography techniques are far from being perfect.[66,67]

1.2.3 Coronary magnetic resonance angiography

1.2.3.1 Imaging Principles

More than decades, magnetic resonance imaging (MRI) has been increasingly used for medical diagnosis and research determination. MRI is used to create anatomical images of soft tissue without exposing subjects to ionizing radiation. MRI can be obtained in any direction and plane, without any restriction to the angulation of the images. Cardiac MRI has experienced tremendous developments and its capability to cardiovascular MR (CMR) imaging which contains sequences capable of diagnosing cardiovascular disease, such as valuation of regional myocardial perfusion measurement in patients with heart diseases.[68]

CMR has a very high sensitivity and specificity for detecting diseases of the thoracic aorta such as aneurysm, acute dissection and intramural haemorrhage. [69]Typically, the perfusion defect is the outcome of severe coronary stenosis, while regional micro-vascular connection

in earlier infarcted segments can similarly principal to a perfusion defect, even in the lack of an epicedial coronary artery obstruction. The occurrence of collateral circulation can decrease a perfusion defect, also in important coronary lesions.[70]

1.2.3.2 Diagnostic accuracy

Cardiovascular MRI (CMR) involves advanced technology, with a high-field magnet such as 1.5 Tesla, although 3.0 Tesla systems are now gradually used, fast switching gradient coils, and coils for transmission and signal response. In contrast to other imaging techniques, MRI has the exclusive capability of tissue description.

Proton density, T1 and T2 relaxation times which can vary significantly for a dissimilar tissue is subjective image contrast. Alternative to change image contrast is by controlling the way that radio-frequency pulses are played. MRI scan is free from radiation and ionizing exposure, and there are no damaging biological side effects of MRI providing that safety guidelines are monitored. [71]

Coronary MR Angiography of the right and left coronary artery systems were imaged using an earlier designated free-breathing electrocardiogram triggered 3D composed steady state free precession coronary magnetic resonance imaging sequence.[72] The delayed enhancement imaging is the most established MRI technique for detecting infarcted myocardium.

Current studies have concentrated on delayed enhancement in the acute phase, with emphasis on assessing peri-infarct border zone areas and myocardium at risk.[73,74] Delayed enhancement magnetic resonance imaging (DE-MRI) precisely displays regional myocardial necrosis in ischaemic heart disease. [75]

Since of the high spatial resolution, DE-MRI has the capability to measure the myocardial infarct, which is important for distinguishing between viable and non-viable. Myocardium Presently DE-MRI is reflected to be the technique of choice for measuring myocardial infarct volume.[76]

Magnetic Resonance Angiography (MRA) perfusion imaging has a sensitivity of 87% and specificity of 85% in detecting more than 50% stenosis.[77,78] MRA perfusion had a sensitivity of 93% and specificity of 75% in identifying 70% stenosis.[79]

Also, MRI has sensitivity of 87%, specificity 77% and accuracy 83%. [80] Recent study indicates that 3-T perfusion CMR is superior to 1.5-T perfusion CMR in the diagnosis of important single-vessel and multi-vessel coronary disease. [81]

Usually, clinical situation, with more than 95% of the registered patients effectively finishing both MR studies, 3-T perfusion CMR had high sensitivity of 98% and negative predictive value of 94%, indicating significant clinical usefulness as a screening instrument. [81]

Though, studies have revealed that visual and semi-quantitative valuation of perfusion CMR at 1.5-Tesla has moderate accuracy for detection of CAD, it is still mainly inadequate by low variances in contrast enhancement between normal and under perfusion myocardium. Compared to perfusion CMR at 1.5-T and 3-T systems distribute improved signal to noise ratio and contrast enhancement, which can be used to increase spatial resolution and image quality. [82-87]

MRI plaque description of the coronary arteries is exactly interesting because of small size and quick signal. Yet, plaque classification is easier in other vessels, for example the carotid artery is more classified than the coronary artery. [88]

1.2.3.3 Limitations

CMR is recognised as a non-invasive method that allows complete valuation of cardiac pathology; however it can be inadequate due to relatively long acquisition times and the essential for ECG and respiratory gating. Recent developments include acoustic gating to cardiac sounds and gating from motion, which may increase image quality in patients with asymmetrical cardiac times, and decrease acquisition times. It is possible that growths in the approaching coming will allow fast acquisition of whole heart 3D data sets, with high temporal and special resolution, which can be recreated for additional analysis.

Similarly, hopeful results for imaging coronary atherosclerotic plaques and more developments in spatial resolution can simplify clinically valuable imaging. [89] Now, the

further technical and safety complications joint with compact contact to patients when performance procedures, limits the technique to highly specialised clinician and a decrease resolution of interventional CMR sequences. [90]

Certain patients will not be suitable for CMR. Several devices like pacemakers and implantable defibrillators could affect the performance of CMR, and all these have been considered as contraindication for CMR. Furthermore, obesity is one of the discontinue factor for CMR, due to a small diameter-size of the magnet. [91]

This is vendor-specific, and then in general a maximal body diameter of greater than 145cm will prevent CMR. Arrhythmias such as atrial fibrillation or frequent ventricular ecotype might compromise image quality and decrease diagnostic accuracy, even when heart rate control is optimal. More significantly patients with resting tachycardia may be unsuitable for stress perfusion CMR.[92]Another limitation of coronary CMR is the limited spatial resolution of MR imaging, which is less than 1.0 mm in z-axis direction. This is inferior to that of multislice CT angiography, which is between 0.4-0.5 mm. This limits the visualisation of distal coronary arteries and branches during coronary CMR. [91]

1.2.4 Coronary CT angiography

Diagnosis of coronary artery disease with multi-detector computed tomography has become possible because of rapid developments in CT technologies. Multi-detector CT can produce images with high spatial and temporal resolution. Since the development of CT over the last three decades imaging of cardiac and coronary artery anatomy is significantly improved. The previous generations of CT scanners are limited in gantry rotation times, inferior spatial and temporal resolution which affect the accurate assessment of coronary artery diseases. The performance of multi-detector row CT enables acquisition of cardiac images with thinner section thickness and reduced scan time. [93,94]

Multi-detector row CT systems are equipped with four or more parallel detector arrays and always apply a third generation technology with synchronously rotating tube and detector array. Dual slice detector systems was available in the early 1990s, but the systems with four detector arrays were introduced in 1998, and systems with eight, 10, 16, or more dynamic detector arrays were developed in 2001 and onwards.

1.2.4.1 Single-slice (single-detector) CT

It was introduced in 1980s and became the most commonly used imaging modality in daily practice. [95]

Axial scanning requires long examination times because of the inter-scan delays necessary to move the table incrementally from one scan position to the next and unwind the cable, thus it is prone to misregistration or loss of anatomical details due to potential movement of the relevant anatomical structures between two scans (by patient breathing, motion or swallowing). [95]

Besides, only a few slices are scanned during maximum contrast enhancement when the contrast medium is used. These problems may be overcome if the scan speed is increased and inters scan delay is eliminated. The development of multi detector CT possesses these features which help to overcome the above problems.[95]

1.2.4.2 Four, eight and 16 detectors row CT

In 1998, a 4-slice CT scanner was introduced by several manufacturers representing an obvious quantum leap in clinical performance. Since then, eight and 16 detectors row CT have been developed with improved temporal and spatial resolution, thus, making imaging of coronary arteries possible and improve as well. [96]

The major advantage of 16-slice scanners over 4-slice CT is the longer z-axis coverage (16 × 0.75 mm vs 4 × 1.0 mm), resulting in significantly shorter breath hold and less motion artefacts. Coronary CT angiography became more clinically practical with retrospective electrocardiogram (ECG) gating to capture cardiac motion plus the z-axis coverage from 16-detector row scanners. However, cardiac motion and stair-step artefacts are the main challenge in this system. Therefore, there are few steps suggested to overcome those problems, which include increasing the number of detector elements and the volume coverage along the z-axis of detector block. Moreover, increase in the sensitivity of detector material and application of iterative image reconstruction algorithms represents another

approach to improve cardiac image quality. During 2003 and 2004, manufacturers introduced different types of multi detector row CT models with less than 16-slice scanners, but most commonly the introduction of more than 16-slice scanners represented the main direction for improving multi detector row systems.[96-98]

1.2.4.3 64 Detectors row Computed Tomography (64-MDCT)

The introduction of 64 detector row CT scanner allows patients to be scanned with high resolution in 5 to 13 seconds with minimal or no motion-related artefacts. With gantry rotation times down to 0.33 second for 64 detectors row CT, temporal resolution for cardiac ECG-gated imaging is again markedly improved. The increased temporal resolution of 64 detectors row CT has the potential to improve the clinical strength of ECG-gated cardiac examinations at higher heart rates, thereby reducing the number of patients requiring heart rate control. In contrast to previous studies, high diagnostic accuracy has been achieved despite the presence of severely calcified coronary plaques. In addition by using 64 detectors row CT, the scanning time is reduced to less than 15 seconds, allowing a decreased breath hold time, better utilization of contrast medium with fewer enhancements of adjacent structures and a lower dose of applied contrast medium. Improvement of image quality has also been reported in the visualization of all coronary artery branches with high sensitivity and specificity achieved.[99]

The 64 detector row CT has sensitivity of 99% and the specificity of 95% when compared with coronary angiography. The 64 detector row CT was accurate and useful in non-invasive discovery of coronary artery stenosis. It had benefits with scanning, including decreased breath holding time compared with the 64 detectors row CT, fewer artefacts, and the quantity of contrast used was smaller than with previous CT scanners.[100] Another study indicated that the 64 detectors row CT has a diagnostic accuracy of 97%, sensitivity of 94%, and specificity of 97% in the detection of patients with coronary artery disease. [100]

The 64 detectors row CT is rapid and competent in screening for coronary artery disease. These changed in technology cause impacts imaging management significantly, decreases avoidable invasive challenging, saves time and cost-effectiveness. Also one of the benefits of the 64 detectors raw CT is possibly subsequent in preventable hospitalization. [101]

The 64 detectors row CT is effective in giving rapid outcomes to health care benefactors by classifying patients with heart disease. Worldwide, 5 million patients were make appointment complaining of chest pain, therefore it is a need for using the 64 detectors row CT as a diagnostic screening instrument. The 64 detectors row CT is suggests a way to exclude disease, without exposing patients to the risks of an invasive procedure. [101]

Yet, the potential of the 64 detectors row CT in non-invasive cardiac diagnostics, many cardiologists referred patients with CAD to undergo cardiac CT.

The main concern is radiation exposure to patients. The radiation dose for the 64 detectors row CT is reported to be about 14 mSv, and the dose for invasive coronary angiography is 6 mSv. These radiation exposures produce period risks of 0.07% and 0.02%, individually, of making a serious cancer in the general population. [102]

Though the 64 detectors row CT involves a higher radiation dose from that practiced throughout a standard catheterization. These complications were sum up to 0.13% overall risk of mortality from coronary angiography compared with the 0.07% risk from the 64 detectors row CT.[102]

1.2.4.4 Dual-Source CT (DSCT)

The new generation of multi-detector row CT is Dual-Source; a current scanner with two x-ray tubes and detectors providing an alternative method to increase temporal resolution. The 360° gantry rotation time is 280 ms, translating to a temporal resolution of approximately 75 ms when the scanner operates with both x-ray tubes collecting data at the same energy.[103]

The second-generation DSCT "SOMATOM Definition Flash" was introduced in 2008. It features even faster gantry rotation (0.28 s), twice the number of detector slices and a larger field of view (332 mm) and a special spectral filter for dual-energy imaging. It has the high-pitch acquisition mode (up to 3.4), only one phase is acquired, which gradually increases with the z-axis table translation. The influence on image quality for different clinical scenarios and heart rates is evaluated with the second generation dual-source CT.[104-110]

The diagnostic accuracy and image quality is mostly incomplete by coronary calcifications and motion artefacts in cardiac MDCT.[111-115] Improved temporal resolution that results in

quicker gantry rotation speed and multi-segmental reconstruction algorithms has been helpful to obtain high diagnostic accuracy.[116] A recent study stated that DSCT has a sensitivity of 96%, specificity of 78%, a positive predictive value of68%, and a negative predictive value of 97%.[114] DSCT coronary angiography with 350 mAs/rotation and 120 kV delivers mean effective dose of 8.8 mSv or 7.8 mSv, depending on the ECG pulsing algorithm used. [117]

Radiation dose is related to the protocols with reduced tube current to 20% outside of the pulsing window considerably with increasing heart rates, despite using wider pulsing windows at higher heart rates in order to maintain diagnostic image quality.

Radiation dose reduces substantially at a considerably lower level with use of ECG-pulsing with saving of tube present to 4%, regardless of the heart rate throughout the examination.[117,118]

1.3 Nuclear cardiology

There are numerous indications that support the usefulness and effectiveness of myocardial perfusion imaging (MPI) and myocardial viability imaging (MVI) by different techniques for the management of patients with suspected or known CAD. In patients with suspected CAD non-invasive assessment is dependent on the primary detection of ischemia and its successive appearance. To detect CAD, it is important to consider cost-effectiveness; optimal application of an imaging modality which enables an accurate evaluation of the incremental amount of information provided by an examination. Currently, nuclear cardiology is widely used as a non-invasive method for evaluating myocardial perfusion and viability.[119]

Myocardial perfusion imaging involves administration of radiopharmaceuticals or radioisotopes to display the circulation of blood flow in the myocardium. Perfusion imaging recognises areas of very concentrated myocardial blood flow related to ischemic change. The regional blood supply or perfusion can be measured either at rest, or through cardiovascular stress, or both. Imaging can also be achieved through emergent procedures.[120]

Viability imaging is important to assess the degree of viable myocardial tissue. The scan is commonly accomplished in patients with earlier heart attacks, and the decision needs to be

made as to plan heart surgery which will offer substantial advantage. Perfusion and viability images can be completed with single photon emission computed tomography (SPECT), hybrid SPECT/CT and positron emission tomography (PET) or hybrid PET/CT techniques. These techniques use radiopharmaceuticals or radioisotopes that are removed and taken for a variable period of time by the myocardium. The data can be analysed by visual review or measurable techniques. [120]

There are a number of radiopharmaceuticals and isotopes which have been approved for use in myocardial perfusion imaging and myocardial viability including ^{82}Rb (Rubidium-82), ^{13}N-ammonia and ^{18}F-FDG for cardiac PET, ^{99m}Tc-tetrofosmin, ^{99m}Tc-sestamibi and ^{201}Tl-thallium for cardiac SPECT in patients with significant coronary artery stenosis or abnormal coronary flow. [120]

1.3.1 Single Photon Emission Computed Tomography (SPECT)

1.3.1.1 Imaging Principles

SPECT uses techniques for constructing images which are acquired by planar images (typically in 64 × 64 or 128 × 128 data-point arrays) at many angles around the patient by single, dual, or three head scintillation cameras which are usually equipped with parallel-hole collimators, which offer plan views of the radioactivity from those angles. Normally, 120 images are acquired at 3° increments for 360° SPECT (60 images at 3° increments for 180° SPECT in cardiac imaging). A single line of data in a planar projection image is a total profile of data developed from a slice of activity. [121]

Yet, consistent lines are clarified and back projected into an image space to concept an image of a transverse slice of the activity delivery as an array of totals at that slice place. SPECT images acquired are frequently used in oncologic applications and deliver physiologic information on localization of radiopharmaceuticals in the regions of interest. However, these images suffer from inferior spatial resolution and regularly deficiency anatomic developments for exact weaknesses of location of areas of abnormal uptake.[122]

Whereas, normal physiologic deliveries necessity frequently stay distinguished from regions of abnormal uptake. This technique lacks of anatomic landmarks for precise correlations. Also, a number of the difficulties in SPECT are encountered that would result from a

rebuilding of the data acquisition procedure. The reconstructed image shows an obvious reduction in activity that extent a minimum at the centre of the image. This result is due to attenuation of photons in the source earlier going the source and presence noticed by the camera system.[122-124]

The camera systems, study protocols and data acquisition vary significantly in studies of different radioisotopes that were reported previously.

Moreover, there is an issue in myocardial perfusion SPECT which was discussed in a clinical setting for long time regarding need to obtain high quality images in a short acquisition time. Surely, efforts are tried to find either superior of data sampling using single and dual head data acquisition.[125,126] Currently, dual head data collection is preferred, while single head data acquisition is still frequently used in a clinical practice.[127-130]

According to the Bucerius J et al. indicated that concerning myocardial viability, positive predictive value for diagnosis of myocardial scar tissue was considerably higher for dual head data as compared to single head data acquisition.[131]

1.3.1.2 Diagnostic accuracy

Subsequently, myocardial perfusion SPECT historical and exercise information is measured to produce incremental prognostic information for prediction of both cardiac death and follow up procedures.[132]

The SPECT has been reported to have a mean value of sensitivity of 82%, specificity of 76% and accuracy 83%.[133] To detect a nonviable myocardium in patients with myocardial infarction using SPECT, the sensitivity was 69.4%, specificity was 81.8% and accuracy was 79.9%.[134]

A systematic review of sensitivity, specificity and the accuracy of SPECT, PET and PET/CT in the detection of CAD showed that PET demonstrated the highest sensitivity, specificity and the accuracy at 91%, 89% and 89%, respectively. Whereas PET/CT had 85%, 83% and 88% while SPECT was found to have 82%, 76% and 83% corresponding to sensitivity, specificity and accuracy. [133,134]

With the moderate results of sensitivity, specificity and accuracy in detecting CAD, therefore, this analysis indicates that SPECT has not reached the diagnostic accuracy to be considered as a reliable technique for assessment of CAD.[133]

1.3.1.3 Limitations

SPECT scanning can be time-consuming. It can take hours or days for the radiotracers to accumulate in some parts of the body under investigation and imaging may take up to several hours to complete though in some cases, newer equipment is available that can substantially shorten the procedure time.[135, 136]

Several studies indicated that in patients with acute myocardial infarction (AMI) the reported rate of undetected infarcts by SPECT ranges from 11% to 25%.[136,137] The spatial resolution of SPECT images is about 10 × 10 × 10 mm and it is similar to the thickness of heart wall, non trans-mural infarcts are difficult to identify.[138,139]

1.3.2 Hybrid SPECT-CT

1.3.2.1 Imaging Principles

The integration of SPECT and CT systems into a single imaging unit shares a common imaging stand and it offers an important improvement in technology since this combination of SPECT and CT data maximises the advantages of each imaging modality in the investigation of coronary artery disease. Therefore, the two datasets can be assimilated into a recorded plane by suitable corrections. Also, this combined acquisition of consistent slices from the two modalities. The CT data can be used to allow accurate assessment of tissue attenuation in the SPECT scans on a slice by slice origin. And the CT data are presented in an advanced resolution matrix than the SPECT data. [140]

It passes through more tissue and clarifying of the beam to eliminate low energy photons is essential. The causing spectrum has an actual energy of about 70 keV. Since attenuation

effects differ with energy, it is necessary to adapt the attenuation data developed with CT to equivalent the energy of the radionuclide required in the SPECT acquisitions. [140]

Yet, it is essential to adapt the attenuation data measured at an actual energy of 70 keV to 140 keV for ^{99m}Tc.

This is typically by spending a bilinear model related attenuation coefficients at the required energy to CT numbers which are measured at the actual energy of the CT beam of x-rays. There are various benefits in the use of CT data for attenuation correction of emission data.[140]

Firstly, the CT scan offers a high photon fluctuation that considerably decreases the statistical noise related to the correction in contrast to other techniques. Similarly, due to the quick acquisition rapidity of CT scanners, the overall imaging time is considerably reduced by using this technology. Also, one of the advantages associated with the high photon fluctuation of CT scanners is that attenuation measurements can be made in the attendance of radionuclide distributions with insignificant influences from photons produced by the radionuclides. [141]

The use of CT also eliminates the need for additional hardware and transmission sources that often must be replaced on a routine basis. The anatomic images developed with CT can be fused with the emission images to deliver useful anatomic records for correct local area of radiopharmaceutical uptake.[141]

The assessment of patients with symptoms of chest pain with coronary CT angiography only proves a low specificity and PPV. The use of hyprid SPECT-CT imaging results in a marked increase in specificity and PPV to distinguish haemodynamically significant coronary lesions. SPECT-CT combined improves the diagnostic value of coronary CT angiography and encourage physiology built development of interventional processes in patients with established CAD.[142]

1.3.2.2 Diagnostic accuracy

Rispler S et al. reported that for assessment of hemodynamically significant coronary artery lesions, integrated (SPECT-CT) had sensitivity, specificity, PPV and NPV of 96%, 95%, 77% and 99%, respectively.[143] SPECT/CT imaging results in improved image quality,

showing improved specificity and PPV to detect hemodynamically significant coronary lesions in patients with chest pain.[143]

The anatomic evidence found with CT matches the functional assessment delivered by SPECT together from a diagnostic and prognostic perception. Numerous procedures for combination of the CT CACS with SPECT have been planned.[144]

Hybrid SPECT-CT and PET-CT are non-invasive imaging modalities cardiovascular that quickly progress with ability to image the structure and function in the heart and cardiovascular system. [145]

It is determining direct measurable evidence almost myocardial perfusion and metabolism with coronary and cardiac anatomy; hybrid imaging offers the prospect for a complete non-invasive assessment of the problem of atherosclerosis. Also, it's provided physiological significances in the coronary arteries and myocardium. [145]

The benefits of prospective study will be to refine these technologies, to establish standard protocols for image acquisition and interpretation, to address the issue of cost-effectiveness, and to confirm a variety of clinical uses in fluctuated clinical decisions.[146]

The conception of joining SPECT studies with CT developed throughout a single examination has encouraged productive elementary and clinical investigation in a selection of diseases.[146]

1.3.2.3 Limitations

Though, the number of integrated SPECT-CT systems remains to grow at a slightly increased rate, the development of SPECT-CT did not monitor the similar movement. One of the main reasons for the slow receiving of SPECT-CT compared to PET-CT is the comparative cost of SPECT and CT which takes into account the low portion of clinical suggestions where SPECT-CT is required[147].

There are new technological and precise expansions enhance substantial difficulty to the current, dynamic discussion almost the possible of conventional, single photon imaging to survive the experiments rising from PET imaging. Since that PET is greater to single photon

imaging for examining the area distribution of agents and as the growing variety of PET radiopharmaceuticals.[148]

1.3.3 Positron Emission Tomography (PET)

1.3.3.1 Imaging Principles

Cardiac positron emission tomography (PET) imaging has progressed rapidly from an initial research instrument to an applied, high performance clinical imaging modality.

The wide availability of PET, the commercial accessibility of perfusion and viability PET imaging radiopharmaceuticals, benefit for PET perfusion and viability procedures by government and private health insurance strategies, and the accessibility of computer software for image demonstration of perfusion, wall motion, and viability images represent the advantages of PET camera. All of these have been a key to cardiac PET imaging which enables it to be attractive for a routine clinical instrument.

Although, myocardial perfusion PET imaging is selected to study patients requiring stress perfusion imaging, there are detectible patient individuals hard to image with conventional SPECT imaging that are principally possible to benefit from PET imaging. For example, obese patients, women, patients with previous no diagnostic tests, and patients with poor left ventricular function attributable to coronary artery disease measured for revascularisation.

Myocardial PET perfusion imaging with rubidium-82 is significant for high efficiency, rapid quantity, and in a high volume setting, low operating costs. PET metabolic viability imaging remains to be a non-invasive typical for diagnosis of viability imaging. Cardiac PET imaging has been exposed to be cost-effective. The possible of routine quantification of resting and stress blood flow and coronary flow reserve in relation to pharmacologic and stress provide teasing potentials of increasing the power of PET myocardial perfusion imaging. This can be concluded by providing declaration of stress quality control. [149]

Also, in improving diagnosis and risk stratification in patients with coronary artery disease. PET has increasing diagnostic imaging into early coronary artery disease and endothelial dysfunction issue to risk factor variation. [150]

While, the clinical value of cardiac PET imaging was established twenty years ago, PET imaging varies from conventional radionuclide imaging. Since, it uses radionuclides that decay with positron emission. A positron has the identical quantity as an electron but has a positive responsibility. [150-152]

The positron movements a short space, up to a few millimetres, interrelates with an electron, and the two experience a joint annihilation, subsequent in the making of two 511-kev gamma photons, 180° apart from each other. PET imaging involves of discovery of these photons in chance. PET imaging is electronic accident localisation by ring detector indications to high acquisition efficiency.[153]

These outcomes in high-quality images developed in a short time and many sequential achievements. The short half-life of ^{82}Rb and ^{13}N ammonia effect in low radiation exposure for the patient from numerous involvement studies or follow-up studies and allow other radionuclide imaging studies on the same day. A consequence of the ability of PET to perform effective non-uniform attenuation correction is high image consistency, therefore reducing attenuation artefact. [154]

The capability to calibrate the PET system allows quantification of myocardial flow and glucose application. PET imaging provides an actual high resolution of 5 to 7mm, parallel with 15mm with resolution of SPECT imaging though in cardiac imaging, resolution is reduced by respiratory and cardiac wall movement. Cardiac PET imaging offers the full potential resolution.[155]

Myocardial PET perfusion imaging requires patient preparation for stress and rest which is similar to SPECT perfusion imaging. Myocardial PET perfusion imaging is frequently achieved with pharmacologic-induced stress, mainly with dipyridamole or adenosine.[155] For myocardial FDG PET viability imaging, this is performed with glucose filling and additional insulin. The patient is injected with FDG. After for a 1-h rest, the patient then undergoes emission PET imaging, along with a transmission scan.[156]

1.3.3.2 Diagnostic accuracy

PET perfusion scan indicates an outstanding prognosis with a low proportion of cardiac procedures.[157-159] At the 70% stenosis severity, sensitivity was 87% for PET and specificity

was 100%, with a resulting significant improvement in overall accuracy of 89%.[160] While, at the 50% stenosis severity, sensitivity was 79% for PET and specificity was 100%, with a resulting significant improvement in overall accuracy by 87%.[160]

There are numerous details why PET influence further SPECT for gated cardiac perfusion imaging. SPECT image superiority arises through low myocardial amounts, soft tissue decrease, and scatter of movement from nearby structures such as the liver and bowel into the cardiac region of concern. PET equipment offers superior myocardial amount mass in a greatly shorter acquisition time.[161,162]

Spatial resolution of PET is in the range of 2 to 4 mm, as is observed with 6 to 8 mm for ^{99m}Tc SPECT. Currently, image resolution is dependent on several patient and processing factors and it ranges from 6 to 10 mm and 10 to 14 mm, individually. The most significantly moving PET effective resolution is the positron range, which gives a characteristic shadow to the images not existing with the gamma emissions of SPECT. [162]

^{82}Rb has relatively high positron emission energy (1.52 MeV), with a mean range of approximately 5.5 mm. One effect of the higher spatial resolution of PET is better parting of the heart from nearby structures and there is less scatter result on myocardial totals. Once there is hot movement in near to the heart in SPECT scans, the filtered back projection method of reconstruction can outcome in artefacts that perform as perfusion defects.[163]

1.3.3.3 Limitations

Yet, PET reconstruction uses an OSEM algorithm, which does not present the ramp-filtering artefact[163]. Patient exposure to radiation is significantly lower with ^{82}Rb PET related with rest/stress ^{99m}Tc SPECT.[164,165]

1.3.4 Hybrid PET-CT

1.3.4.1 Imaging Principles

In spite of the fact that the introduction of dual-modality imaging systems planned exactly for medical exercise is quite new. The possible advantages of joining anatomical and functional imaging have been accepted for numerous years by radiological scientists and physicians.[166]

Several of the developers of nuclear medicine accepted that a radionuclide imaging system might be increased by count peripheral radioisotope basis to obtain show data for anatomical association of the emission image. [167]

But, the theoretical plans were never concentrated to practice or applied in any an experimental or a clinical background until established in the 1990s the progress of SPECT/CT and coming established in 1998 the improvement of combined PET/CT imaging systems, which have the ability to detected individually radionuclide and CT data for connected functional structural imaging[167-170].

Later, SPECT/CT and PET/CT dual-modality imaging systems were presented by the main scanner manufacturers for routine clinical practice where about more than 80% of PET systems sold yearly are combined PET/CT units. Dual-modality SPECT/CT and PET/CT scanners now are available from all of the major medical imaging department's producers (GE Healthcare Technologies, Siemens Medical Solutions, and Philips Medical Systems) contribution the show obtainable on state-of-the-art diagnostic CT systems. [170]

1.3.4.2 Diagnostic accuracy

Many SPECT/CT systems join a dual-headed SPECT camera fixed to a single detector, 4 detectors, 8 detectors or a 16 detectors diagnostic CT scanner however present PET/CT systems have up to 64 slice CT ability. It has detectors with either 2D/3D or only 3D PET imaging capability. This is demonstrates a high resolution anatomical information from CT. Also, dual-modality imaging compares functional and anatomical data to progress disease zone and helps management development for radiation oncology or surgery. [171-175]

A current study using PET/CT indicated that a sensitivity of 93%, a specificity of 83%, with a regularity rate of 100%. In this study of patients without known previous CAD, the PPV and NPV of PET/CT were 80% and 94%, respectively, with an overall accuracy of 87%. [176] In

addition, both SPECT/CT and PET/CT have confirmed their capability to enable attenuation correction by a patient particular attenuation map resulting from CT. It can be produced faster and more accurately than attenuation maps generated with external radionuclide sources. [177]

PET scanners have intense enhancements in routine over the past years. Dual modality, these developments are in together hardware and software, with new radiopharmaceuticals, improved spatial resolution, advanced sensitivity, more accurate reconstruction techniques, and the newer-establishment of time of flight measurements.

As the improvements in PET technology confirm a more stable examination; a whole PET/CT inspection can currently be done in 10–15 min. An increasing supports the better accuracy of performance with PET/CT, associated with any CT or PET developed individually.[178,179]

There are significant developments in specificity and, sensitivity and in early detection of CAD. These are enhancements that are related with a technique (PET) that previously establishes high levels of sensitivity and specificity for an extensive disease states. The sensitivity that software combination is a viable another to PET/CT and certainly offers several advantages.[180]

Software combination techniques will continuously have a clinical role, improving the registration of images developed with PET/CT, supporting images from modalities if there is no alternative hardware solution and combining PET/CT images with MRI for treatment development. Combination software may be extensively obtainable, however that is not the similar as being normally accessible.

It is the routine, practically easy, accessibility of registered CT and PET images for every patient that gives PET/CT the advantage. PET/CT operators have just been combined by a increasing of SPECT/CT users. The distribution of PET/CT and SPECT/CT into the clinical practice has been determined by physician request founded on gradually fixed clinical results. As long as this movement remains, the future of hybrid imaging and of PET/CT, in particular, will be guaranteed.[178,179]

1.3.4.3 Limitations

PET/CT combined equipment cannot determination entirely the matters related with precise position of two modalities. [180]

The use of CT for attenuation correction may create artefacts that do not appear with a conventional radionuclide scan. Moreover, there is debate connected to some extra radiation dose associated with using the CT scan.

This situation has created the application for preparation of separately the technologists and the physicians. Instructions have been available and new ethics recognised making an actual dissimilar condition currently from the technique radiology and nuclear medicine was worked.[180]

Furthermore, addressing the training of practician for a different feature in imaging is essential. While, the original PET/CT strategies might have performed too expensive by joining two costly modalities. Also, high performance PET/CT scanners are now accessible for a financial amount similar to that of various PET alone earlier 2001. The most worry that the 45 min PET scan would create sufficient use of the related CT scanner[182].

1.3.5 Radioisotopes used for nuclear cardiology used for SPECT/ SPECT-CT

A patient who has significant coronary artery stenosis or abnormal coronary flow replacement will have a region of reduced radiopharmaceutical absorption in the area of quite reduced perfusion. Each of the area or the severity of reduced tracer absorption is inferior when the tracer is controlled through stress and at rest. The region of reduced tracer absorption is recorded due to ischemia. If the region of reduced tracer absorption is still unaffected from rest to stress, it is most likely that the defect is scar. While, in particular circumstances it could characterise viable, under-perfused myocardium. Abnormalities may also indicate high obstruction to regions of viable, about myocardium. The available SPECT flow agents are considered a quick myocardial abstraction by a cardiac uptake related to blood flow.

1.3.5.1 ^{99m}Tc-tetrofosmin

^{99m}Tc labelled tetrofosmin is relative to regional myocardial blood flow with a first-pass extraction portion inferior to that of ^{201}Tl and sestamibi. Myocardial uptake is relative to blood flow completed the physiological range of blood flow.

Blood flow and tetrofosmin myocardial movement demonstrate a direct relationship to about 2 mL/min/m. For sestamibi, tetrofosmin uptake is not direct related to the growing blood flow.

Also, tetrofosmin establishes a table during stress at a blood flow level inferior to that of sestamibi.[181] During intravenous injection tetrofosmin is cleared quickly from the blood. Myocardial subtraction from the blood into the myocardium is less effective than for ^{201}Tl.

Tetrofosmin is similar to sestamibi which is considered by a speedy heart uptake and stable holding, no evidence of reorganisation for up to 3 hours next injection within reversible ischemic segment. Tetrofosmin is offers the similar benefits of sestamibi concerning the energy level. The half-life and the larger doses can be controlled to the patient in evaluation with ^{201}Tl. [184] ^{99m}Tc-tetroforsmin intravenously administrated with an activity of 740–1,480 MBq (20–40 mCi) and effective dose of 0.0067 mSv/MBq (0.025 rem/mCi).

1.3.5.2 ^{99m}Tc-sestamibi

^{99}Tc labelled sestamibi is related to area myocardial blood flow with a first-pass extraction fraction lower than that of ^{201}Tl. Yet, the considerably higher dose of sestamibi used more than inferior removal as associated to ^{201}Tl. The relationship between regional blood flow and myocardial uptake is to almost 2 mL/min/m.[185] A sestamibi myocardial uptake is not directly related to growing flow. The myocardial management of sestamibi is associated with screen across biological membranes.[186]

After sestamibi collects inside the myocardial cell, it is sure in a quite stable method. The parenchymal cell absorbent and volume of supply of sestamibi are much superior to ^{201}Tl. Subsequent, in a longer time is inside the myocardial cells for sestamibi. Thus, at clinical imaging following tracer injection, remaining myocardial tracer satisfied is related for ^{201}Tl and sestamibi is higher and more rapid extraction of ^{201}Tl. Sestamibi has uncertain indication of variance from ischemic to normal tissue. So, images achieved at 1 hour reproduce perfusion at the time of injection. The ^{99}Tc energy level (140 KeV) is perfect for imaging

with conventional gamma camera, reducing difficulties for soft tissue reduction. Besides, the 6 hours half-life gives a higher dose that can be managed to the patient as related to ^{201}Tl. [187] ^{99}Tc-sestamibiis intravenously administrated with an activity of 740–1,480 MBq (20–40 mCi) and effective dose0.0085 mSv/MBq (0.031 rem/mCi).

1.3.5.3 ^{201}TI-thallium

Thallium-201 (^{201}TI) is relative to area myocardial blood flow with a high first-pass removal in the range of 85%. The relative between blood flow and myocardial uptake is practically direct at low and sensible flow level, to at least 3 mL/min/gm. Also, there achieves to be a decrease in the uptake of ^{201}Tl in relation to blood flow. But, at almost 3 mL/min/gm, there is a table result such that, growths in blood flow, ^{201}Tl movement does not have variation. The growth and absorbent of ^{201}Tl inside the myocardium is affected by together coronary blood flow and cellular viability. Yet, an intracellular uptake of ^{201}Tl across the sarcolemma membrane is continued for as extended as essential blood flow. Blood flow current to transmit the tracer to the myocardial cell. After,^{201}Tl has arrived into myocardial cells; a continuous altercation precedes location through the cell membrane.

In the presence of an ischemia, the essential degree for ^{201}Tl is concentrated. This gives to viable of late tracer activity between originally ischemic and normally perfused areas. That is stated to as tracer redistribution. Later ^{201}Tl injection, the initial images acquired reproduce the area distribution of myocardial blood flow. In spite of ^{201}Tl has been the maximum used tracer to measure myocardial blood flow, its physical features represent model. The energy level (69 to 83 KeV) is slightly appropriate for imaging by conventional gamma camera. It creates particular difficulties for attenuation in the body.

The quite extended physical half-life 73 hours and biological half-life 10 days principal to a radiation dose to the kidneys and only a small amount (74 to 111 MBq) of ^{201}Tl can be controlled.[187] ^{201}Tl-thallium is intravenously administrated activity of 74–148 MBq (2–4 mCi) and effective dose of 0.23 mSv/MBq (0.85 rem/mCi).

1.3.6 Radiopharmaceuticals used of nuclear cardiology used for PET/ PET-CT

The capabilities of radionuclide methods are to measure myocardial perfusion or viability in the incidence of coronary artery stenosis. This is associated to the myocardial supply of a perfusion tracer and consistent regional blood flow.

Consequently, myocardial perfusion can be imaged and hypo-perfusion can be distinguished as a relation uptake defect as associated with the usually perfused myocardium. In addition, dissimilar PET tracers could be used for the measurement of qualified myocardial blood flow and Coronary Flow Reserve (CFR).

Although, several tracers have been used for evaluating myocardial perfusion with PET, the most widely used in clinical practice are as listed on the following subtopics.[188]

1.3.6.1 Rubidium-82 (^{82}Rb)

^{82}Rb is apotassium equivalent that is a generator produced with a half-life of 76 s and moving stuffs related to^{201}Tl. The different benefit of not requiring a cyclotron, ^{82}Rb is the extensively used radionuclide for assessment of myocardial perfusion with PET. Next, intravenous injection of ^{82}Rb quickly crosses the vessel membrane.[187] Myocardial uptake of ^{82}Rb needs dynamic passage through the sodium and potassium adenosine triphosphate transporter. It is dependent on coronary blood flow.[189]

The only vessel passage extraction portion of ^{82}Rb exceeds 50%. Nevertheless, its remaining removal portion declines in an indirect method with growing myocardial blood flow [190].The determined dynamic energy of positrons produced through^{82}Rb degeneration is considerably higher than that of ^{18}F or ^{13}N. Thus, the spatial improbability in the position of the decaying nucleus which depends on the moved by the positrons earlier their extermination is more for ^{82}Rb 2.6-mm complete width at half extreme than for ^{18}F 0.2 mm or ^{13}N 0.7 mm.

While,^{82}Rb imaging produces an excellent image quality with current PET technology. Its longer positron variety and short half-life needs important image quality to suppress noise. Individually alleviate slightly the better quality spatial resolution of PET.[191] Rubidium-82 (^{82}Rb) is intravenously administrated with an activity of 1,100–1,850 MBq (30–50 mCi) and for effective dose of 0.0048 mSv/MBq (0.018 rem/mCi).

1.3.6.2 ^{13}N-ammonia

^{13}N-ammonia is a cyclotron produced and a half-life of 9.96 min. ^{13}N-ammonia quickly no display from the movement, positive the acquisition of images of excellent superiority. Though, the appropriation of ^{13}N-ammonia in the lungs is usually minimal, it may be enlarged in patients with low left ventricular (LV) systolic function or chronic pulmonary disease. This might be in shot affect the excellence of the images.

It could be essential to rise the time between injection and image accomplishment to enhance the contrast in myocardial.^{13}N-ammonia contains of neutral ammonia NH_3 in stability with its stimulating ammonium NH_4 ions. The neutral NH_3 particle is readily through plasma and cell membranes; this is leading to almost removal from the vascular pool.[192]

^{13}N-ammonia is combined into the glutamine pool and develops metabolically surrounded. It's retaining by the myocardium an indirect and opposite association with blood flow. The portion of ^{13}N-ammoniaengaged by the myocardium throughout its principal pass is 0.83 when blood flow is 1 mL/min/g, and reductions to 0.60 as flow rises to 3 mL/min/g.[193]

The remaining tissue removal reduces as myocardial blood flow growths. ^{13}N-ammoniarelative between remaining tissue extraction and blood flow is direct for standards of blood flow up to 2.5 mL/min/g. A metabolic trapping of 13N-ammonia develops the rate restrictive factor moving tracer retention. This is indication to under assessment of blood flow at high flow rates.[194]

Consequently, to quantify myocardial blood flow using ^{13}N-ammonia, it develops essential to accurate for flow dependent fluctuations in remaining tissue removal. Myocardial retaining of ^{13}N-ammonia is dissimilar the lateral left ventricular (LV) wall being about 10% lower than that of other segments, even in healthy subjects. ^{13}N-ammonia images can be low-quality by infrequent powerful liver activity. It cause affect with the assessment of the inferior wall. Yet, the appropriation of ^{13}N-ammonia in the lungs is commonly insignificant. It could be improved in patients with low LV systolic purpose or chronic pulmonary disease.[195]

It could be essential to growth the time between injection and image acquisition of the contrast amongst myocardial and background activity.

^{13}N-Ammonia allows the acquisition of no gated and gated images of good quality. These studies take complete benefit of the higher resolution of PET qualified to SPECT, as the half-life of ^{13}N is adequately extended. Its usual positron variety is very short.

Gated ^{13}N-ammonia imaging can deliver exact assessments of both regional and overall cardiac function. But, this imaging agent is not well suitable for peak stress gated imaging. For the reason that of the 3- to 4-min time interval between radiotracer injection and the start of imaging with the quite long 20 min acquisition times.[196] ^{13}N-ammonia is intravenously administrated with an activity of 370–740 MBq (10–20 mCi) and effective dose of 0.0022 mSv/MBq (0.0081 rem/mCi).

1.3.6.3 ^{18}F-FDG

Myocardial imaging using ^{18}F-FDG is the greatest recurrent clinical request of cardiac PET. It is achieved in patients with dysfunctional, hypo-perfused myocardial regions to indicate the possibility of advantage from revascularisation. Remaining metabolic activity is a meter of myocardial viability, and therefore of reversibility of contractile dysfunction.

^{18}F-FDG has a better regional uptake which makes it most suitable for assessing myocardial perfusion and viability. However, regional reduction of ^{18}F-FDG uptake in quantity to perfusion is shows irreversibly damaged myocardium.

Myocardial ^{18}F-FDG uptake can be imaged by SPECT using extreme high energy collimators. Methodological issues specific to SPECT need to be measured for image interpretation.

This also relates to combinations of SPECT perfusion imaging and ^{18}F-FDG PET imaging for viability assessment. Cardiac PET has been accessible for a quite short time and the techniques have been under quick progress. Also, some studies reported the actual tasteless patients who are typical applicants for cardiac PET.[197,198] ^{18}F-FDG is intravenously administrated with an activity of 350 – 750MBq (4.5-6 mCi) and effective dose of 0.027 mSv/MBq (0.10 rem/mCi).

1.4 Thesis outline

This thesis contains seven chapters. An overview of background, different imaging modalities and radiopharmaceuticals/radioisotopes is presented in this chapter which consists of the relevance and the interconnection to the topic of nuclear cardiology in the diagnosis of coronary artery disease. The overall aim of this thesis is to investigate the recently developed imaging technique, PET with regard to its diagnostic value in the assessment of coronary artery disease. This technique is compared to the standard method cardiac SPECT in terms of diagnostic value of myocardial viability.

Chapter 2 is a systemic review of the diagnostic value of SPECT, PET and PET/CT in the diagnosis of coronary artery disease. The analysis of all eligible articles shows that PET has the highest diagnostic value in the diagnosis of coronary artery disease.

Chapter 3 is a head to head comparison of the coronary calcium score by computed tomography with myocardial perfusion imaging in predicting coronary artery disease. Research findings of this study show that coronary calcium score and SPECT provide complimentary information, thus should be used together in the diagnostic management of patients with coronary artery disease.

Chapter 4 is a phantom experiment on the myocardial perfusion imaging using ^{99m}Tc-sestamibi SPECT. A cardiac phantom is manufactured to simulate the normal cardiac anatomy, and myocardial perfusion imaging with SPECT is tested on the phantom. Results indicate that the cardiac phantom can be used for further experimental studies, in particular cardiac SPECT and PET imaging.

Chapter 5 is a prospective study on diagnostic value of ^{18}F-FDG PET in the assessment of myocardial viability in comparison with ^{99m}Tc SPECT and echocardiography with invasive coronary angiography as the gold standard. Patients with known or proven coronary artery disease are recruited to undergo all of these imaging examinations. Results show that ^{18}F-FDG PET has high diagnostic value in myocardial viability assessment when compared to SPECT or echocardiography, and it can be used as a reliable and accurate modality in diagnosing coronary artery disease and guiding patient management.

Chapter 6 is a summary and conclusion of the thesis.

1.5 References

1. Waller BF. Five coronary ostia: Duplicate left anterior descending and right conus coronary arteries. The American Journal of Cardiology. 1983;51(9):1562-1563.

2. Waller BF. Anatomy, histology, and pathology of coronary arteries: A review relevant to new interventional and imaging techniques—Part I. Clinical cardiology. 1992;15(6):451-452.

3. Bastarrika Alemañ G, Alonso Burgos A, Azcárate Agüero PM, et al. [Normal anatomy,anatomical variants, and anomalies of the origin and course of the coronary arterieson multislice CT]. Radiologia 2008 May–Jun;50(3):197–206.

4. Angelini P, Villason S, Chan AV Jr, Diez JG. Normal and anomalous coronary arteries in humans. In: Angelini P, editor. Coronary artery anomalies: a comprehensive approach. Philadelphia: Lippincott Williams & Wilkins; 1999. p. 27-150.

5. Netter FH. Colacino S (ed). Atlas of HumanAnatomy. Summit, NJ: Ciba-Geigy Corp.; 1989.

6. Berdoff R, Haimowitz A, Kupersmith J. Anomalousorigin of the right coronary artery from the left sinus ofValsalva. Am J Cardiol. 1986; 58:656-657.
7. Australian Institute of Health and Welfare (AIHW) 2001. Heart, stroke and vascular diseases Australian facts 2001. Cardiovascular Disease Series No. 14. AIHW Cat. No. CVD 13. Canberra: AIHW, National Heart Foundation of Australia, National Stroke Foundation of Australia.
8. Australian Institute of Health and Welfare (AIHW) 2008a. Australia's health 2008: the ninth biennial health report of the Australian Institute of Health and Welfare. Canberra: AIHW.
9. Centres for Disease Control and Prevention. Morbidity and Mortality Weekly Report (MMWR), Prevalence of Coronary Heart Disease in United States, 2010;60:40-14.
10. Coy KM, Maurer G, Siegel RJ. Intravascular ultrasound imaging: a currentperspective. J Am Co Cardiol 1991; 18:1811-23.
11. Nissen SE, Gurley JC, Booth DC, Demaria AM. Intravascular ultrasound of the coronary arteries: current applications and future directions. Am J Cardiol 1992; 69: lSH-29H.
12. Hodgson JMcB, Reddy KG, Suneja R, Nair RN, Lesnefsky EJ, Sheehan HM. Intracoronary ultrasound imaging: correlation of plaque morphology with angiography, clinical syndrome and procedural results in patientsundergoing coronary angioplasty. J Am Coll Cardiol 1993;21:35-44.
13. Davignon J, Ganz P. Role of endothelial dysfunction in atherosclerosis. Circulation 2004;109(Suppl 1):III27-32.
14. Naghavi M, Libby P, Falk E, Casscells SW, Litovsky S, Rumberger J, et al. From vulnerable plaque to vulnerable patient: a call for new definitions and risk assessment strategies: part I. Circulation 2003;108:1664-72.
15. Mannebach H, Hamm C, Horstkotte D. 17th report of performance statistics of heart catheterization laboratories in Germany. Results of a combined survey by the

Committee of Clinical Cardiology and the Interventional Cardiology (for ESC) and Angiology Working Groups of the German Society of Cardiology–Cardiovascular Research for the year 2000. ZKardiol 2001;90:665–667.
16. Smith SC Jr, Feldman TE, Hirshfeld JW Jr, Jacobs AK, Kern MJ, King SB III, Morrison DA, O'Neill WW, Schaff HV, Whitlow PL, Williams DO, Antman EM, Adams CD, Anderson JL, Faxon DP, Fuster V, Halperin JL, Hiratzka LF, Hunt SA, Nishimura R, Ornato JP, Page RL, Riegel B. ACC/AHA/ SCAI 2005 Guideline Update for Percutaneous Coronary Intervention summary article: a report of the American College of Cardiology/American Heart Association Task Force on Practice Guidelines (ACC/AHA/SCAI Writing Committee to Update the 2001 Guidelines for Percutaneous Coronary Intervention). Circulation 2006; 113:156–175.
17. Morgan Hughes GJ. Highly accurate coronary angiography with submillimetre, 16 slice computed tomography. Heart. 2005;91(3):308-309.
18. Piers LH. Computed tomographic angiography or conventional coronary angiography in therapeutic decision-making. Eur heart J. 2008;29(23):2902-2903.
19. Braunwald E, Antman EM, Beasley JW, et al. ACC/AHA guideline update for the management of patients with unstable angina and non-ST-segment elevation myocardial infarction–2002: summary article: a report of the American College of Cardiology/American Heart Association Task Force on Practice Guidelines (Committee on the Management of Patients With Unstable Angina). Circulation. 2002;106:1893-1900.
20. Bertrand ME, Simoons ML, Fox KA, et al. Management of acute coronary syndromes in patients presenting without persistent ST-segment elevation. Eur Heart J. 2002;23:1809-1840.
21. Reddy BK, Brewster PS, Walsh T, et al. Randomized comparison of rapid ambulation using radial, 4 French femoral access, or femoral access with AngioSeal closure. Catheter Cardiovasc Interv. 2004;62:143-149.
22. Koo B-K, Waseda K, Kang H-J, Kim H-S, Nam C-W, Hur S-H, et al. Anatomic and Functional Evaluation of Bifurcation Lesions Undergoing Percutaneous Coronary Intervention. Circulation: Cardiovascular Interventions. 2010;3(2):113-119.
23. Ryan TJ, Faxon DP, Gunnar RM, et al. Guidelines for percutaneous transluminal coronary angioplasty. A report of the American College of Cardiology/American Heart Association Task Force on Assessment of Diagnostic and Therapeutic Cardiovascular Procedures (Subcommittee on Percutaneous Transluminal Coronary Angioplasty). Circulation. 1988;78:486-502.
24. Jacobs, Alice K., Sheryl F. Kelsey, Maria Mori Brooks, David P. Faxon, Bernard R. Chaitman, Vera Bittner, Michael B. Mock et al. "Better outcome for women compared with men undergoing coronary revascularization a report from the bypass angioplasty revascularization investigation (BARI). Circulation 1988;13: 1279-1285.
25. Ehara M, Kawai M, Surmely J-F, Matsubara T, Terashima M, Tsuchikane E, et al. Diagnostic Accuracy of Coronary In-Stent Restenosis Using 64-Slice Computed Tomography Comparison With Invasive Coronary Angiography. J Am Ccoll Cardiol. 2007;49:951-959.
26. Gorenoi V, Schönermark MP, Hagen A. CT coronary angiography vs. invasive coronary angiography in CHD. GMS Health Technology Assessment. 2012;8: 786-792.

27. Members C, Scanlon PJ, Faxon DP, Audet A-M, Carabello B, Dehmer GJ, et al. ACC/AHA Guidelines for Coronary Angiography: Executive Summary and Recommendations: A Report of the American College of Cardiology/American Heart Association Task Force on Practice Guidelines (Committee on Coronary Angiography) Developed in collaboration with the Society for Cardiac Angiography and Interventions. Circulation. 1999;99:2345-2357
28. Mehta Sr CCPFKA, et al. Routine vs selective invasive strategies in patients with acute coronary syndromes: A collaborative meta-analysis of randomized trials. JAMA. 2005;293:2908-2917.
29. Dewey M, Vavere AL, Arbab-Zadeh A, Miller JM, Sara L, Cox C, et al. Patient Characteristics as Predictors of Image Quality and Diagnostic Accuracy of MDCT Compared With Conventional Coronary Angiography for Detecting Coronary Artery Stenoses: CORE-64 Multicenter International Trial. Am J Roentgenol. 2010;194:93-102.
30. Tavakol M. Risks and Complications of Coronary Angiography: A Comprehensive Review. Global Journal of Health Science. 2011;4:1-2.
31. Scanlon PJ, Faxon DP, Audet AM, Carabello B, Dehmer GJ, Eagle KA, et al. ACC/AHA guidelines for coronary angiography. J Am Coll Cardiol 1999;33:1756-824.
32. Pons-Lladó G, Carreras F, Borrás X, Subirana M, Jiménez- Borreguero LJ. Atlas of practical cardiac applications of MRI. 1st ed. Dordrecht: Kluwer Academic Publishers, 1999; p. 73-77.
33. Achenbach S, Ropers D, Regenfus M, Pohle K, Giesler T, Moshage W, et al. Noninvasive coronary angiography by magnetic resonance imaging, electron-beam computed tomography, and multislice computed tomography. Am J Cardiol 2001;88(2-A):E70-73.
34. Qayyum R. Systematic review: comparing routine and selective invasive strategies for the acute coronary syndrome. Annals of Internal Medicine. 2008;148(3):186.
35. Bashein G, Detmer P, Sidebotham D, Merry A, Legget M. Physical principles, ultrasonic image formation and artifacts. Practical perioperative transoesophageal echocardiography. 2003;1:13-23.
36. Maslow A, Perrino AC. Principles and technology of two dimentional echocardiography. In: Perinno AC, Reeves ST (Eds). A practical approach to transesophageal echocardiography (2nded). Lippincott Williams & Wilkins, 2008; 3-23.
37. Weyman AE (Ed). Principles and practice of echocardiography (2nd ed). Philadelphia: Lea and Febiger, 1994;3-55.
38. Savord B, Solomon R. Fully sampled matrix transducer for real time 3D ultrasonic imaging. Ultrasonics, 2003 IEEE Symposiumon, 2003;Vol 1:945–953.
39. Salgo IS. Three-dimensional echocardiographic technology. Cardiol Clin. 2007;25(2):231–239.
40. Brekke S, Rabben SI, Støylen A, Haugen A, Haugen GU, Steen EN,Torp H. Volume stitching in three-dimensional echocardiography:distortion analysis and extension to real time. Ultrasound Med Biol.2007;33(5):782–796.
41. Steen E, Olstad B. Volume rendering of 3D medical ultrasound data using direct feature mapping. IEEE Trans Med Imaging. 1994;13(3):517–525.
42. Yang HS, Pellikka PA, McCully RB, Oh JK, Kukuzke JA, Khandheria BK, Chandrasekaran K. Role of biplane and biplane echocardiographically guided 3-dimensional echocardiography during dobutamine stress echocardiography. J Am Soc Echocardiogr. 2006;19:1136–1143.

43. Nucifora G, Badano LP, Dall'Armellina E, Gianfagna P, Allocca G, Fioretti PM. Fast data acquisition and analysis with real time triplane echocardiography for the assessment of left ventricular size and function: a validation study. Echocardiography. 2009;26(1):66–75.
44. Monaghan, M. Multi-plane and four-dimensional stress echocardiography new solutions to old problems? Eur Cardiovasc Dis. 2006; 72: 133–135.
45. Zamorano J, Cordeiro P, Sugeng L, Perez de Isla L, Weinert L, Macaya C, Rodríguez E, Lang RM. Real-time three-dimensional echocardiography for rheumatic mitral valve stenosis evaluation: an accurate and novel approach. J Am Coll Cardiol. 2004;43: 2091–2096.
46. Jenkins C, Moir S, Chan J, Rakhit D, Haluska B, Marwick TH. Left ventricular volume measurement with echocardiography: a comparison of left ventricular opacification, three-dimensional echocardiography, or both with magnetic resonance imaging. Eur Heart J.2009;30(1):98–106.
47. Gerard O, Allain P, Zamorano JL, de Isla LP, Mor-Avi V, Lang RM. Rapid online quantification of left ventricular volume from realtime three-dimensional echocardiographic data. Eur Heart J. 2006; 27(4):460–468.
48. Pouleur AC, le Polain de Waroux JB, Pasquet A, Gerber BL, Gérard O, Allain P, Vanoverschelde JL. Assessment of left ventricular mass and volumes by three dimensional echocardiography in patients with or without wall motion abnormalities: comparison against cine magnetic resonance imaging. Heart. 2008; 94(8):1050–1057.
49. Suh IW, Song JM, Lee EY, Kang SH, Kim MJ, Kim JJ, Kang DH, Song JK. Left atrial volume measured by real-time 3-dimensional echocardiography predicts clinical outcomes in patients with severe left ventricular dysfunction and in sinus rhythm. J Am Soc Echocardiogr. 2008;21:439–445.
50. Niemann PS, Pinho L, Balbach T, Galuschky C, Blankenhagen M, Silberbach M, Broberg C, Jerosch-Herold M, Sahn DJ. Anatomically oriented right ventricular volume measurements with dynamic three-dimensional echocardiography validated by 3-Tesla magnetic resonance imaging. J Am Coll Cardiol. 2007; 50(17):1668–1676.
51. Walimbe V., Jaber WA, Garcia MA, Shekhar R. Multimodality cardiac stress testing: combining real-time 3-dimensional echocardiography and myocardial perfusion SPECT. J Nucl Med. 2009; 50:226–230.
52. Gorcsan Iii J, Gorcsan. Quantitative assessment of alterations in regional left ventricular contractility with color-coded tissue Doppler echocardiography: comparison with sonomicrometry and pressure-volume relations. Circulation. 1997;95(10):2423-2424.
53. Gulati VK. Mitral annular descent velocity by tissue Doppler echocardiography as an index of global left ventricular function. Am J Cardiol. 1996;77:979-980.
54. Gatti G. Noninvasive dynamic assessment with transthoracic echocardiography of a composite arterial Y-graft achieving complete myocardial revascularization. Ann Thor Surg. 2005;79:1217-1274.
55. Kaul S. Myocardial Contrast Echocardiography. Curr Probl Cardiol. 1997;22:549–640.
56. Kuersten B, Murthy T, Li P, et al. Ultraharmonic myocardial contrast imaging. In vivo experimental and clinical data from a novel technique. J Am Soc Echocardiogr. 2001;14:910–916.
57. Janardhanan R, Moon JC, Pennell DJ. Myocardial contrast echocardiography accurately reflects transmurality of myocardial necrosis and predicts contractile reserve after acute myocardial infarction. Am Heart J. 2005;149:355–362.

58. Cholley BP, Vieillard-Baron A, Mebazaa A. Echocardiography in the ICU: time for widespread use! Intensive Care Med. 2006;32:9-10.
59. Vieillard-Baron A, Slama M, Cholley BP, Janvier G, Vignon P. Echocardiography in the intensive care unit: from evolution to revolution? Intensive Care Med. 2008;34:243-249.
60. Jensen MB, Sloth E. Echocardiography for cardiopulmonary optimization in the intensive care unit: should we expand its use? Acta Anaesthesiol Scand. 2004;48:1069-1070.
61. Seppelt IM. All intensivists need echocardiography skills in the 21st century. Crit Care Resusc. 2007;9:286-288.
62. McLean A, Yastrebov K. Echocardiography training for the intensivist. Crit Care Resusc 2007;9:319-322.
63. Breitkreutz R, Walcher F, Seeger F. Focused echocardiographic evaluation in resuscitation management: concept of an advanced life support-conformed algorithm. Crit Care Med. 2007;35:S150-161.
64. Manasia AR, Nagaraj HM, Kodali RB, et al. Feasibility and potential clinical utility of goal-directed echocardiography performed by noncardiologist intensivists using a small hand-carried device (SonoHeart) in critically ill patients. J Cardiothorac Vasc Anesth. 2005;19:155-159.
65. Hellmann DB, Whiting-O'Keefe Q, Shapiro EP, Martin LD, Martire C, Ziegelstein RC. The rate at which residents learn to use hand-held echocardiography at the bedside. Am J Med. 2005;118:1010-1018.
66. Bodenham AR. Ultrasound imaging by anaesthetists: training and accreditation issues. Br J Anaesth 2006;96:414-7.
67. Pibarot P. Doppler echocardiographic evaluation of prosthetic valve function. Heart. 2012;98:69-70.
68. Wilke N, Jerosch-Herold M, Wang Y, Huang Y, Christensen BV, Stillman AE, et al. Myocardial perfusion reserve: assessment with multisection, quantitative, first-pass MR imaging. Radiology. 1997;204:373-384.
69. Karamitsos TD, Francis JM, Myerson S, Selvanayagam JB, Neubauer S. The role of cardiovascular magnetic resonance imaging in heart failure. J Am Coll Cardiol. 2009; 54: 1407e-1424e.
70. Cullen JHS, Horsfield MA, Reek CR, Cherryman GR, Barnett DB, Samani NJ. A myocardial perfusion reserve index in humans using first-pass contrast-enhanced magnetic resonance imaging. J Am Coll Cardiol. 1999;33:1386-1394.
71. Pennell DJ, Sechtem UP, Higgins CB, et al. Clinical indications for cardiovascular magnetic resonance (CMR): consensus panel report. Eur Heart J. 2004; 25: 1940e-1965.
72. Spuentrup E, Bornert P, Botnar RM, Groen JP, Manning WJ, Stuber M. Navigator-gated free-breathing three-dimensional balanced fast field echo (TrueFISP) coronary magnetic resonance angiography. Invest Radiol. 2002;37:637– 642.
73. Phrommintikul A, Abdel-Aty H, Schulz-Menger J, Friedrich MG, Taylor AJ. Acute oedema in the evaluation of microvascular reperfusion and myocardial salvage in reperfused myocardial infarction with cardiac magnetic resonance imaging. Eur J Radiol. 2010; 74:e12-e17.
74. O'Regan DP, Ahmed R, Neuwirth C, et al. Cardiac MRI of myocardial salvage at the peri-infarct border zones after primary coronary intervention. Am J Physiol Heart Circ Physiol. 2009;297: H340–346.
75. Azevedo Filho CF, Hadlich M, Petriz JL, Mendonca LA, Moll Filho JN, Rochitte CE. Quantification of left ventricular infarcted mass on cardiac magnetic resonance

imaging: comparison between planimetry and the semiquantitative visual scoring method. Arq Bras Cardiol. 2004; 83: 118–124.
76. Choi KM, Kim RJ, Gubernikoff G, Vargas JD, Parker M, Judd RM. Transmural extent of acute myocardial infarction predicts long-term improvement in contractile function. Circulation. 2001; 104: 1101– 1107.
77. Budoff MJ, Cohen MC, Garcia MJ, et al. ACCF/AHA clinical competence statement on cardiac imaging with computed tomography and magnetic resonance: a report of the American College of Cardiology Foundation/American Heart Association/American College of Physicians Task Force on Clinical Competence and Training. J Am Coll Cardiol. 2005;46:383–402.
78. Weinreb JC, Larson PA, Woodard PK, et al. American college of radiology clinical statement on noninvasive cardiac imaging. Radiology. 2005;235:723–727.
79. Wolff SD, Schwitter J, Coulden R, et al. Myocardial first-pass perfusion magnetic resonance imaging: a multicenter dose-ranging study. Circulation 2004;110:732–737.
80. Hamdan A, Asbach P, Wellnhofer E, Klein C, Gebker R, Kelle S, et al. A Prospective Study for Comparison of MR and CT Imaging for Detection of Coronary Artery Stenosis. JACC: Cardiovasc Imaging. 2011;4(1):50-61.
81. Cheng ASH, Pegg TJ, Karamitsos TD, Searle N, Jerosch-Herold M, Choudhury RP, et al. Cardiovascular Magnetic Resonance Perfusion Imaging at 3-Tesla for the Detection of Coronary Artery Disease: A Comparison With 1.5-Tesla. J Am Coll Cardiol. 2007;49(25):2440-2449.
82. Schwitter J, Nanz D, Kneifel S, et al. Assessment of myocardial perfusion in coronary artery disease by magnetic resonance: a comparison with positron emission tomography and coronary angiography. Circulation. 2001;103:2230 –2235.
83. Nagel E, Klein C, Paetsch I, et al. Magnetic resonance perfusion measurements for the noninvasive detection of coronary artery disease. Circulation. 2003;108:432–437.
84. Arai AE, Gaither CC, 3rd, Epstein FH, Balaban RS, Wolff SD. Myocardial velocity gradient imaging by phase contrast MRI with application to regional function in myocardial ischemia. Magn Reson Med. 1999;42:98 –109.
85. Klem I, Heitner JF, Shah DJ, et al. Improved detection of coronary artery disease by stress perfusion cardiovascular magnetic resonance with the use of delayed enhancement infarction imaging. J Am Coll Cardiol. 2006;47:1630–1638.
86. Gutberlet M, Noeske R, Schwinge K, Freyhardt P, Felix R, Niendorf T. Comprehensive cardiac magnetic resonance imaging at 3.0 Tesla: feasibility and implications for clinical applications. Invest Radiol. 2006;41:154–167.
87. Araoz PA, Glockner JF, McGee KP, et al. 3 Tesla MR imaging provides improved contrast in first-pass myocardial perfusion imaging over a range of gadolinium doses. J Cardiovasc Magn Reson. 2005;7: 559–564.
88. Boussel L, Arora S, Rapp J, et al. Atherosclerotic plaque progressionin carotid arteries: monitoring with high-spatial-resolution MRimaging multicenter trial. Radiology 2009; 252:789 –796.
89. E.R. McVeigh, M.A. Guttman, R.J. Lederman, M. Li, O. Kocaturk, T. Hunt, S. Kozlov, K.A. Horvath, Real-time interactive MRI-guided cardiac surgery: aortic valve replacement using a direct apical approach, Magn Reson Med. 2006; 56: 958–964.
90. A.N. Raval, J.D. Telep, M.A. Guttman, C. Ozturk, M. Jones, R.B. Thompson, V.J. Wright, W.H. Schenke, R. DeSilva, R.J. Aviles, V.K. Raman, M.C. Slack, R.J. Lederman, Real-time magnetic resonance imaging-guided stenting of aortic coarctation with commercially available catheter devices in swine, Circulation. 2005; 112: 699–706.

91. Myerson SG, Holloway CJ, Francis JM, Meubauer S. Cardiovascular magnetic resonance (CMR)–An update and review. Prog Nucl Magn Reson Spectrosc. 2011;59(3):213-222.
92. Christiansen JP. Stress perfusion imaging using cardiovascular magnetic resonance: a review. Heart, lung and circulation. 2010;19(12):697-700.
93. Klingenbeck-Regn K, Schaller S, Flohr T, Ohnesorge B, Kop AF, Baum U. Subsecond multi-slice computed tomography: basics and applications. Eur J Radiol. 1999;31:110-124.
94. Mahesh M. The AAPM/RSNA physics tutorial for residents: search for isotropic resolution on CT from conventional through multiple-row detector. Radiographics. 2002;22:949-962.
95. Hong C, Becker CR, Huber A, et al. ECG-gated reconstructed multi-detector row CT coronary angiography: effect of varying trigger delay on image quality. Radiology. 2001; 220:712–717.
96. Giesler T, Baum U, Ropers D, et al. Noninvasive visualization of coronary arteries using contrastenhanced multidetector CT: influence of heartrate on image quality and stenosis detection. AJR 2002; 179:911–916.
97. Jhaveri KS, Saini S, Levine LA, Piazzo DJ, Doncaster RJ, Halpern EF, Jordan PF. Thrall JH. Effect of multislice CT technology on scanner productivity. AJR Am J Roentgenol. 2001;177:769-772.
98. Prokop M. Radiation exposure and image quality. In; Prokop M, Galanski M (eds.) Spiral and multislice computed tomography of the body. Thieme; Stuttgart, New York 2003:131-160.
99. Hu H, He HD, Foley WD, Fox SH. Four multidetector-row helical CT: image quality and volume coverage speed. Radiology. 2000;215:55-62.
100. Mollet N, Cademartiri F, van Mieghem C, et al. High-resolution spiral computed tomography coronary angiography in patients referred for diagnostic conventional coronary angiography. Circulation. 2005;112(15):2318-2323.
101. Ropers D, Rixe J, Anders K, et al. Usefulness of multidetector row spiral computed tomography with 64- x 0.6-mm collimation and 330-ms rotation for the noninvasive detection of significant coronary artery stenoses. Am J Cardiol. 2006;97(3):343-348.
102. Schuijf JD, Pundziute G, Jukema JW, et al. Diagnostic accuracy of 64-slicemultislice computed tomography in the noninvasive evaluation ofsignificant coronary artery disease. Am J Cardiol. 2006;98(2):145-148.
103. Kopp A, Heuschmid M, Reismann A, et al. Advances in imaging protocols for cardiac MDCT: from 16- to 64-row multidetector computed tomography. Eur Radiol Suppl. 2005;15:E71-E77.
104. Flohr TG, McCollough CH, Bruder H, Petersilka M, Gruber K, Suss C, Grasruck M, Stierstorfer K, Krauss B, Raupach R, et al. First performance evaluation of a dual-source CT (DSCT) system. Eur Radiol. 2006;16:256 –268.
105. Achenbach S, Ropers D, Kuettner A, Flohr T, Ohnesorge B, Bruder H, Theessen H, Karakaya M, Daniel WG, Bautz W, et al. Contrastenhanced coronary artery visualization by dual-source computed tomography initial experience. Eur J Radiol. 2006;57:331–335.
106. Johnson TR, Nikolaou K, Wintersperger BJ, Leber AW, von Ziegler F, Rist C, Buhmann S, Knez A, Reiser MF, Becker CR. Dual-source CT cardiac imaging: initial experience. Eur Radiol. 2006;16:1409 –1415.
107. Halliburton SS, Do segmented reconstruction algorithms for cardiac multi-slice computed tomography improve image quality? Herz. 2003;28(1):20–31

108. Johnson TR, Material differentiation by dual energyCT: initial experience. Eur Radiol. 2006; 17(6):1510–1517
109. Winters perger BJ, Nikolaou K, von Ziegler F, Johnson T, Rist C, Leber A, Flohr T, Knez A, Reiser MF, Becker CR. Image quality, motion artifacts, and reconstruction timing of 64-slice coronary computed tomography angiography with 0.33-second rotation speed. Invest Radiol. 2006;41:436–442.
110. Bley TA, Ghanem NA, Foell D, Uhl M, Geibel A, Bode C, Langer M. Computed tomography coronary angiography with 370-millisecond gantry rotation time: evaluation of the best image reconstruction interval. J Comput Assist Tomogr. 2005;29:1–5.
111. Brodoefel H, Reimann A, Heuschmid M, Kuettner A, Beck T, Burgstahler C, Claussen CD, Schroeder S, Kopp AF. Non-invasive coronary angiography with 16-slice spiral computed tomography: image quality in patients with high heart rates. Eur Radiol. 2006;16:1434– 1441.
112. Herzog C, Arning-Erb M, Zangos S, Eichler K, Hammerstingl R, Dogan S, Ackermann H, Vogl TJ. Multi-detector row CT coronary angiography: influence of reconstruction technique and heart rate on image quality. Radiology. 2006;238:75–86.
113. Leschka S, Wildermuth S, Boehm T, Desbiolles L, Husmann L, PlassA, Koepfli P, Schepis T, Marincek B, Kaufmann PA, Alkadhi H.Noninvasive coronary angiography with 64-Section CT: effect of averageheart rate and heart rate variability on image quality. Radiology. 2006;241:378 –385.
114. Heuschmid M. Usefulness of noninvasive cardiac imaging using dual-source computed tomography in an unselected population with high prevalence of coronary artery disease. Am J Cardiol. 2007;100:587-589.
115. Heuschmid M, Kuettner A, Schroeder S, Trabold T, Feyer A, Seemann MD, Kuzo R, Claussen CD, Kopp AF. ECG-gated 16-MDCT of the coronary arteries: assessment of image quality and accuracy in detecting stenoses. AJR Am J Roentgenol. 2005;184:1413–1419.
116. Halliburton SS, Stillman AE, Flohr T, Ohnesorge B, Obuchowski N, Lieber M, Karim W, Kuzmiak SA, Kasper JM, White RD. Do segmented reconstruction algorithms for cardiac multi-slice computed tomography improve image quality? Herz. 2003; 28:20 –31.
117. Stolzmann P. Radiation dose estimates in dual-source computed tomography coronary angiography. Eur Radiol. 2008;18(3):592-602.
118. Krauss B, Schmidt B, Flohr TG. Dual-energy CT with single-and dual-source scanners: current applications in evaluating the genitourinary tract. Dual source CT 2011:11-20.
119. Cuocolo A, Acampa W, Imbriaco M, De Luca N, Iovino G, Salvatore M. The many ways to myocardial perfusion imaging. The quarterly journal of nuclear medicine and molecular imaging: official publication of the Italian Association of Nuclear Medicine (AIMN)[and] the International Association of Radiopharmacology (IAR),[and] Section of the Society of. 2005;49:4-7
120. Strauss HW, Miller DD, Wittry MD, Cerqueira MD, Garcia EV, Iskandrian AS, et al. Procedure guideline for myocardial perfusion imaging 3.3. J N Medi Tech. 2008;36:155-161.
121. Patton JA. SPECT/CT physical principles and attenuation correction. J N Medi Tech. 2008;36:-11.

122. Cherry SR, Sorenson JA, Phelps ME. Tomographic reconstruction in nuclear medicine. In: Physics in Nuclear Medicine. 3rd ed. Philadelphia, PA: Saunders; 2003:273–297.
123. Cherry SR, Sorenson JA, Phelps ME. Single photon emission computed tomography. In: Physics in Nuclear Medicine. 3rd ed. Philadelphia, PA: Saunders; 2003:299–324.
124. Zaidi H, Hasegawa BH. Determination of the attenuation map in emission tomography. J Nucl Med. 2003;44:291–315.
125. Bax JJ, Visser FC, van Lingen A, Sloof GW, Cornel JH, Visser CA. Comparison between 3608 and 1808 data sampling in thallium-201 rest-redistribution single-photon emission tomography to predict functional recovery after revascularization. Eur J Nucl Med. 1997; 24:516–522.
126. Wallis JW. Increased sensitivity through use of overlapping 1808 orbits in clinical myocardial perfusion imaging. Eur J Nucl Med. 1995; 22:543–547.
127. Zheng, X. M. Changes of rCBF on major depressed patients following TMS treatment: An SPM analysis. Nuclear Medicine Communications 2000, 21(5), 473.
128. Go RT, MacIntyre WJ, Houser TS, et al. Clinical evaluation of 3608 and 1808 data sampling techniques for transaxial SPECT thallium-201 myocardial perfusion imaging. J Nucl Med. 1985;26: 695– 706.
129. Knesaurek K, King MA, Glick SJ, Penney BC. Investigation of causes of geometric distortion in 1808 and 3608 angular sampling in SPECT. J Nucl Med. 1989;30:1666–16 75.
130. Coleman RE, Jaszczak RJ, Cobb FR. Comparison of 1808 and 3608 data collection in thallium-201 imaging using single-photon emission computerized tomography (SPECT): concise communication. J Nucl Med. 1982;23:655–660.
131. Bucerius J. Single-vs. dual-head SPECT for detection of myocardial ischemia and viability in a large study population. Clin imaging. 2007;31:228-232.
132. Hachamovitch R, Berman DS, Shaw LJ, Kiat H, Cohen I, Cabico JA, et al. Incremental prognostic value of myocardial perfusion single photon emission computed tomography for the prediction of cardiac death: differential stratification for risk of cardiac death and myocardial infarction. Circulation. 1998;97:535-543.
133. Al Moudi M, Sun Z, Lenzo N. Diagnostic value of SPECT, PET and PET/CT in the diagnosis of coronary artery disease: A systematic review. Biomed Imaging Interv J. 2011;7:1-10.
134. Lee IH, Choe YH, Lee KH, Jeon E-S, Choi J-H. Comparison of multidetector CT with F-18-FDG-PET and SPECT in the assessment of myocardial viability in patients with myocardial infarction: A preliminary study. Eur J Radiol. 2009;72:401-405.
135. Kang X, Shaw LJ, Hayes SW, Hachamovitch R, Abidov A, Cohen I, et al. Impact of body mass index on cardiac mortality in patients with known or suspected coronary artery disease undergoing myocardial perfusion single-photon emission computed tomography. Am J Cardiol. 2006;47(7):1418-1426.
136. Miller TD, Christian TF, Hopfenspirger MR, Hodge DO, Gersh BJ, Gibbons RJ. Infarct size after acute myocardial infarction measured by quantitative tomographic 99mTc sestamibi imaging predicts subsequent mortality. Circulation. 1995;92:334–341.
137. Kontos MC, Kurdziel K, McQueen R, et al. Comparison of 2-dimensional echocardiography and myocardial perfusion imaging for diagnosing myocardial infarction in emergency department patients. Am Heart J. 2002;143:659–667.

138. Wackers FJ, Sokole EB, Samson G, et al. Value and limitations of thallium-201 scintigraphy in the acute phase of myocardial infarction. N Engl J Med. 1976;295:1–5.
139. MA, Glick SJ, Pretorius PH, et al. Attenuation, scatter, and spatial resolution compensation in SPECT. In: Wernick MN, Aarsvold JN, eds. Emission Tomography: The Fundamentals of PET and SPECT. London, U.K.: Elsevier Academic Press; 2004:473–494.
140. Kinahan PE, Hasegawa BH, Beyer T. X-ray-based attenuation correction for positron emission tomography/computed tomography scanners. Semin Nucl Med. 2003;23:166–179.
141. Blankespoor SC, Xu X, Kalki CK, et al. Attenuation correction of SPECT using x-ray CT on an emission-transmission CT system: myocardial perfusion assessment. IEEE Trans Nucl Sci. 1996;NS-43:2263–2274.
142. Rispler S, Keidar Z, Ghersin E, Roguin A, Soil A, Dragu R, et al. Integrated single-photon emission computed tomography and computed tomography coronary angiography for the assessment of hemodynamically significant coronary artery lesions. Am J Cardiol. 2007;49(10):1059-1067.
143. Husmann L, Herzog BA, Gaemperli O, Tatsugami F, Burkhard N, Valenta I, et al. Diagnostic accuracy of computed tomography coronary angiography and evaluation of stress-only single-photon emission computed tomography/computed tomography hybrid imaging: comparison of prospective electrocardiogram-triggering vs. retrospective gating. Eur heart J. 2009;30: 600-607.
144. Mahmarian JJ. Hybrid SPECT-CT: integration of CT coronary artery calcium scoring and angiography with myocardial perfusion. Curr Cardiol Rep. 2007;9:129-135.
145. Kaufmann PA. Hybrid SPECT/CT and PET/CT imaging: the next step in noninvasive cardiac imaging. Semin Nucl Med. 2009;39(5):341-347.
146. Kao P-F, Chou Y-H. Clinical Applications and Usefulness of Integrated Single Photon Emission Computed Tomography/Computed Tomography Imaging. Tzu Chi Medical Journal. 2008;20:253-269.
147. Rahmim A, Zaidi H. PET versus SPECT: strengths, limitations and challenges. Nucl Med Commun. 2008;29:193-202.
148. Mariani G, Bruselli L, Kuwert T, Kim EE, Flotats A, Israel O, et al. A review on the clinical uses of SPECT/CT. Eur J N Med Mol Imaging. 2010;37:1959-1985.
149. Machac J, editor. Cardiac positron emission tomography imaging. Semin Nucl Med. 2005: 5:17-36.
150. Gould KL, Schelbert H, Phelps M, et al: Noninvasive assessment of coronary stenoses with myocardial perfusion imaging during pharmacologic coronary vasodilation. Am J Cardiol. 1979; 43:200-208.
151. Schelbert H, Wisenberg G, Phelps M, et al: Noninvasive assessment of coronary stenoses by myocardial imaging during pharmacological coronary vasodilation, VI: Detection of coronary artery disease in man with intravenous 14-NH3 and positron computed tomography. Am J Cardiol. 1982; 49:1197-1207.
152. Tillisch J, Brunken R, Marshall R, et al: Reversibility of cardiac wall motion abnormalities predicted by positron emission tomography. N Engl J Med. 1986;314:884-888.
153. Klein C, Nekolla SG, Bengel FM, Momose M, Sammer A, Haas F, et al. Assessment of myocardial viability with contrast-enhanced magnetic resonance imaging comparison with positron emission tomography. Circulation. 2002;105; 162-167.

154. Phelps ME, Cherry SR: The changing design of positron imaging systems. Clin Positron Imaging. 1998;1:31-45.
155. Chow BJ, Ruddy TD, Dalipaj MM, et al: Feasibility of exercise rubidium-82 positron emission tomography myocardial perfusion imaging. J Am Coll Cardiol. 2003;41:428A-430A.
156. Bacharach SL, Bax JJ, Case J, et al: PET myocardial glucose metabolism and perfusion imaging. Part I-Guidelines for patient preparation and data acquisition. J Nucl Cardiol. 2003;10:543-554.
157. Yoshinaga K, Chow BJ, Williams K, et al. What is the prognostic value of myocardial perfusion imaging using rubidium-82 positron emission tomography? J Am Coll Cardiol. 2006;48:1029 –1039.
158. Metz LD, Beattie M, Hom R, Redberg RF, Grady D, Fleischmann KE. The prognostic value of normal exercise myocardial perfusion imaging and exercise echocardiography: a meta-analysis. J Am Coll Cardiol. 2007;49:227–237.
159. Lerakis S, McLean DS, Anadiotis AV, et al. Prognostic value of adenosine stress cardiovascular magnetic resonance in patients with low-risk chest pain. J Cardiovasc Magn Reson. 2009;11:37-41.
160. Bateman TM, Heller GV, McGhie AI, Friedman JD, Case JA, Bryngelson JR, et al. Diagnostic accuracy of rest/stress ECG-gated Rb-82 myocardial perfusion PET: comparison with ECG-gated Tc-99m sestamibi SPECT. J Nucl Cardiol. 2006;13:24-33.
161. Links JM, DePuey EG, Taillefer R, Becker LC. Attenuation correction and gating synergistically improve the diagnostic accuracy of myocardial perfusion SPECT. J Nucl Cardiol. 2002;9:183-187.
162. Heller GH, Bateman TM, and the Multicenter Investigators. Clinical value of attenuation correction in stress-only Tc-99m sestamibi SPECT imaging. J Nucl Cardiol. 2004;11:273-281.
163. Taillefer R, DePuey EG, Udelson JE, Beller GA, Latour Y, Reeves F. Comparative diagnostic accuracy of Tl-201 and Tc-99m sestamibi SPECT imaging (perfusion and ECG-gated SPECT) in detecting coronary artery disease in women. J Am Coll Cardiol 1997;29:69-77.
164. Hudson HM, Larkin RS. Accelerated image reconstruction using ordered subsets of projection data. IEEE Trans Med Imaging. 1994;13:601-9.
165. Nuyts J, Dupont P, Van den Maegdenbergh V, Vleugels S, Suetens P, Mortelmans L. A study of the liver-heart artifact in emission tomography. J Nucl Med. 1995;36:133-139.
166. Hasegawa, B., Zaidi, H.: Dual-modality imaging: more than the sum of its components. I In: Zaidi, H. (Ed.): Quantitative analysis in nuclear medicine imaging. Springer, New York 2005; 35–81.
167. Hasegawa, B.H., Gingold, E.L., Reilly, S.M., Liew, S.C., Cann, C.E.: Description of a simultaneous emission-transmission CT system. Proc SPIE. 1990; 1231 :50–60.
168. Hasegawa, B.H., Iwata, K., Wong, K.H., et al.: Dual-modality imaging of function and physiology. Acad Radiol. 2002; 9: 1305–1321.
169. Beyer, T., Townsend, D.W., Brun, T., et al.: A combined PET/CT scanner for clinical oncology. J Nucl Med. 2000; 41: 1369–1379.
170. Townsend, D.W.: From 3-D positron emission tomography to 3-D positron emission tomography/computed tomography: what did we learn? Mol Imaging Biol. 2004; 6: 275–290.
171. Wahl, R.L.: Why nearly all PET of abdominal and pelvic cancers will be performed as PET/CT. J Nucl Med. 2004; 45: 82S–95S.

172. Goerres, G.W., von Schulthess, G.K., Steinert, H.C.: Why most PET of lung and head-and-neck cancer will be PET/CT. J Nucl Med. 2004; 45: 66S–71S.
173. Cohade, C., Osman, M.M., Leal, J., Wahl, R.L.: Direct comparison ofF-18-FDG PET and PET/CT in patients with colorectal carcinoma. J Nucl Med. 2003; 44: 1797–1803.
174. Israel, O., Keidar, Z., Iosilevsky, G., et al.: The fusion of anatomic andphysiologic imaging in the management of patients with cancer. Semin Nucl Med. 2001; 31:191–205.
175. Pfannenberg, A.C., Eschmann, S.M., Horger, M., et al.: Benefit of anatomical-functional image fusion in the diagnostic work-up of neuroendocrine neoplasms. Eur J Nucl Med Mol Imaging. 2003; 30:835–843.
176. Zaidi, H., Hasegawa, B.H.: Determination of the attenuation map in emission tomography. J Nucl Med. 2002; 44: 291–315.
177. Sampson UK, Limaye A, Dorbala S, et al. Diagnostic accuracy of rubidium-82 myocardial perfusion imaging with hybrid positron emission tomography/ computed tomography (PET-CT) in the detection of coronary artery disease. J Am Coll Cardiol. 2007;49:1052–1058.
178. Czernin J, Auerbach MA. Clinical PET/CT imaging: promises and misconceptions. Nuklearmedizin. 2005;44:S18–S23.
179. Czernin J, Allen-Auerbach M, Schelbert HR. Improvements in cancer staging with PET/CT: literature-based evidence as of September 2006. J Nucl Med. 2007;48:78S–88S.
180. Israel O, Kuten A. Early detection of cancer recurrence: 18F-FDG PET/CT can make a difference in diagnosis and patient care. J Nucl Med. 2007;48: 28S–35S
181. Sinusas AJ, Shi Q, Saltzberg MT, Vitols P, Jain DJ, Wackers FJ et al. Technetium-99m-tetrofosmin to assess myocardial blood flow: experimental validation in an intact canine model of ischemia. J Nucl Med. 1994;35:664-671.
182. Coleman RE, Delbeke D, Guiberteau MJ, Conti PS, Royal HD, Weinreb JC, et al. Concurrent PET/CT with an integrated imaging system: intersociety dialogue from the joint working group of the American College of Radiology, the Society of Nuclear Medicine, and the Society of Computed Body Tomography and Magnetic Resonance. J Nucl Med. 2005;46:1225–1239.
183. Hicks RJ. A new world order: training clinicians for a new era in imaging. Biomed Imaging Interv J. 2006;2:e49-e57.
184. Higley B, Smith FW, Smith T, Gemmell HG, Das Gupta P, Gvozdanovic DV et al. Technetium-99m-1,2 bis (bis(2-ethoxyethyOphosphino) ethane: human biodistribution, dosimetry and safety of a new myocardial perfusion imaging agent. J Nucl Med. 1993;34:30-38.
185. DePuey EG, Berman DS, Garcia EV. Cardiac SPECT imaging. Philadelphia: Lippincott-Raven; 1996.
186. Okada RD, Glover D, Gaffney T, Williams S. Myocardial kinetics of technetium-99m hexakis-2methoxy-2-methylpropyl-isonitril. Circulation. 1988;77:491-498.
187. Leppo J, Meerdink D. Comparison of the myocardial uptake of a technetium-labeled isonitrile analog and thallium. Circ Res. 1989;65:632-639.
188. Schelbert HR. Evaluation of myocardial blood flow in cardiac disease. In:Skorton DJ, Schelbert HR, Wolf GL, Brundage BH, eds. Cardiac Imaging: A Companion to Braunwald's Heart Disease. Philadelphia, PA: W.B. Saunders;1991:1093–1112.
189. Selwyn AP, Allan RM, L'Abbate A, et al. Relation between regional myocardial uptake of rubidium-82 and perfusion: absolute reduction of cation uptake in ischemia. Am J Cardiol. 1982;50:112–121.

190. Mullani NA, Goldstein RA, Gould KL, Marani SK, Fisher DJ, O'Brien HA Jr, et al. Myocardial perfusion with rubidium-82. I. Measurement of extraction fraction and flow with external detectors. J Nucl Med. 1983;24:898–906.
191. Goldstein RA, Mullani NA, Marani SK, Fisher DJ, Gould KL, O'Brien HA Jr. Myocardial perfusion with rubidium-82. II. Effects of metabolic and pharmacologic interventions. J Nucl Med. 1983;24:907–915.
192. Schelbert HR, Phelps ME, Hoffman EJ, Huang SC, Selin CE, Kuhl DE. Regional myocardial perfusion assessed with N-13 labeled ammonia and positron emission computerized axial tomography. Am J Cardiol. 1979;43:209–218.
193. Schelbert HR, Phelps ME, Huang SC, et al. N-13 ammonia as an indicator of myocardial blood flow. Circulation. 1981;63:1259–1272.
194. Hutchins GD, Schwaiger M, Rosenspire KC, Krivokapich J, Schelbert H, KuhlDE. Noninvasive quantification of regional blood flow in the human heart usingN-13 ammonia and dynamic positron emission tomographic imaging. J Am Coll Cardiol. 1990;15:1032–1042.
195. Tamaki N, Ruddy TD, Dekamp R. Myocardial perfusion. In: Wahl RL, Buchanan JW, eds. Principles and Practice of Positron Emission Tomography. Philadelphia, PA: Lippincott, Williams & Wilkins; 2002:320–333.
196. Hickey KT, Sciacca RR, Bokhari S, et al. Assessment of cardiac wall motion and ejection fraction with gated PET using N-13 ammonia. Clin Nucl Med. 2004; 29:243–248.
197. Schinkel AF, Bax JJ, Valkema R, Elhendy et al. Effect of diabetes mellitus on myocardial 18F-FDG SPECT using acipimox for the assessment of myocardial viability. J Nucl Med. 2003;44(6):877-883.
198. Hoekstra CJ, Stroobants SG, Smit EF, Vansteenkiste J, van Tinteren H, Postmus PE, et al. Prognostic relevance of response evaluation using [F-18]-2-fluoro-2-deoxy-D-glucose positron emission tomography in patients with locally advanced nonsmall-cell lung cancer. J Clin Oncol. 2005;23:8362–8370.

Chapter 2 Diagnostic value of SPECT, PET and PET/CT in the diagnosis of coronary artery disease: A systematic review

2.1 Introduction

Coronary artery disease (CAD) remains the leading cause of mortality and morbidity in Western countries. [1]Invasive coronary angiography is currently the gold standard for diagnosis and treatment of CAD; however, it is an invasive procedure associated with risks and complications. [2]Moreover, it is reported that around 20% to 40% of all diagnostic invasive coronary angiography procedures were performed for diagnostic purposes without any interventional procedures being applied, [3-5] Thus, investigation of less invasive imaging modalities is important for reducing or avoiding the use of invasive coronary angiography examinations. [6]

Currently, multislice computed tomography (CT) angiography is widely used in clinical practice for the diagnosis of CAD, and its diagnostic accuracy has been significantly enhanced with the recent development of64-, 256- and 320-slice scanners.[7-10] Studies have shown that multislice CT angiography can be used as are liable alternative to invasive coronary angiography in selected patients, due to its high sensitivity and specificity. [7-10]

Myocardial perfusion imaging with SPECT is a widely established method for non-invasive evaluation of coronary artery stenosis.[11] However, the most important applications of SPECT are in the diagnosis of CAD, prediction of disease prognosis, selection of patients for revascularisation and assessment of acute coronary syndromes. Moreover, SPECT holds special value in some particular patient subgroups.[11-13] Generally speaking, the sensitivity of stress SPECT for detecting angiographically-defined CAD is consistently above 70%, but in the better-designed studies, it is within the range of 85-90%.[14, 15]

Positron emission tomography (PET) has contributed significantly to advancing our understanding of heart physiology and pathophysiology for more than 25 years. The diagnostic accuracy of myocardial perfusion by PET in the assessment of CAD has been reported to be superior to SPECT.[16-17] PET with rest-stress myocardial perfusion is regarded as an exact imaging modality for diagnosing and managing patients with CAD.[17] Moreover, the combined modality of PET/CT further increases the diagnostic accuracy in CAD.[13-17]

Despite promising results reported in the literature,[18, 19] the diagnostic value of SPECT and PET to detect CAD has not been well established. This is mainly due to the fact that the diagnostic accuracy reported by these studies is variable and the radiopharmaceuticals used in these studies are different. Thus, the purpose of our study was to investigate the diagnostic value of SPECT, PET and PET/CT when compared to invasive coronary angiography for detection of CAD, based on a systematic review of the current literature.

2.2 Materials and methods

A search of the English-language literature was performed using two main databases, PubMed/Medlineand Science Direct. The search included articles published between 1985 and 2009 on the topics of SPECT, PET and PET/CT in CAD. The research was limited to peer-reviewed articles on human subjects and studies published in the English language. The keywords used for the search were "Positron Emission Tomography", "Single Photon Emission Computed Tomography", "integrated Positron Emission Tomography and Computed Tomography", "Coronary Artery Disease", "Myocardial perfusion", "Nuclear Medicine Imaging in cardiac disease".

The reference lists for studies matching these criteria were also reviewed to identify additional articles which were not found through the initial search. The last search was performed in September 2010 to ensure inclusion of all recent publications in the analysis. Articles that met the following criteria were included for analysis: SPECT, PET, or PET/CT studies were performed in patients who underwent myocardial perfusion imaging (MPI) rest/stress test while invasive coronary angiography was used as the standard of reference; at least ten patients were included in each study; diagnosis of CAD was based on >50% stenosis.

The reason >50% stenosis was chosen was because it has become a routine clinical practice to consider coronary stenosis >50% as haemodynamically significant.[20-22]Also, the diagnostic value in terms of sensitivity and specificity was reported in the study. The exclusion criteria included: review articles or case study reports; animal or phantom studies; studies dealing with myocardial perfusion without addressing the diagnostic accuracy of coronary artery stenosis or occlusion, and studies including patients treated with coronary stents or bypass grafts.

Two reviewers checked the references independently and the following information was extracted from each study: year of publication; number of participants in the study; prevalence of patients with suspected or confirmed CAD; mean age; percentage of male patients affected; type of radiotracer used in each study; rest and stress imaging protocols; diagnostic value of SPECT, PET and PET/CT in terms of sensitivity and specificity; and the accuracy of SPECT, PET and PET/CT for detection of CAD.

The main findings were summarised in terms of the extent to which studies were reported to have shown the value of using SPECT, PET and PET-CT to diagnose CAD towards improving patient management and cost-effectiveness. All of the statistical analyses were undertaken using SPSS software version 17.0 (SPSS Inc., Chicago, ILL).Each of the study estimates for sensitivity and specificity were independently combined across studies using one sample test. Comparison was performed by Chi Square test using n-1 degree of freedom to test if there are any significant differences between different imaging modalities (SPECT vs PET, SEPCT vs PET/CT, PET vs PET/CT). Statistical hypotheses (2-tailed) were tested at the 5% level of significance.

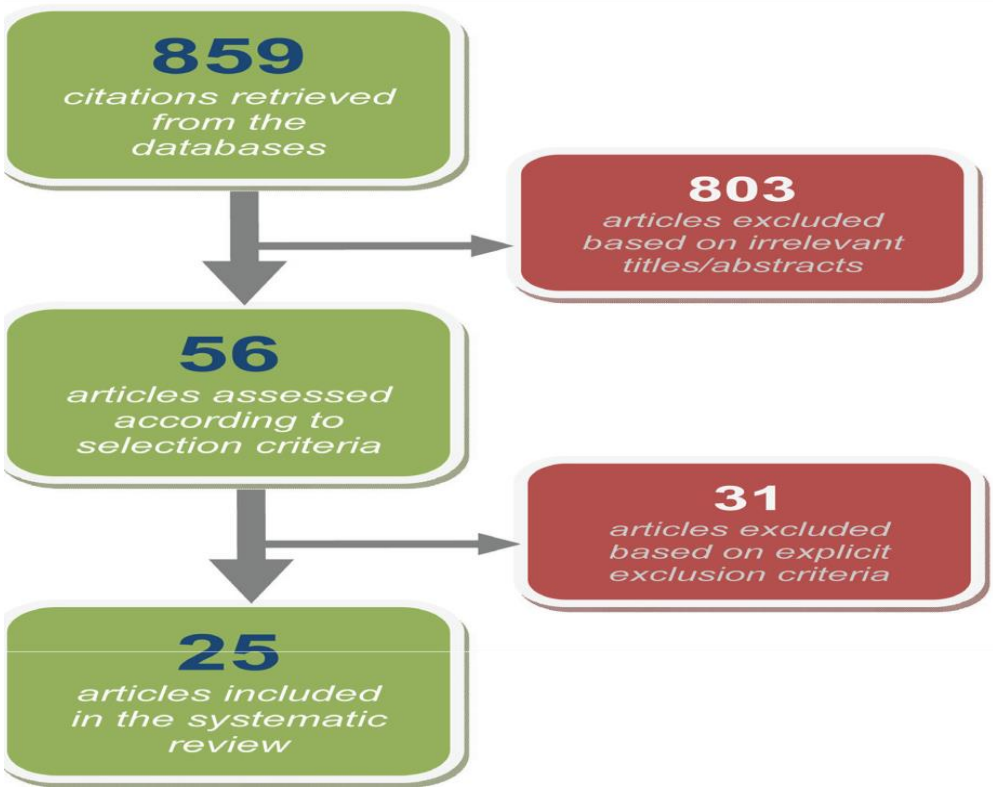

Figure 2.1 Flow chart shows the searching strategy of eligible References.

2.3 Results

Twenty-five studies (with 25 comparisons) met the selection criteria and were included in the analysis.[20- 44]Ten of these studies were performed with SPECT alone,[20-25, 40-42, 44]while six of the studies were performed with PET alone.[31-36]Five studies were carried out with both PET and SPECT modalities [26-30]and the remaining four studies were investigated within teg rated PET/CT.[37-39, 43]

The total number of patients included in these studies was 4,114 with 53.5%of the patients suspected of CAD, 72.2 % being male and the mean age of patients being 48-years-old. Table 2.1 summarises the number of patients, the radiotracers used in each study, and the reported sensitivity, specificity and accuracy with use of SPECT, PET and PET/CT imaging modalities, respectively.

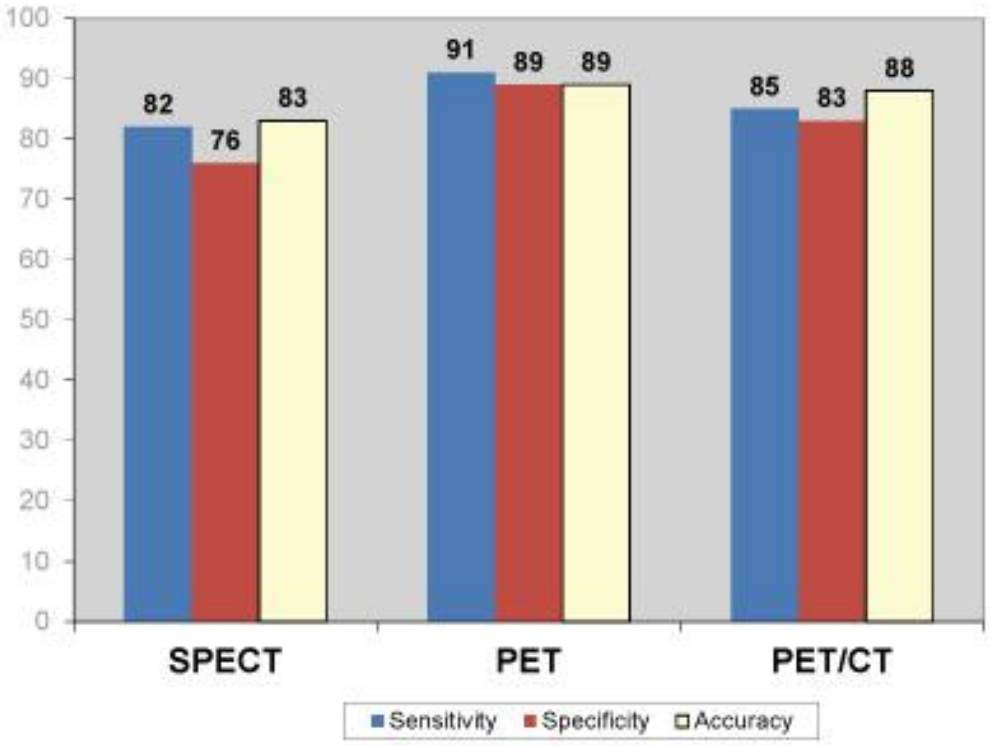

Figure 2.2 Overall pooled mean diagnostic values of SPECT, PET and PET/CT for detection of coronary artery disease.

The degree of coronary artery stenosis was assessed based on the criterion of >50%, which was determined by invasive coronary angiography in all studies.

Of these 20 studies, ^{82}Rubidium was the most commonly-used radiopharmaceutical which was utilised in 10 studies;[27–29, 31-34, 37-39] ^{99}mTc-Sestamibi was used in seven studies;[20-22, 24, 25, 27, 42] ^{201}Thallium was used in four studies;[26, 27, 29, 30] a combination of ^{201}Thallium and ^{99}mTc-Sestamibi was used in one study;[23] ^{99}mTc-Tetrofosmin was used in three studies;[40, 41, 44] and combinations of ^{13}N Ammonia and ^{82}Rubidium were used in the remaining two studies.[35,36]

Analysis of diagnostic value of SPECT in CAD

A total of 2,208 patients were included in 15 SPECT studies based on significant CAD which was determined by visual assessment of coronary angiography. Figure 2.2 shows the mean sensitivity, specificity and accuracy of SPECT for diagnosis of CAD. As shown in the figure, the diagnostic value of SPECT was moderate when compared to invasive coronary angiography.

Analysis of diagnostic value of PET in CAD

A total 1,376 patients were included in another 11 studies performed with PET tests based on significant CAD which was determined by visual assessment of coronary angiography. Figure 2.3 shows the mean sensitivity, specificity and accuracy of PET for diagnosis of CAD. As shown in the figure, PET imaging was found to have high diagnostic value in the detection of CAD.

Analysis of diagnostic value of PET/CT in CAD

A total 518 patients were included in four studies performed with PET/CT studies based on significant CAD which was determined by visual assessment of coronary angiography. Again Figure 2.4 demonstrates that moderate sensitivity, specificity and accuracy of PET/CT were reached for diagnosis of CAD.

Table 2.1 Study characteristics of SPECT, PET and PET/CT for detection of coronary artery disease.

Authors	Year	Patients (n)	Male (%)	Mean age (yr)	Stenosis	Radiotracer	Stress type	Sensitivity (%)	Specificity (%)	Accuracy (%)
Husmann et al[26]	2008	80 70	85 80	56 54.5	>50%	^{201}Thallium ^{13}N ammonia	Dipyridamole	77% 97%	84% 84%	NA
Fallahi et al[20]	2008	51	85	34	>50%	^{99m}Tc-sestamibi	18 patients exercise and 33 patients dipyridamole	91%	71%	88%
Di Carli et al[37]	2007	110	54.5	57.3	>50%	^{82}Rubidium	Adenosine	65%	75%	NA
Cesar et al[38]	2007	281	51.6	38.3	>50%	^{82}Rubidium	Adenosine	93%	75%	91%
Sampson et al[39]	2007	102	59	37	>50%	^{82}Rubidium	Dipyridamole or dobutamine	93%	83%	85%
Schepis T et al[44]	2007	77	62	55	>50%	^{99m}Tc-tetrofosmin	Bicycle ergometry	76%	91%	NA
Bateman et al[27]	2006	112 112	52 52	65 66.7	>50%	^{99m}Tc-sestamibi ^{82}Rubidium	Dipyridamole	82% 87%	73% 93%	79% 89%
Namdar el at[43]	2005	25	92	62	>50%	^{13}N ammonia	Adenosine	90%	98%	NA
Giorgetti et al[40]	2004	23	80	40	>50%	^{99m}Tc-tetrofosmin	Nitrates (Intravenous isosorbide dinitrate, 0.2 mg/ml, 10mL/h)	61%	88%	72%
Elhendy et al[21]	2001	332	77	57	>50%	^{99m}Tc-sestamibi	Upright bicycle ergometry	77%	74%	77%
Leoncini et al[22]	2001	33	93	37	>50%	^{99m}Tc-sestamibi	Dobutamine	85%	55%	NA
Elhendy et al[41]	2000	124	69.5	35	>50%	^{99m}Tc-tetrofosmin	Dobutamine	80%	72%	77%
Nakamura et al[23]	1999	81	80	37	>50%	^{201}Thallium & ^{99m}Tc-sestamibi	Exercise	83%	99%	95%
Levine et al[24]	1999	50	76	36	>50%	^{99m}Tc-sestamibi	No stress	86%	55%	85%
Milavetz et al[25]	1998	209	77	36.5	>50%	^{99m} Tc-sestamibi	16 patients Dipyridamole, 2 patients dobutamine and 191 patients exercise	95%	73%	88%
Santana-Boado et al[42]	1998	702	56	34	>50%	^{99m}Tc-sestamibi	Bicycle ergometry	89%	90%	91%
Williams et al[31]	1994	287	75	NA	>50%	^{82}Rubidium	Dipyridamole	87%	88%	88%
Simone et al[32]	1992	225	80	NA	>50%	^{82}Rubidium	Dipyridamole	92%	91%	91%
Marwick et al[33]	1992	74	NA	34	>50%	^{82}Rubidium	Treadmill exercise	90%	100%	91%
Grover-McKay et al[34]	1992	31	84	34.5	>50%	^{82}Rubidium	Dipyridamole	100%	73%	87%
Fallahi et al[20]	2008	51	85	34	>50%	^{99m}Tc-sestamibi	18 patients exercise and 33 patients dipyridamole	91%	71%	88%
Di Carli et al[37]	2007	110	54.5	57.3	>50%	^{82}Rubidium	Adenosine	65%	75%	NA
Cesar et al[38]	2007	281	51.6	38.3	>50%	^{82}Rubidium	Adenosine	93%	75%	91%

*NA-not available.

Table 2.2 Mean diagnostic value of SPECT, PET and PET/CT for detection of coronary artery disease by individual coronary branches.

Authors	Radiotracer			Sensitivity (%)			Sensitivity (%)			Specificity (%)		
	SPECT	PET	PET/CT	SPECT	PET	PET/CT	SPECT	PET	PET/CT	SPECT	PET	PET/CT
Bateman et al[11]												
>50% stenosis	^{99m}Tc-	^{99m}Tc-		61	79		92	95		75	87	
LAD	sestamibi/	sestamibi /		33	58		86	93		68	79	
LCx	^{82}Rubidium	^{82}Rubidium		60	58		87	100		73	78	
RCA												
Tamaki et al[28]												
>50% stenosis	^{201}Thallium /	^{201}Thallium /		90	93		89	100				
LAD	^{13}N ammonia	^{13}N ammonia		65	85		93	90		NA	NA	
LCx				79	76		95	86				
RCA												
Cesar et al[36]												
>50% stenosis						70			69			70
LAD			^{82}Rubidium			76			86			83
LCx						66			92			77
RCA												
Husmann et al[26]												
>50% stenosis	^{99m}Tc-			64	95		76	86				
LAD	sestamibi	^{13}N ammonia		80	100		93	80		NA	NA	
LCx				87	100		86	87				
RCA												
Overall												
>50% stenosis				72	89	70	86	94	69	75	87	70
LAD				59.	81	76	91	88	86	68	79	83
LCx				75	78	66	89	91	92	73	78	77
RCA												

*NA-not available, LAD-left anterior descending, LCx-left circumflex, RCA-right coronary artery.

Table 2.3 Mean diagnostic value of nuclear medicine imaging with use of different radiotracers.

Radiotracer	Patients (n)	Male (%)	Mean age (yr)	Stenosis	Sensitivity (%)	Specificity (%)	Accuracy (%)
^{201}Thallium	414	74.6	42.3	>50%	80 (95% CI: 74 to 86)	77 (95% CI: 71 to 83)	78 (95% CI: 72 to 84)
^{99m}Tc-sestamibi	760	76.6	45.7	>50%	86 (95% CI: 80 to 92)	66 (95% CI: 60 to 72)	83 (95% CI: 77 to 89)
^{99m}Tc-tetrofosmin	224	75	37.5	>50%	74 (95% CI: 64 to 76)	86 (95% CI: 74 to 86)	75 (95% CI: 68 to 80)
^{201}Thallium & ^{99m}Tc-sestamibi	81	80	37	>50%	83 (95% CI: 77 to 89)	99 (95% CI: 93 to 100)	95 (95% CI: 90 to 100)
^{13}N ammonia	121	71	42.5	>50%	92 (95% CI: 86 to 98)	86 (95% CI: 80 to 92)	90 (95% CI: 84 to 96)
^{82}Rubidium	985	71	42.5	>50%	90 (95% CI: 84 to 96)	88 (95% CI: 82 to 94)	92 (95% CI: 86 to 98)
^{82}Rubidium and ^{13}N ammonia	243	74	NA	>50%	89 (95% CI: 83 to 95)	97 (95% CI: 91 to 100)	91 (95% CI: 75 to 87)

*NA-not available.

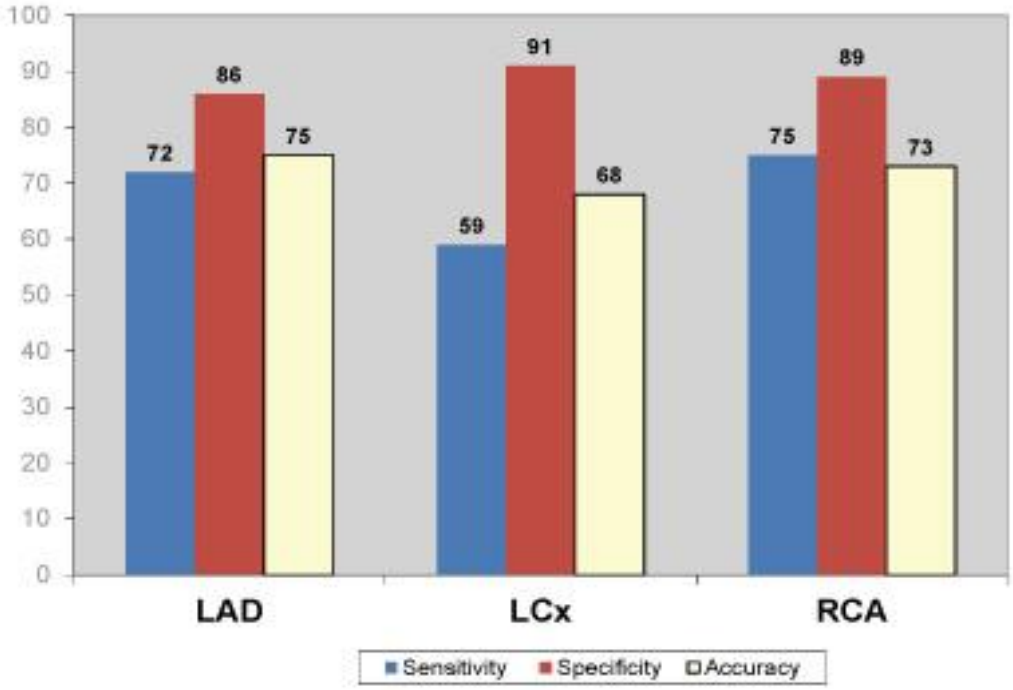

Figure 2.3 Pooled diagnostic value of SPECT for detection of coronary artery disease based on individual coronary artery assessment.

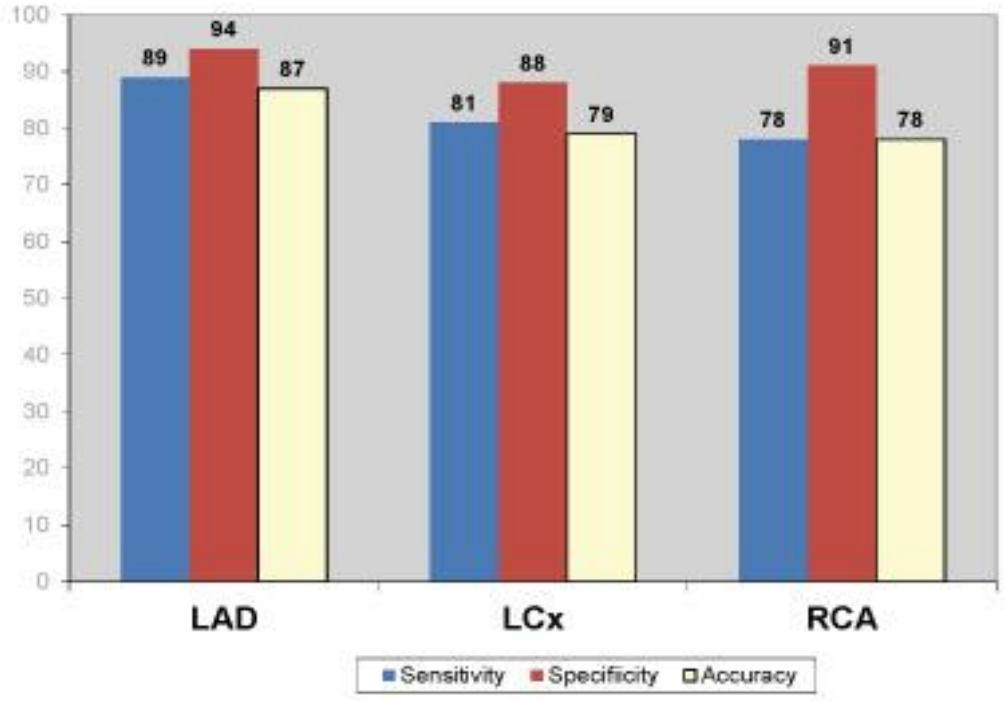

Figure 2.4 Pooled diagnostic value of PET for detection of coronary artery disease based on individual coronary artery assessment.

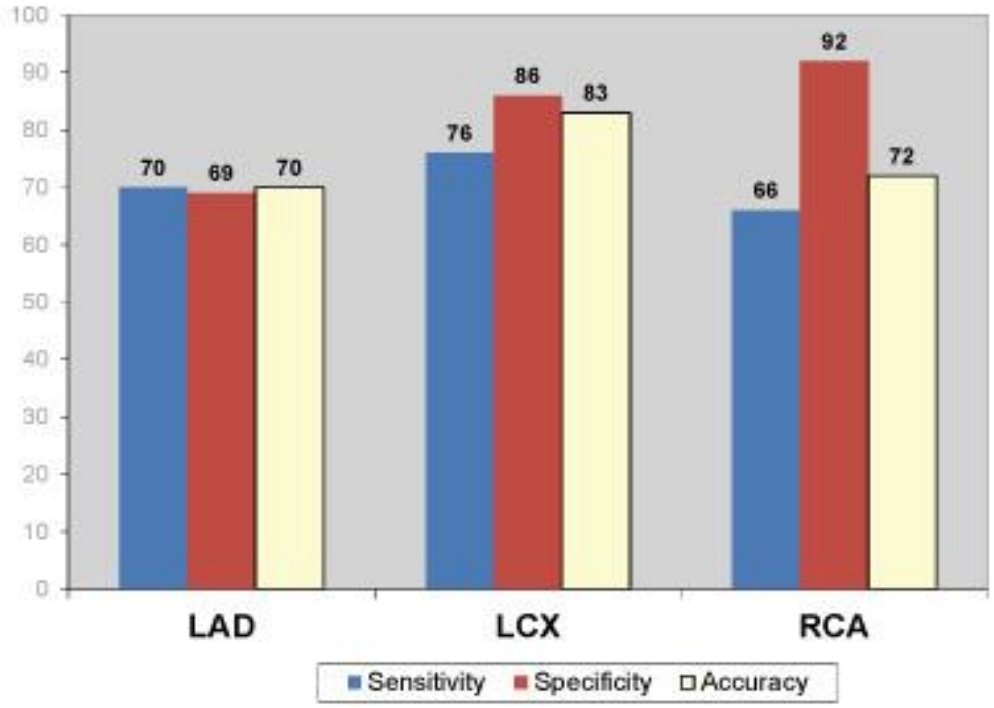

Figure 2.5 Pooled diagnostic value of PET/CT for detection of coronary artery disease based on individual coronary artery assessment.

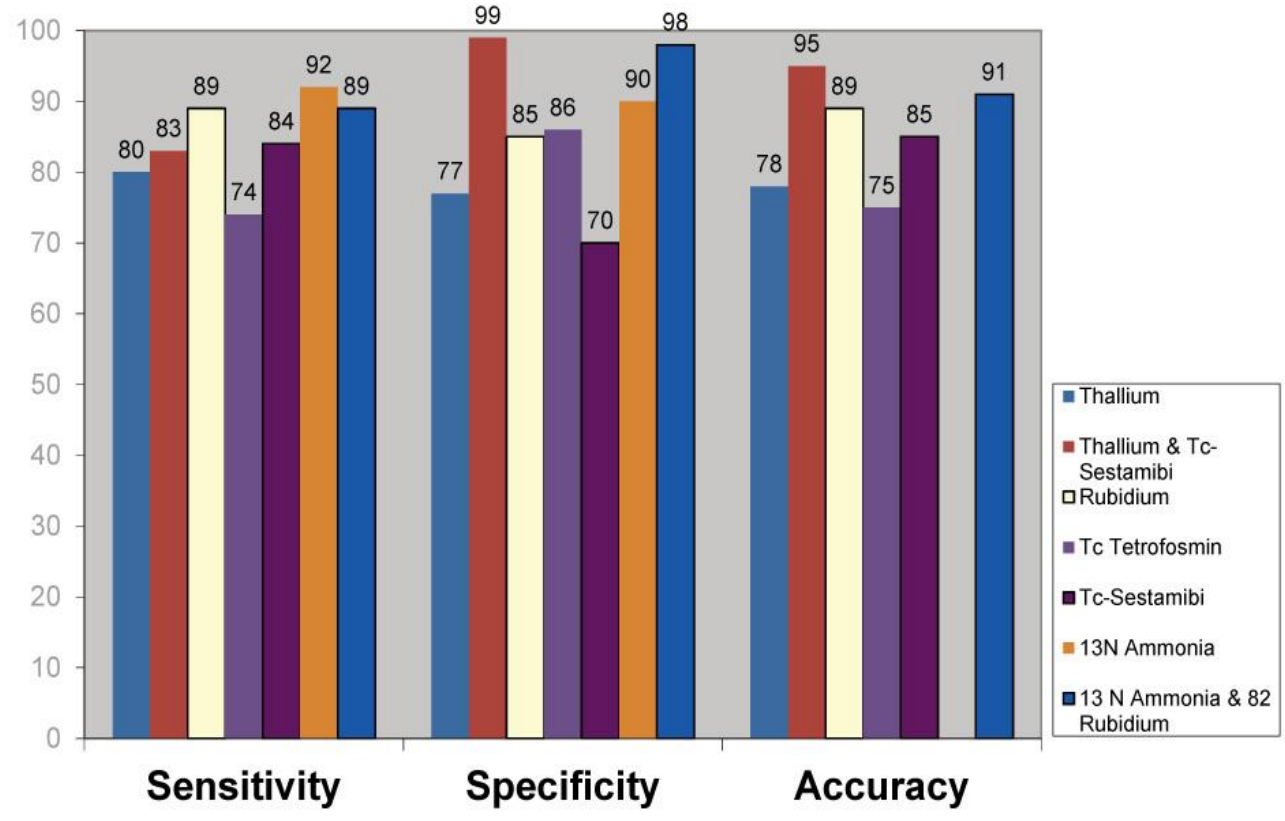

Figure 2.6 Pooled diagnostic value of nuclear medicine imaging with use of variable radiotracers for detection of coronary artery disease.

Comparison of SPECT, PET and PET/CT

There is a significant difference in sensitivity, specificity and accuracy between PET and SPECT, PET and PET/CT, SPECT and PET/CT for the diagnosis of CAD ($p<0.05$), with PET demonstrating the highest diagnostic value among these three imaging modalities as shown in Figure 2.2.

Analysis of diagnostic value for assessment of individual coronary artery disease

Table 2.2 demonstrates the diagnostic value of SPECT, PET and PET/CT in three studies with five comparisons based on analysis of three main coronary arteries. Figures 2.3 to 2.5 demonstrate the overall results of sensitivity, specificity and accuracy analysed with three different nuclear medicine modalities at left anterior descending (LAD), left circumflex (LCx) and right coronary artery (RCA). As shown in the figures, PET has the highest diagnostic value among the 3 imaging modalities for diagnosis of CAD.

Analysis of effects of different Radiotracers on diagnostic value

Since different types of radiotracers were used in these 20 studies, analyses of the diagnostic value of variable radiotracers for detection of CAD were investigated. Table 2.3 shows the radiotracers used in these studies and their corresponding diagnostic value. As demonstrated in the table, using ammonia as a radiotracer produced the highest diagnostic value for detection of CAD. Figure 2.6 shows the differences in sensitivity and specificity between both ^{201}Thallium and 99mTcsestamibi for the diagnosis of CAD ($p<0.05$), and also significant differences in the specificity and accuracy between both ^{201}Thallium and ^{99}mTc-sestamibi and individual radiotracers for the diagnosis of CAD ($p<0.05$).

Significant differences in sensitivity and accuracy was found between ^{13}N ammonia, 82Rubidium and both ^{13}N ammonia with 82Rubidium for the diagnosis of CAD ($p<0.05$) as shown in Figure 2.6 Significant differences were found in the sensitivity and specificity between use of combined radiotracers (13N ammonia and ^{82}Rubidium, ^{201}Thallium and ^{99}mTc-sestamibi) and use of individual radiotracers alone for the diagnosis of CAD ($p<0.05$).

2.4 Discussion

This systematic review presents three significant findings which are considered to be important from a clinical perspective. First, the diagnostic value of SPECT and PET/CT in the detection of CAD is moderate when compared to invasive coronary angiography. Second, PET has higher sensitivity and specificity than SPECT or PET/CT for detection of CAD, indicating the increasing diagnostic accuracy of PET in cardiac imaging. Lastly, there are significant differences when different radiotracers are used for the diagnosis of CAD, with the use of combined radiotracers resulting in improved diagnostic value.

SPECT has been used as a routine technique in clinical practice for myocardial perfusion imaging for decades.[29] Previous studies have shown that the diagnostic value of SPECT in cardiac imaging is variable, ranging from low to moderate.[30] Di Carli et al.[45] compared three studies using SPECT with PET, looking particularly at the diagnostic accuracy for detection of CAD. Only the sensitivity and specificity were provided in their study while the analysis of diagnostic accuracy was not identified. This analysis confirms their results to a greater extent, as the mean sensitivity, specificity and accuracy of SPECT for detection of CAD are moderate.

This indicates that SPECT has not reached the diagnostic accuracy to be considered as a reliable technique for assessment of CAD. PET has been used more recently in cardiac imaging, and early results look promising.[46] PET offers potential advantages in a clinical practice over myocardial perfusion scintigraphy.[47] PET is able to assess myocardial blood flow and is superior in detecting multivessel disease.[48] Our analysis identifies PET as having the highest diagnostic value for CAD among the three different nuclear imaging modalities analysed.

Husmann et al.[26] compared SPECT and PET in respect to diagnostic accuracy of myocardial perfusion imaging. Only the sensitivity and specificity were reported in their study, while the diagnostic accuracy was not available. In contrast, the sensitivity, specificity and accuracy of PET for detection of CAD were analysed in our report. This review provides a comprehensive analysis of the diagnostic value of these nuclear modalities, including sensitivity, specificity and accuracy.

Thus, it is believed that the analysis offers additional and valuable diagnostic information, as compared to the previous reports in the literature. Recently, cardiac imaging has been further enhanced by the use of integrated PET/CT, a combined modality which provides the considerable benefit of anatomical and physiologic assessment in patients with CAD.[37, 38] PET/CT allows precise detection and localisation of CAD.[39] CT coronary angiography provides superior anatomical details but lacks the functional information of cardiac perfusion.

The latest refinements in CT technology, including multidetector CT with faster gantry rotations, and dual-source devices, have advanced CT angiography as a promising alternative to conventional angiography in the diagnosis of CAD selected patients.[49] Recent studies have shown that 64-slice CTA has high sensitivity (73%- 100%) and specificity (90%-90%) in the detection of CAD. [50-52] PET offers evidence of sub-clinical coronary atherosclerosis as it is superior in demonstrating metabolic activities, but its spatial resolution is limited when demonstrating coronary anatomical structures.[48]

Thus, combined PET/CT overcomes the limitations of each individual modality while maximising the advantages of both PET and CT in cardiac imaging.[45-47] However, the analysis of integrated PET/CT for detection of CAD was not as good as initially expected since PET/CT was shown to have moderate sensitivity, specificity and accuracy. This may be due to the selection of patients with different risk factors in the studies analysed. Therefore, results of this analysis should be interpreted with caution. PET/CT may show improved diagnostic accuracy in other areas, such as tumour imaging, but not in the diagnosis of CAD, based on this analysis.

This analysis also involves a comparison of radiotracers used in SPECT and PET imaging which includes seven different types of radioisotopes, namely ^{201}Thallium, ^{99m}Tc-tetrofosmin, ^{99m}Tc-Sestamibi, a combination of ^{201}Thallium and ^{99m}Tc-Sestamibi, ^{13}N Ammonia, ^{82}Rubidium, and a combination of ^{13}N Ammonia and ^{82}Rubidium. The comparative analysis indicates significant benefits of using ^{13}N ammonia for MPI to detect CAD by PET, leading to the highest sensitivity and accuracy. Both ^{13}N ammonia and ^{82}Rubidium have significantly high specificity in MPI by PET.

PET imaging with use of 13N ammonia, ^{82}Rubidium, and a combination of 13N ammonia and ^{82}Rubidium for diagnosis of CAD, has been found to result in significant differences in sensitivity, specificity and accuracy than those using ^{201}Thallium, ^{99m}Tc-sestamibi, and a combination of ^{201}Thallium and ^{99m}Tc-sestamibi by SPECT imaging.

This is consistent with results reported by other studies. Go and colleagues [29] compared PET and SPECT in 202 patients. Their results showed there was no significant difference between PET imaging with use of ^{82}Rubidium and SPECT imaging with ^{201}Thallium. Tamaki and colleagues [30] compared ^{13}N ammonia PET with ^{201}Thallium SPECT and reported similar findings. Hence, this analysis confirms that 13N ammonia PET and ^{201}Thallium SPECT provide high diagnostic value for detection of CAD.

In addition, the analysis of individual coronary arteries demonstrates the superiority of PET over the other two modalities, but a significant difference in diagnostic value was only found between PET and SPECT, PET/CT in LAD. PET/CT was found to be significantly higher than PET in the assessment of RCA in terms of diagnostic accuracy. However, only a few studies presented the analysis of individual coronary arteries, thus a robust conclusion cannot be drawn based on the current analyses.

2.5 Conclusion

This analysis shows that PET has higher sensitivity, specificity and accuracy for detection of CAD than SPECT and PET/CT. PET can be used as a reliable, less invasive modality for functional analysis of patients suspected of CAD. Further studies comprising a large sample size are needed to verify these results.

2.6 References

1. Thom T. Heart disease and stroke statistics-2006 update a report from the American Heart Association Statistics Committee and Stroke Statistics Subcommittee. Circulation 2006;113(6):e85.
2. Cuocolo A, Acampa W, Imbriaco M, De Luca N, Iovino GO,Salvatore M. The many ways to myocardial perfusion imaging. Q J Nucl Med Mol Imaging 2005;49(1):4-18.
3. American Heart Association, American Stroke Association. 2002 Heart and stroke statistics update. Dallas, TX: The American Heart Association, 2002.
4. Noto Jr TJ, Johnson LW, Krone R, et al. Cardiac catheterization 1990: a report of the registry of the Society for Cardiac Angiography and Interventions, (SCA&I). Cathet Cardiovasc Diagn 1991; 24: 75-83.
5. Achenbach S, Daniel WG. Noninvasive Coronary Angiography-An Acceptable Alternative? N Engl J Med 2001;345(26):1909-1910.
6. Noto TJ Jr, Johnson LW, Krone R, Weaver WF, Clark DA, Kramer JR Jr, et al. Cardiac catheterization 1990: a report of the registry of the Society for Cardiac Angiography and Interventions. (SCA&I). Cathet Cardiovasc Diagn 1991; 24: 75-83.
7. Kido T, Kurata A, Higashino H, et al. Cardiac imaging using 256-detecror row four-dimensional CT: preliminary clinical report. Radiat Med 2007; 25: 38-44.
8. Rybicki F, Otero H, Steigner M, et al. Initial evaluation of coronary images from 320-detector row computed tomography. Int J Cardiovasc Imaging 2008; 24: 535-546.
9. Sun Z, Jiang W. Diagnostic value of multislice computed tomography angiography in coronary artery disease: A metaanalysis. Eur J Radiol 2006;60(2):79-86.
10. Marwick TH, Shan K, Patel S, Go RT, Lauer MS. Incremental Value of Rubidium-82 Positron Emission Tomography for Prognostic Assessment of Known or Suspected Coronary Artery Disease. Am J Cardiol 1997;80(7):65-70.
11. Hachamovitch R. Comparison of the short-term survival benefit associated with revascularization compared with medical therapy in patients with no prior coronary artery disease undergoing stress myocardial perfusion single photon emission computed tomography. Circulation 2003;107(23):2900-2906.
12. Hachamovitch R, Berman DS, Shaw LJ, et al. Incremental Prognostic Value of Myocardial Perfusion Single Photon Emission Computed Tomography for the Prediction of Cardiac Death: Differential Stratification for Risk of Cardiac Death and Myocardial Infarction. Circulation 1998; 97(6):535-543.
13. Van der Vaart MG, Meerwaldt R, Slart RHJA, van Dam GM, Tio RA, Zeebregts CJ. Application of PET/SPECT imaging in vascular disease. Eur J Vasc Endovasc Surg 2008;35(5):507-513.
14. Di Carli MF, Hachamovitch R. Should PET replace SPECT for evaluating CAD? The end of the beginning. J Nucl Cardiol 2006; 13: 2-7.
15. Iomka PJ, Le Meunier L, Hayes SW, et al. Comparison of Myocardial Perfusion 82Rb PET Performed with CT- and Transmission CT-Based Attenuation Correction. J Nucl Med 2008 12/1;49(12):1992-1998.
16. Santana CA, Folks RD, Garcia EV, et al. Quantitative 82Rb PET/CT: Development and Validation of Myocardial Perfusion Database. J Nucl Med 2007;48: 1122-1128.
17. Donati OF, Stolzmann P, Desbiolles L, et al. Coronary artery disease: Which degree of coronary artery stenosis is indicative of ischemia? Eur J Radiol 2011; 80: 120-126.
18. Oncel D. Detection of significant coronary artery stenosis with 64- section MDCT angiography. Eur J Radiol 2007;62: 394-405.

19. D'Othee BJ, Siebert U, Cury R, Jadvar H, Dunn EJ, Hoffmann U. A systematic review on diagnostic accuracy of CT-based detection of significant coronary artery disease. Eur J Radiol 2008;65: 449- 461.
20. Fallahi B, Beiki D, Gholamrezanezhad A, et al. Single Tc99m Sestamibi injection, double acquisition gated SPECT after stress and during low-dose dobutamine infusion: a new suggested protocol for evaluation of myocardial perfusion. Int J Cardiovasc Imaging 2008;24: 825-835.
21. Elhendy A, van Domburg RT, Sozzi FB, Poldermans D, Bax JJ, Roelandt JR. Impact of hypertension on the accuracy of exercise stress myocardial perfusion imaging for the diagnosis of coronary artery disease. Heart 2001;85(6):655-661.
22. Leoncini M, Marcucci G, Sciagrà R, et al. Prediction of functional recovery in patients with chronic coronary artery disease and left ventricular dysfunction combining the evaluation of myocardial perfusion and of contractile reserve using nitrate-enhanced technetium-99m sestamibi gated single-photon emission computed tomography and Dobutamine stress. Am J Cardiol 2001;87:1346- 1350.
23. Nakamura M, Takeda K, Ichihara T, et al. Feasibility of simultaneous stress 99mTc-sestamibi/rest 201Tl dual-isotope myocardial perfusion SPECT in the detection of coronary artery disease. J Nucl Med 1999;40: 895-903.
24. Levine MG, McGill CC, Ahlberg AW, et al. Functional assessment with electrocardiographic gated single-photon emission computed tomography improves the ability of technetium-99m sestamibi myocardial perfusion imaging to predict myocardial viability in patients undergoing revascularization. Am J Cardiol 1999;83:1-5.
25. Milavetz JJ, Miller TD, Hodge DO, Holmes DR, Gibbons RJ. Accuracy of single-photon emission computed tomography myocardial perfusion imaging in patients with stents in native coronary arteries. Am J Cardiol 1998;82:857-861.
26. Husmann L, Wiegand M, Valenta I, et al. Diagnostic accuracy of myocardial perfusion imaging with single photon emission computed tomography and positron emission tomography: a comparison with coronary angiography. Int J Cardiovasc Imaging 2008; 24: 511-518.
27. Bateman TM, Heller GV, McGhie AI, et al. Diagnostic accuracy of rest/stress ECG-gated Rb-82 myocardial perfusion PET: Comparison with ECG-gated Tc-99m sestamibi SPECT. J Nucl Cardiol 2006;13:24-33.
28. Stewart RE, Schwaiger M, Molina E, et al. Comparison of rubidium-82 positron emission tomography and thallium-201 SPECT imaging for detection of coronary artery disease. Am J Cardiol 1991;67:1303-1310.
29. Go RT, Marwick TH, MacIntyre WJ, et al. A prospective comparison of rubidium-82 PET and thallium-201 SPECT myocardial perfusion imaging utilizing a single dipyridamole stress in the diagnosis of coronary artery disease. J Nucl Med 1990;31:1899-1905.
30. Tamaki N, Yonekura Y, Senda M, et al. Value and limitation of stress thallium-201 single photon emission computed tomography: comparison with nitrogen-13 ammonia positron tomography. J Nucl Med 1988;29:1181-1188.
31. Williams BR, Mullani NA, Jansen DE, Anderson BA. A retrospective study of the diagnostic accuracy of a community hospital-based PET center for the detection of coronary artery disease using rubidium-82. J Nucl Med 1994;35:1586-1592.
32. Simone GL, Mullani NA, Page DA, Anderson BA. Utilization statistics and diagnostic accuracy of a nonhospital-based positron emission tomography center for the detection of coronary artery disease using rubidium-82. Am J Physiol Imaging 1992;7:203-209.

33. Marwick TH, Nemec JJ, Stewart WJ, Salcedo EE. Diagnosis of coronary artery disease using exercise echocardiography and positron emission tomography: comparison and analysis of discrepant results. J Am Soc Echocardiog 1992;5:231 238.
34. Grover-McKay M, Ratib O, Schwaiger M, et al. Detection of coronary artery disease with positron emission tomography and rubidium 82. Am Heart J 1992;123:646-652.
35. Demer LL, Gould KL, Goldstein RA, et al. Assessment of coronary artery disease severity by positron emission tomography. Comparison with quantitative arteriography in 193 patients. Circulation 1989;79:825-835.
36. Gould KL, Goldstein RA, Mullani NA, et al. Noninvasive assessment of coronary stenoses by myocardial perfusion imaging during pharmacologic coronary vasodilation. VIII. Clinical feasibility of positron cardiac imaging without a cyclotron using generator-produced rubidium-82. J Am Coll Cardiol 1986;7:775- 789.
37. Di Carli MF, Dorbala S, Curillova Z, et al. Relationship between CT coronary angiography and stress perfusion imaging in patients with suspected ischemic heart disease assessed by integrated PETCT imaging. J Nucl Cardiol 2007;14:799-809.
38. Santana CA, Folks RD, Garcia EV, et al. Quantitative 82Rb PET/CT: Development and validation of myocardial perfusion database. J Nucl Med 2007;48:1122-1128.
39. Sampson UK, Dorbala S, Limaye A, Kwong R, Di Carli MF. Diagnostic Accuracy of Rubidium-82 Myocardial Perfusion Imaging with Hybrid Positron Emission Tomography/Computed Tomography in the Detection of Coronary Artery Disease. J Am Coll Cardiol 2007; 49:1052-1058.
40. Giorgetti A. Baseline/post-nitrate Tc-99m tetrofosmin mismatch for the assessment of myocardial viability in patients with severe left ventricular dysfunction: comparison with baseline Tc-99m tetrofosmin scintigraphy/FDG PET imaging. J Nucl Cardiol 2004;11(2):142-151.
41. Elhendy A. Dobutamine technetium-99m tetrofosmin SPECT imaging for the diagnosis of coronary artery disease in patients with limited exercise capacity. J Nucl Cardiol 2000;7(6):649-656.
42. Santana-Boado C. Diagnostic accuracy of technetium-99m-MIBI myocardial SPECT in women and men. J Nucl Med 1998;39(5):751-755.
43. Namdar M. Integrated PET/CT for the assessment of coronary artery disease: a feasibility study. J Nucl Med 2005;46(6):930-935.
44. Schepis T. Added value of coronary artery calcium score as an adjunct to gated SPECT for the evaluation of coronary artery disease in an intermediate-risk population. J Nucl Med 2007;48(9):1424-1430.
45. Di Carli MF, Dorbala S. Integrated PET/CT for cardiac imaging. Q J Nucl Med Mol Imaging 2006;50(1):139-144.
46. Fricke H, Elsner A, Weise R, et al. Quantitative myocardial perfusion PET combined with coronary anatomy derived from CT angiography: Validation of a new fusion and visualisation software. Med Phys 2009;19(3):182-188.
47. Di Carli MF, Dorbala S, Meserve J, et al. Clinical myocardial perfusion PET/CT. J Nucl Med 2007;48(5):783- 793.
48. Machac J, Machac. Cardiac positron emission tomographyimaging. Seminars in Nucl Med 2005;35(1):17-36.
49. Gaemperli O. Functionally Relevant Coronary Artery Disease: Comparison of 64-Section CT Angiography with Myocardial Perfusion SPECT1. Radiology 2008;248(2):414-423.
50. Raff GL. Diagnostic accuracy of non-invasive coronary angiography using 64-slice spiral computed tomography. J Am Coll Cardiol 2005;46(3):552-557.

51. Pugliese F. Diagnostic accuracy of non-invasive 64-slice CT coronary angiography in patients with stable angina pectoris. Eur Radiol 2006;16(3):575-582.
52. Scheffel H. Accuracy of dual-source CT coronary angiography: first experience in a high pre-test probability population without heart rate control. Eur Radiol 2006;16(12):2739-2747.
53. Fisher LD. Reproducibility of coronary arteriographic reading in the coronary artery surgery study (CASS). Cathet Cardiovasc Diagn 1982;8(6):565-575.

Chapter 3 A head to head comparison of the coronary calcium score by computed tomography with myocardial perfusion imaging in predicting coronary artery disease

3.1 Introduction

Multi-slice computed tomography (CT) has been increasingly used to detect coronary artery calcium and diagnose coronary artery stenosis. Quantifying the amount of coronary artery calcium (CAC) with non-enhanced CT scans has been widely accepted as a reliable non-invasive technique for screening patients with a potential risk of developing major cardiac events, and is usually quantified using the Agatston score.[1-4] The clinical application of CAC scoring has been supported by evidence showing that the absence of calcium reliably excludes obstructive coronary artery stenosis,[5] and that the amount of CAC is a strong predictor for risk assessment of myocardial infarction and sudden cardiac death, independent of conventional coronary risk factors.[6,7]

However, its predictive value is, in the end, determined by the patients' symptoms. In symptomatic patients, CAC scoring is considered as being only marginally related to the degree of coronary stenosis, and it is well known that both obstructive and non-obstructive coronary artery disease (CAD) can occur in the absence of calcification.[8,9] According to these reports, low CAC scores are less valuable in the prediction of the prevalence, or severity, of coronary artery disease caused by the non-calcified coronary plaques.

Myocardial perfusion imaging (MPI) with gated single photon emission computed tomography (SPECT) has been widely used in the diagnosis of CAD and risk stratification with high diagnostic accuracy[10,11] when compared to CT angiography. The presence of ischemia could be used to classify the patients as having CAD and candidates for receiving aggressive medical therapy and management. However, a normal MPI does not necessarily exclude significant coronary stenosis, while high CAC scores sometimes do not result in abnormal perfusion on MPI.[12-14]

Thus, the exact relationship between CAD and MPI is not very clear. The purpose of this study is to correlate CAC scores with MPI by SPECT in a group of patients with suspected CAD.

An important strength of this study is that simultaneous assessment of MPI and CAC scores was performed on all consecutive patients with suspected CAD, thus, the results could be applicable to similar populations of patients undergoing MPI examination.

3.2 Materials and methods

Patient data collection

This retrospective study consisted of 48 patients (33 men and 15 women; mean age 61.7 years; range 44–81 years) with suspected coronary artery disease that underwent both multi-slice CT and MPI-SPECT examinations within two weeks. Patients who were referred first by general practitioners for coronary CT scans, and then, for MPI-SPECT by nuclear physicians, met the following inclusion criteria: no previous history of CAD; typical or atypical chest pain, dyspnea or signs of myocardial perfusion on a resting or stress ECG test.

Medical history, including cardiovascular risk factors, blood pressure, lipid profile, electrocardiography (ECG) and 10-year CAD risk, predicted on the basis of the Framingham risk score, was obtained for all patients (pretest probability: low to moderate).

Patients were excluded if they had a previous history of myocardial infarction, unstable angina, percutaneous coronary intervention (angioplasty) or coronary bypass surgery; allergy to contrast medium and renal insufficiency (serum creatinine > 1.5 mg/dL). All patients were in a stable condition at the time of the study. The study was approved by the local ethics research committee and written informed consent was obtained from all patients. The characteristics of the study population are summarised in table 3.1.

Table 3.1 Patient demographics.

Males	33 (69%)
Females	15 (31%)
Age (years, mean ± SD)	61.7 (9.8)
Cardiovascular risk factors	
Smoking	13 (27%)
Hypertension	41 (83%)
Diabetes	8 (17%)
Dyslipidemia	13 (27%)
Angina pectoris	
Atypical	7 (14.6)
Typical	41 (85.4%)

Coronary CT scanning protocol

All patients were scanned on a dual-source CT scanner (Somatom Definition, Siemens Medical Solutions, Forchheim, Germany). A non-enhanced scan was performed for CAC scoring. Scanning parameters were as follows: detector collimation 2 × 32 × 0.6 mm, slice collimation 2 × 64 × 0.6 mm by means of a z-flying focal spot, gantry rotation time 330 ms, pitch of 0.2–0.5 depending on the heart rate, tube current time product 350 mAs and tube potential 120 kV.

CT scans were performed from the level of the tracheal bifurcation to the diaphragm. Non-enhanced CT scans were performed with prospective ECG-triggering with images acquired at three mm slice thickness.

Coronary artery calcium scoring

Coronary artery calcifications were quantified using calcium scoring software (Syngo CaScore, Siemens) and measurments were performed by a qualified CT technologist using the standard Agatston calcium scoring algorithm.[4] The extent of CAD was determined according to the recommended CT calcium score guidelines using five CAC score categories: none (0), minimal or low (1–10), mild (11–100), moderate (101–400) and extensive or high (401 or greater).

MPI-SPECT imaging protocol

Rest and stress ECG-gated MPI protocols were performed in all patients using technetium (^{99m}Tc)-tetrofosmin (500 MBq). The stress test was performed on an exercise-modified Bruce treadmill and associated (such as adenosine infusion) protocol. Images were acquired on a triple-head SPECT camera (ADAC Vertex with VXGP collimators) using a low-energy, high-resolution, parallel-hole collimator with a 360 rotation in a continuous mode. All projection images were stored in a 64 × 64 × 16 acquisition and processing frame matrix size.

MPI-SPECT image analysis

The myocardial perfusion assessment was performed by a nuclear physician with more than 10 years of experience in nuclear cardiology using a 20-segment model, and myocardial perfusion for each segment was evaluated using a five-point continuous scoring system as recommended by Xu et al.[15] (0: normal; 1: mildly abnormal; 2: moderately abnormal; 3: severely abnormal; 4: absence of segmental uptake). The observer was blinded to any clinical information and CAC scores.

The segmental perfusion scores during rest and stress were added to calculate the summed rest score (SRS) and the summed stress score (SSS). The summed difference score (SDS) was calculated by subtracting the SRS from the SSS.

Statistical analysis

Data were entered into SPSS V 19.0 for analysis (SPSS, Chicago, Illinois). All continuous variables were expressed as mean ± SD. A one way analysis of variance (ANOVA) was used for analysis of continuous variables and a Pearson test was used to demonstrate the correlation between CAC and MPI scores. A *P* value of less than 0.05 indicated statistically significant difference.

3.3 Results

Table 3.2 lists the CAC and MPI-SPECT scores as assessed in these patients. There are variable degrees of differences between the CAC and corresponding MPI-SPECT scores. Figure 3.1 shows the distribution of CAC and MPI scores among these 48 patients. Forty-seven percent of the patients had moderate and extensive calcifications with CAC scores more than 100, while 42% of these patients demonstrated abnormal, or probably abnormal, MPI assessments. Analysis of the relationship between overall CAC scores and MPI assessments indicated no correlation with a Pearson correlation factor *r* of 0.019 (Figure 3.2).

Table 3.2. Percentages of coronary artery calcium score and MPI-SPECT results.

CAC score	Total number of patients (%)
0	12 (25%)
1-10	3 (6%)
11-100	10 (21%)
101-400	11 (23%)
>400	12 (25%)
TOTAL	48 (100%)
MPI score	**Total number of patients (%)**
0	3 (6%)
1	8 (17%)
2	16 (33%)
3	7 (15%)
4	14 (29%)
TOTAL	48 (100%)

CAC: coronary artery calcium; MPI: myocardial perfusion imaging.

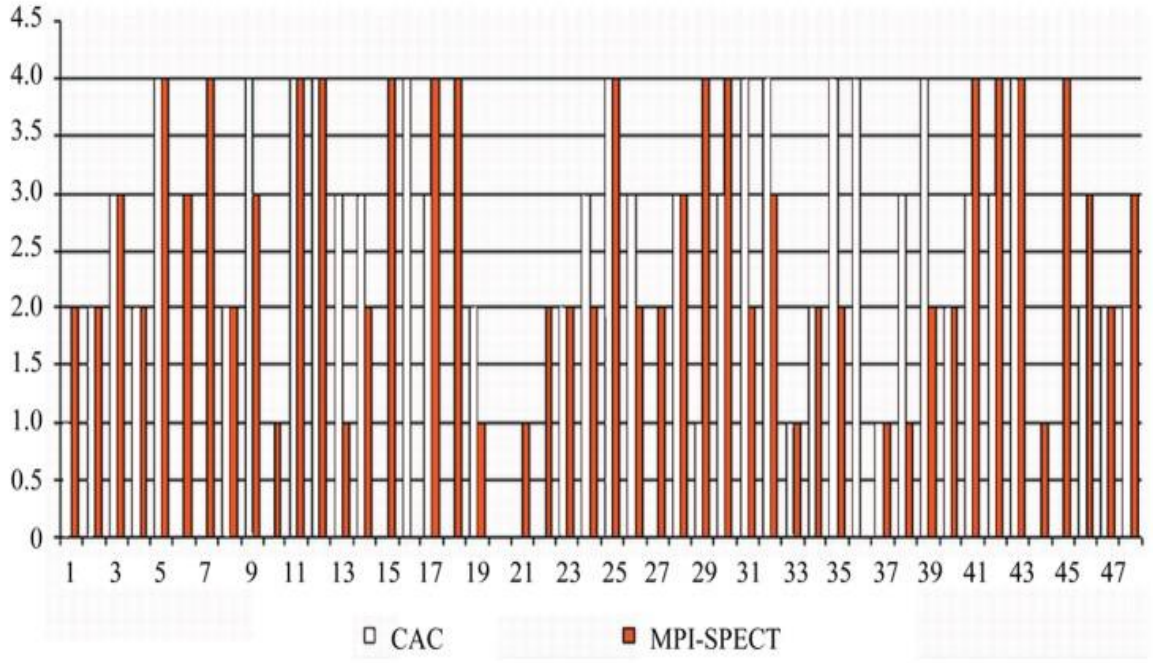

Figure 3.1. Distribution of the CAC scores with myocardial perfusion imaging among the 48 patients with suspected coronary artery disease.

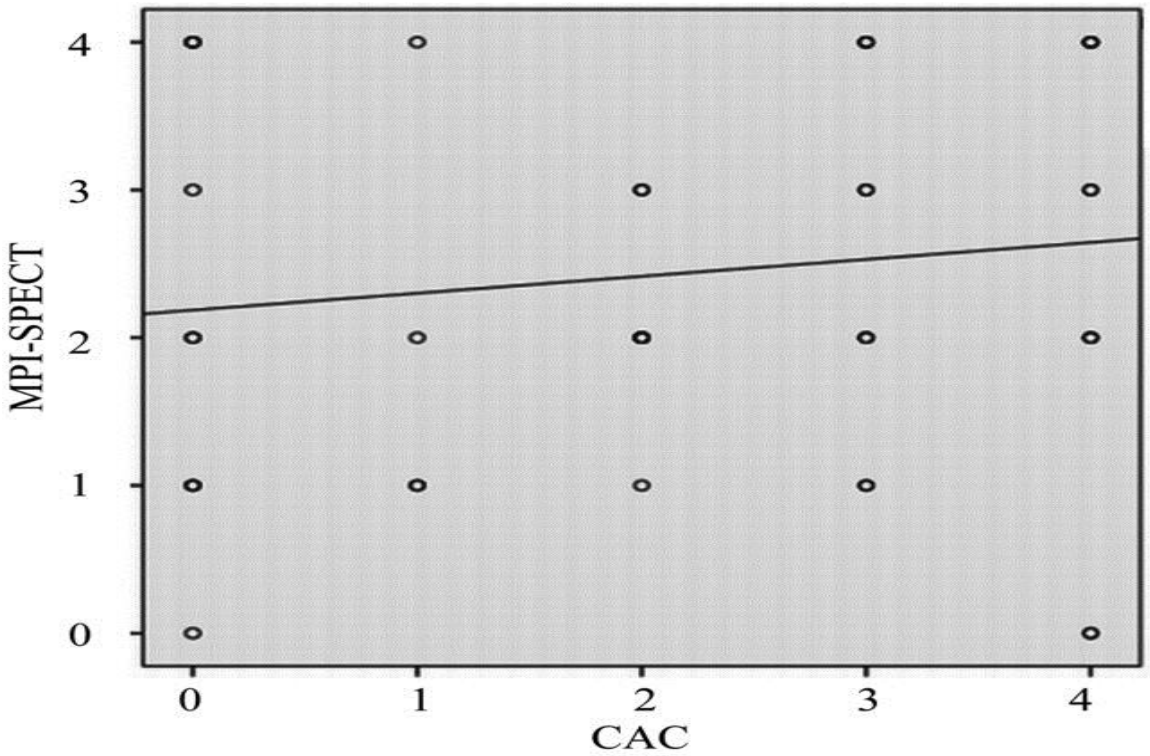

Figure 3.2. Graph shows that there is a lack of correlation between coronary artery calcium scores and the corresponding myocardial perfusion SPECT assessments, with r value of 0.019.

A zero CAC score was found in 25% of the patients; however, only 6% of these were noted to demonstrate the normal MPI-SPECT results. Of 10 patients with a zero CAC score, abnormal MPI-SPECT scores were found to range from 1 to 4 (mean score 2.6). In contrast, normal MPI-SPECT scores were found in two patients with a CAC score of four. A CAC score of 1–10 was identified in 6% of the patients with probably normal MPI-SPECT findings in 17% of the patients. A CAC score of 11–100 was found in 21% of patients with equivocal MPI-SPECT findings in 33% of the patients. A CAC score of the 101–400 was reported in 23% of the patients with probably abnormal MPI-SPECT findings in 15% of these patients. Similarly, there was no correlation between the CAC scores and MPI assessments in the group of patients with low to moderate calcification, with a Pearson correlation factor *r* of 0.012.

Extensive calcifications (CAC score > 400) were noticed in 25% patients, while 29% of patients were found to have abnormal MPI. Again, there was no correlation between the CAC scores and MPI assessments in the group of patients with extensive calcification, with a Pearson correlation factor *r* of 0.080.

3.4 Discussion

Although based on a relatively small sample size, this study presents important findings which are considered valuable for the clinical diagnosis of patients with suspected coronary artery disease. There is a lack of correlation between the CAC scores and MPI-SPECT assessments, with a significant difference observed between these scoring techniques, especially in the patients with zero or mild calcification (CAC scores 0–100). Thus, CAC scores cannot be reliably used as single parameters to predict the disease prognosis in this group of patients.

CAC score using multi-slice CT has been validated as a useful imaging tool for risk stratification and reclassification of risk of coronary artery disease.[16] The CAC score is a highly sensitive marker with increased prognostic value for determining the atherosclerotic disease compared with conventional cardiovascular risk factors. However, issues have been raised as to whether using only a CAC score is a reliable tool of determining the extent of CAD, since non-calcified coronary artery plaque may not be detected.

There is growing evidence to show the discrepancy between low CAC and corresponding myocardial perfusion findings.[8,17,18] This is confirmed by the results in this analysis as there is no correlation between the CAC scores and MPI assessments, whether the analysis is based on a comparison of overall CAC scores and MPI assessments, or on low or high CAC scores with corresponding MPI assessments.

Several studies have reported the presence of obstructive non-calcified plaque in 8.7% of symptomatic patients with zero or low calcium scores.[8,17] Cheng et al.[17] reported that low, but detectable, CAC scores were less reliable in predicting the plaque burden due to their association with high overall non-calcified coronary artery plaque. Similarly, Greenland, et al.[18] demonstrated a CAC of zero did not usually eliminate the risk of future CAD events. Our results are in line with those findings. Twenty-three percent patients had a zero CAC score with only 7% of these patients verified by the myocardial perfusion SPECT to be normal. It could be concluded that low CAC scores are significantly less predictive of the prevalence, or severity, of underlying non-calcified coronary plaque,[19] although further studies based on a larger cohort of patients should be conducted.

It has been reported that the MPI-SPECT in cardiac imaging is a widely accepted test for the diagnostic and prognostic evaluation of patients with known, or suspected, CAD.[10,20] This study indicates that MPI-SPECT may provide more accurate assessments of the extent of CAD, or the prediction of disease outcomes, than CAC alone, given that, in patients with zero CAC, some could demonstrate abnormal myocardial perfusion. Schaap, et al.[21] in their recent study concluded that a CAC score did not significantly improve the diagnostic performance of SPECT in patients with significant CAD. The association between CAC and MPI-SPECT demonstrates that as the CAC score increases, so does the occurrence and severity of myocardial perfusion abnormalities.[22,23]

High values of CAC often indicate the presence of stenotic lesions and are associated with an increased risk of adverse cardiovascular events.[16,24,25] Similarly, our study shows that patients with a high calcium score had abnormal, or probably abnormal, MPI-SPECT results, although the correlation between these imaging modalities was not significant. However, studies have been reported that patients with a high CAC score did not demonstrate a significantly different percentage of abnormal MPI findings than in patients with a low CAC score.[12,14]

A high CAC in patients with normal MPI-SPECT reflects non-obstructive atherosclerosis, which is regarded as a preclinical state with strong predictive value for the development of CAD, thus, aggressive risk factor modification should be recommended according to the guidelines.[26] A CAC score and MPI should be considered complementary approaches rather than individual parameters in the assessment of patients with suspected CAD.

Several limitations in this study should, however, be acknowledged. Firstly, only a limited number of patients were included in this study and further studies based on a larger cohort are needed.

Secondly, this study is only a retrospective analysis of the diagnostic reports without the inclusion of follow-up details on patients, thus, there is no information available about the disease outcomes, such as major cardiac events relative to the CAC or MPI scores.

Thirdly, the cut off value for CAC at 401 or greater in this study is much lower than the suggested value in the literature (> 700),[27,28] thus, this could affect the diagnostic specificity in detecting significant CAD.

Lastly, the diagnostic accuracy of coronary CT angiography was not assessed with regard to the evaluation of the degree of coronary stenosis, with no correlation to subsequent myocardial perfusion analysis, thus, no information is available about the diagnostic value in terms of sensitivity and specificity.

This could be explained by the fact that the current study only focused on the correlation between CAC and MPI-SPECT. Recent evidence shows that coronary calcium scores assessed with non-enhanced CT might be supported by coronary CT angiography or coronary CT angiography might be performed alone with the aim of acquiring more diagnostic information.[29,30] Further studies are required to investigate the potential value of coronary CT angiography for both calcium scoring and assessment of coronary stenosis.

In conclusion, this study demonstrates the lack of direct correlation between the CAC score and the corresponding myocardial perfusion assessed by SPECT in patients with suspected coronary artery disease. In particular, in patients with a zero or low CAC scores, myocardial perfusion imaging shows potential abnormalities in some patients which indicate significant lack of agreement between these two methods.

This highlights the limitations in using CAC scores alone as a predictor of coronary disease outcomes. Coronary calcium score should be combined with myocardial perfusion imaging in low-to-intermediate risk patients to improve the diagnostic performance.

3.5 References

1. Oudkerk M, Stillman AE, Halliburton SS, et al. Coronary artery calcium screening: current status and recommendations from the European Society of Cardiac Radiology and North American Society for Cardiovascular Imaging. Int J Cardiovasc Imaging. 2008;24:645–671.
2. Greenland P, Bonow RO, Brundage BH, et al. ACCF/AHA 2007 clinical expert consensus document on coronary artery calcium scoring by computed tomography in global cardiovascular risk assessment and in evaluation of patients with chest pain: a report of the American College of Cardiology Foundation Clinical Expert Consensus Task Force (ACCF/AHA Writing Committee to Update the 2000 Expert Consensus Document on Electron Beam Computed Tomography) Circulation. 2007;115:402–426.
3. Hoffmann U, Siebert U, Bull-Stewart A, et al. Evidence for lower variability of coronary artery calcium mineral mass measurements by multidetector computed tomography in a community based cohort—consequences for progression studies. Eur J Radiol. 2006;57:396–402.
4. Agatston AS, Janowitz WR, Hildner FJ, et al. Quantification of coronary artery calcium using ultrafast computed tomography. J Am Coll Cardiol. 1990;15:827–832.
5. Keelan PC, Bielak LF, Ashai K, et al. Long-term prognostic value of coronary calcification detected by electron-beam computed tomography in patients undergoing coronary angiography. Circulation. 2001;104:412–417.
6. Wong ND, Hsu JC, Detrano RC, et al. Coronary artery calcium evaluation by electron beam computed tomography and its relation to new cardiovascular events. Am J Cardiol. 2000;86:495–498.
7. Arad Y, Spadaro LA, Goodman K, et al. Prediction of coronary events with electron beam computed tomography. J Am Coll Cardiol. 2000;36:1253–1260.
8. Gottlieb I, Miller JM, Arbab-Zadeh A, et al. The absence of coronary calcification does not exclude obstructive coronary artery disease or the need for revascularization in patients referred for conventional coronary angiography. J Am Coll Cardiol. 2010;55:627–634.
9. Chang SM, Nabi F, Xu J, et al. The coronary artery calcium score and stress myocardial perfusion imaging provide independent and complementary prediction of cardiac risk. J Am Coll Cardiol. 2009;54:1872–1882.
10. Fallahi B, Beiki D, Gholamrezanezhad A, et al. Single Tc99m Sestamibi injection, double acquisition gated SPECT after stress and during low-dose dobutamine infusion: a new suggested protocol for evaluation of myocardial perfusion. Int J Cardiovasc Imaging. 2008;24:825–835.
11. Elhendy A, van Domburg RT, Sozzi FB, Poldermans D, Bax JJ, Roelandt JR. Impact of hypertension on the accuracy of exercise stress myocardial perfusion imaging for the diagnosis of coronary artery disease. Heart. 2001;85:655–661.
12. Rosman J, Shapiro M, Pandey A, VanTosh A, Bergmann SR. Lack of correlation between coronary artery calcium and myocardial perfusion imaging. J Nucl Cardiol. 2006;13:333–337.
13. Thompson RC, McGhie AI, Moser KW, et al. Clinical utility of coronary calcium scoring after nonischemic myocardial perfusion imaging. J Nucl Cardiol. 2005;12:393–400.

14. Schuijf JD, Wijns W, Jukema W, et al. Relationship between noninvasive coronary angiography with multi-slice computed tomography and myocardial perfusion imaging. J Am Coll Cardiol. 2006;48:2508–2514.
15. Xu Y, Fish M, Gerlach J, et al. Combined quantitative analysis of attenuation corrected and non-corrected myocardial perfusion SPECT: method development and clinical validation. J Nucl Cardiol. 2010;17:591–599.
16. Detrano R, Guerci AD, Carr JJ, et al. Coronary calcium as a predictor of coronary events in four racial or ethnic groups. N Engl J Med. 2008;358:1336–1345.
17. Cheng VY, Lepor NE, Madyoon H, et al. Presence and severity of noncalcified coronary plaque on 64-slice computed tomographic coronary angiography in patients with zero and low coronary artery calcium. Am J Cardiol. 2007;99:1183–1186.
18. Greenland P, Labree L, Azen SP, Doherty TM, Detrano RC. Coronary artery calcium score combined with Framingham score for risk prediction in asymptomatic individuals. JAMA. 2004;291:210–215.
19. Sun Z, Cao Y, Li H. Multislice computed tomography angiography in the diagnosis of coronary artery disease. J Geriatric Cardiol. 2011;8:104–113.
20. Bateman TM, Heller GV, McGhie AI, et al. Diagnostic accuracy of rest/stress ECG-gated Rb-82 myocardial perfusion PET: comparison with ECG-gated Tc-99m sestamibi SPECT. J Nucl Cardiol. 2006;13:24–33.
21. Schaap J, Kauling RM, Boekholdt SM, et al. Usefulness of coronary calcium scoring to myocardial perfusion SPECT in the diagnosis of coronary artery disease in a predominantly high risk population. Int J Cardiovasc Imaging. doi: 10.1007/s10554-012-0118-1.
22. Oudkerk M, Stillman AE, Halliburton SS, et al. Coronary artery calcium screening: current status and recommendations from the European Society of Cardiac Radiology and North American Society for Cardiovascular Imaging. Eur Radiol. 2008;18:2785–2807.
23. Bybee KA, Lee J, Markiewicz R, et al. Diagnostic and clinical benefits of combined coronary calcium and perfusion assessment in patients undergoing PET/CT myocardial perfusion stress imaging. J Nucl Cardiol. 2010;17:188–196.
24. Arad Y, Goodman KJ, Roth M, et al. Coronary calcification, coronary disease risk factors, C-reactive protein, and atherosclerotic cardiovascular disease events: the St. Francis Heart Study. J Am Coll Cardiol. 2005;46:158–165.
25. Berman DS, Wong ND, Gransar H, et al. Relationship between stress-induced myocardial ischemia and atherosclerosis measured by coronary calcium tomography. J Am Coll Cardiol. 2004;44:923–930.
26. Choudhary G, Shin V, Punjani S, et al. The role of calcium score and CT angiography in the medical management of patients with normal myocardial perfusion imaging. J Nucl Cardiol. 2010;17:45–51.
27. Schepis T, Gaemperli O, Koepfli P, et al. Added value of coronary artery calcium score as an adjunct to gated SPECT for the evaluation of coronary artery disease in an intermediate-risk population. J Nucl Med. 2007;48:1424–1430.
28. Ghardri JR, Pazhenkottil AP, Nkoulou RN, et al. Very high coronary calcium score unmasks obstructive coronary artery disease in patients with normal SPECT MPI. Heart. 2011;97:998–1003.
29. Rubinshtein R, Gaspar T, Halon DA, et al. Prevalence and extent of obstructive coronary artery disease in patients with zero or low calcium score undergoing 64-slice cardiac multidetector computed tomography for evaluation of a chest pain syndrome. Am J Cardiol. 2007;99:472–475.

30. Van Werkhoven, Shuijf JD, Gaemperli O, et al. Incremental prognostic value of multi-slice computed tomography coronary angiography over coronary artery calcium scoring in patients with suspected coronary artery disease. Eur Heart J. 2009;30:2622–2629.

Chapter 4 Myocardial Perfusion Imaging Using 99mTc-MIBI Single Photon Emission Computed Tomography: A Cardiac Phantom Study

4.1 Introduction

Ischemic heart disease continues to be the most common aetiology for myocardial infarction in developed countries.[1,2] Medical imaging modalities have undergone rapid developments over the last decade, such as multislice CT, magnetic resonance imaging and radionuclide imaging with excellent visualisation of anatomical structures and functional assessment of cardiac disease.[3-9]

Of these imaging techniques, myocardial perfusion single photon emission computed tomography (SPECT) has been established as a non-invasive method for the diagnosis of coronary artery disease with flow-limiting lesions with a sensitivity and specificity of 87–89% and 73–75%, respectively, depending on the selection of radioisotope and stress modality.[10]

Furthermore, SPECT has been reported to be a valuable diagnostic modality for risk stratification with a normal perfusion scan being associated with very low risk of death or non-fatal myocardial infarction.[10] SPECT myocardial perfusion imaging performed with Technetium-99 (^{99M}Tc)-based radiopharmaceuticals is widely used in daily clinical practice for diagnosing coronary artery disease and stratifying patients according to cardiac risk factors.[11,12]

Despite these advantages, myocardial perfusion SPECT has been challenged by the emergence of positron emission tomography (PET) as PET has higher spatial and temporal resolution than SPECT, which allows more accurate quantification of regional myocardial perfusion.[13-15] However, both SPECT and PET suffer from radiation exposure to patients, thus, selection of protocols for individual patients is essential to ensure the implementation of an “as low as reasonably achievable” approach.[16]

The purpose of this study was to develop a cardiac phantom and test SPECT myocardial perfusion imaging using ^{99m}Tc-MIBI under normal and simulated conditions in the left ventricle.

It is expected that this preliminary study will lay the foundation for further experiments on the cardiac imaging comparing SPECT with PET with regard to minimizing radiation dose of myocardial perfusion protocols.

4.2 Materials and methods

Phantom Design and Experimental Setup

A realistic thorax-heart phantom was designed to serve as purpose of performing myocardial perfusion imaging. The phantom consists of left ventricle, right ventricle, vertebral column and lungs (Fig. 4.1). The phantom was made from Perspex and Acrylic materials with two cylinders consisting of a half-spherical end and inner cylinder which forms the ventricular chambers. The space between two cylinders represents the myocardial wall chamber. The left and right ventricles were located between the lung cavities (Fig. 4.2).

The defects which were made from solid inserts caused cold spot which represents myocardial perfusion defects (Fig. 4.3). Sponges were used to support the position of heart phantom in an angle of about 45◦ which is similar to the normal heart position within the chest (Fig. 4.4).

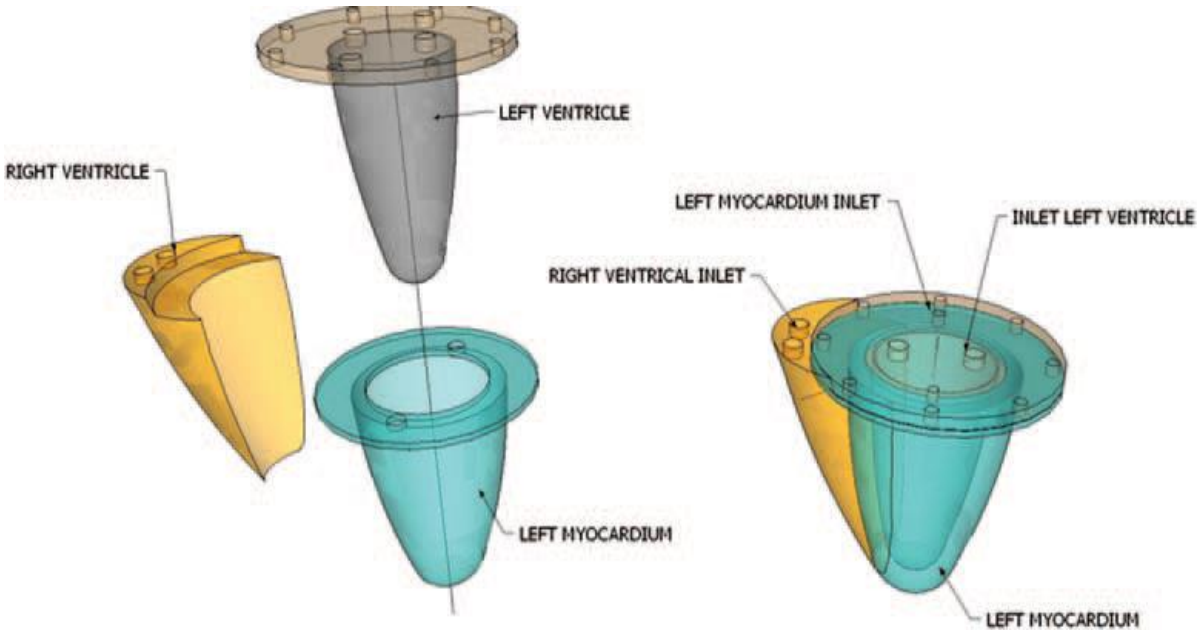

Figure 4.1. Diagrams show the anatomical structures of cardiac phantom consisting of left and right ventricles. (A) lateral view, (B) superior view.

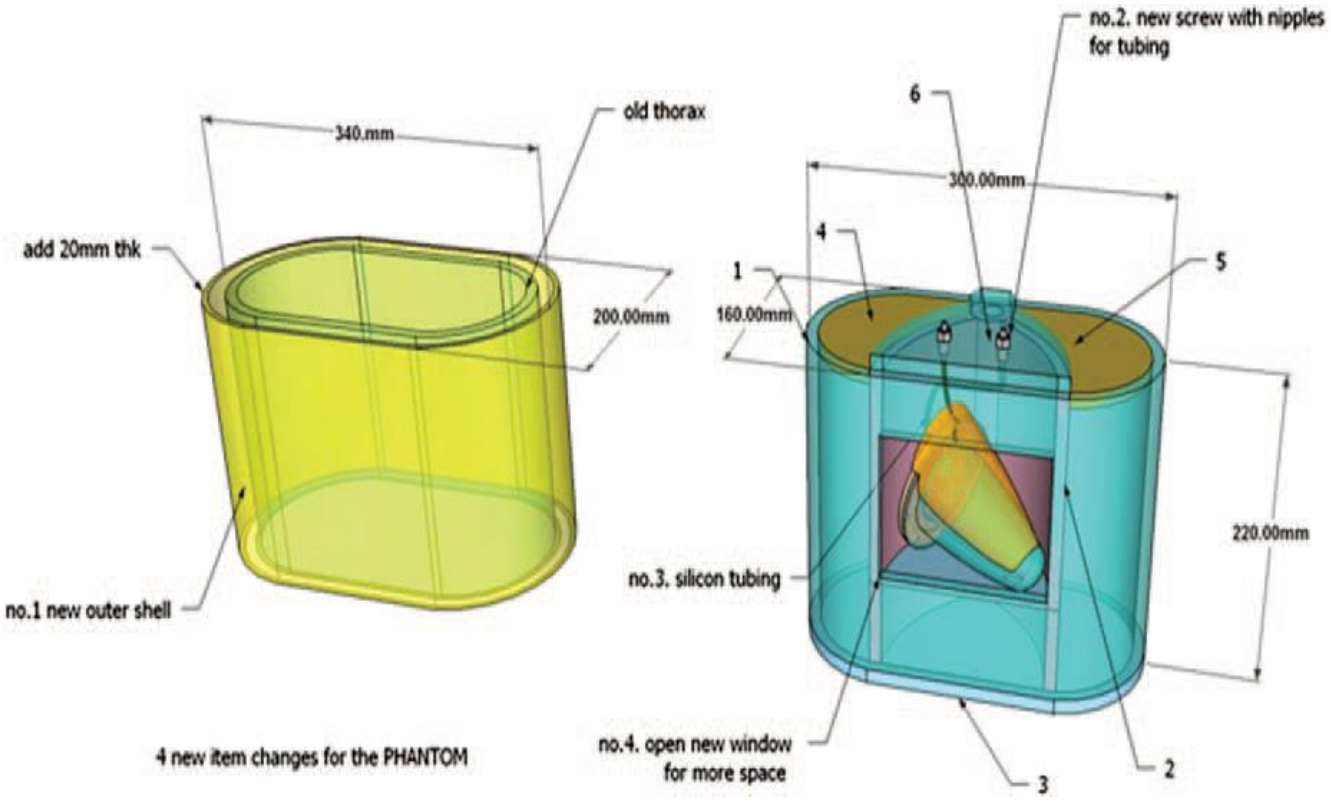

Figure 4.2. Diagrams show the phantom position in relation to the chest wall and lungs.

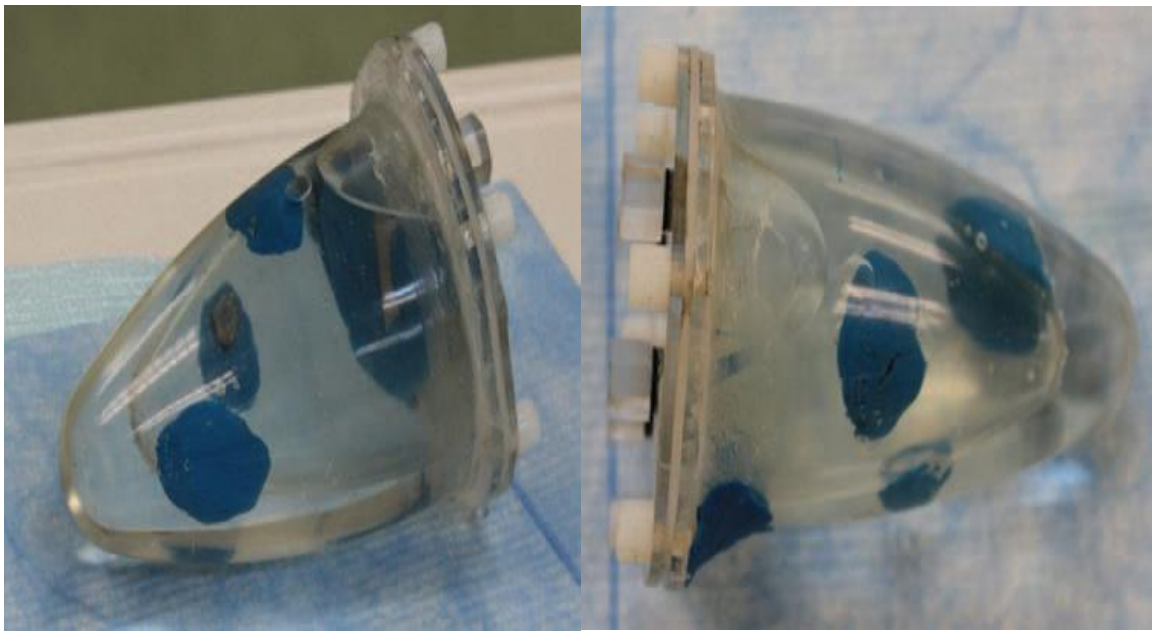

(A) (B)

Figure 4.3. External views of cardiac phantom showing the simulated infarcted areas at different locations of the left ventricular wall (blue solid areas).

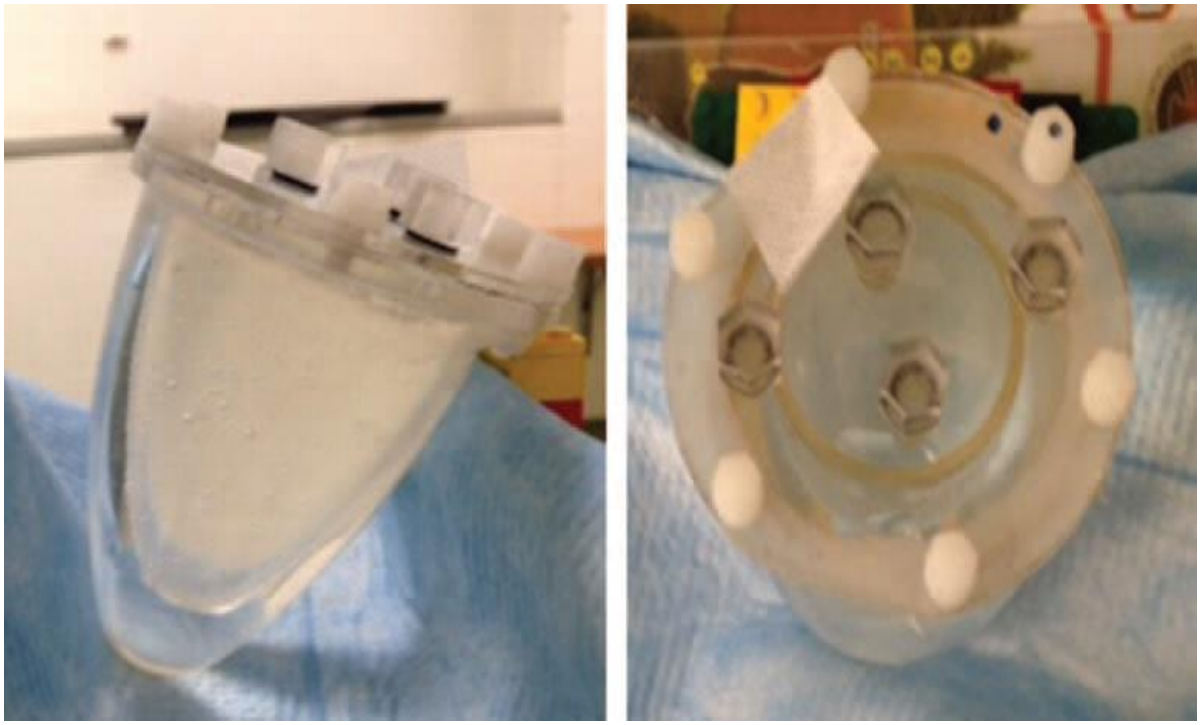

(A) (B)

Figure 4.4. Cardiac phantom with water and radioisotope filled in the left ventricular wall and positioned in an angle similar to the normal heart position within the chest. (A) lateral view, (B) superior view.

SPECT Image Acquisition

All phantom image acquisitions were performed on a three-head SPECT/CT camera (IRIX 300D, Philips) with low-energy collimator at 140 keV. A rest myocardial perfusion imaging protocol without ECG-gating was performed in the phantom. A step-and-shoot mode was used for SPECT acquisition, with a 64×64 acquisition and processing frame matrix size and zoom of 1.49. The time per frame was 30 sec.

SPECT data were processed using standard reconstruction software based on a filtered back projection method. The CT images were used to provide attenuation factors for correction of the SPECT data. Phantom acquisitions were single-isotope studies with injection of a small amount of radioisotope of 0.6 mCi of ^{99m}Tc sestamibi mixed with 160 ml of water into the left ventricular wall to simulate myocardial perfusion.

Simulated infarcts were located in the anterior and septal regions of the left ventricular wall to produce moderate and severe defects.

4.3 Results

Cardiac SPECT imaging was successfully performed on the phantom with demonstration of both normal myocardium and ischemic defects due to presence of simulated infarction. Figure 4.5 (A) shows circumferential profiles of the short-axis and long-axis (vertical and horizontal) slices of normal myocardium, while Figure 4.6 (A) demonstrates the severity of the inserts from the ^{99m}Tc SPECT study.

The simulated infarcted areas were clearly visualised on both axes in the left ventricular wall. Using a simple 20-segment polar map, all tomographic slices of the myocardium under both normal and infarcted conditions (Figs. 4.5 (B) and 4.6 (B) were shown with similar appearance to that observed on the short and long-axis slices.

The ischemic change due to simulated moderate and severe infarcted lesions was demonstrated at the anterolateral and apical anteroseptal segments, which are shown in Figure 4.6 (B).

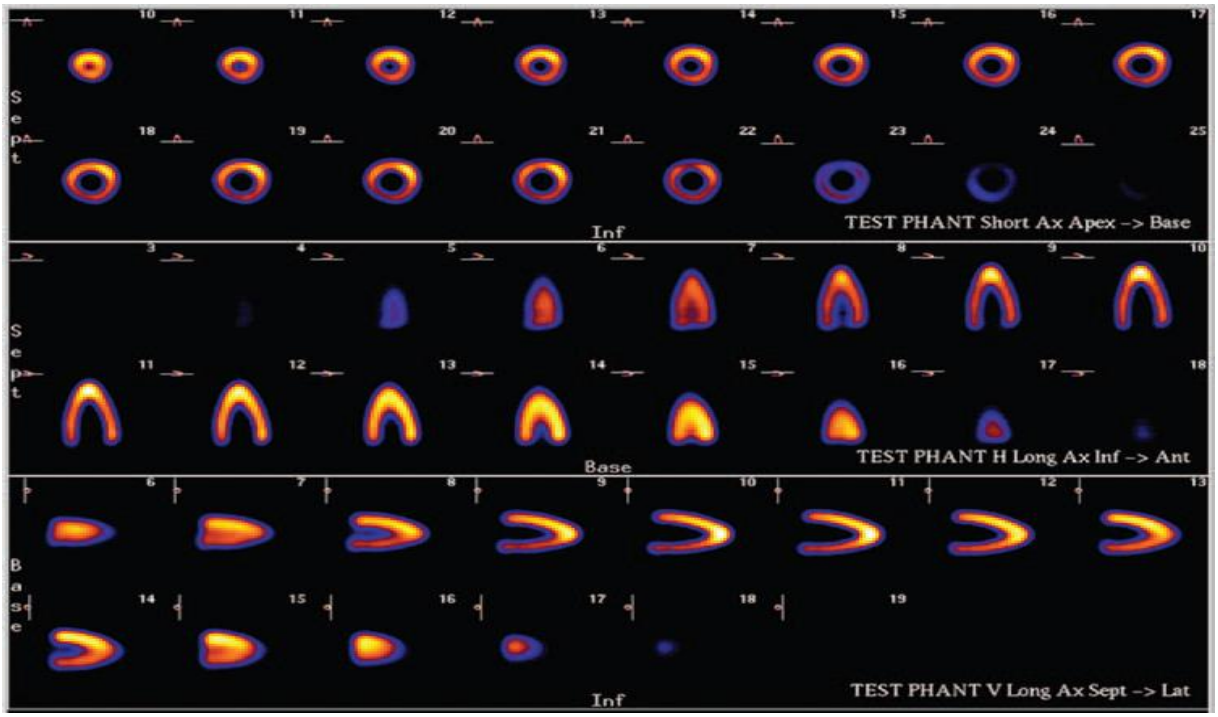

(A)

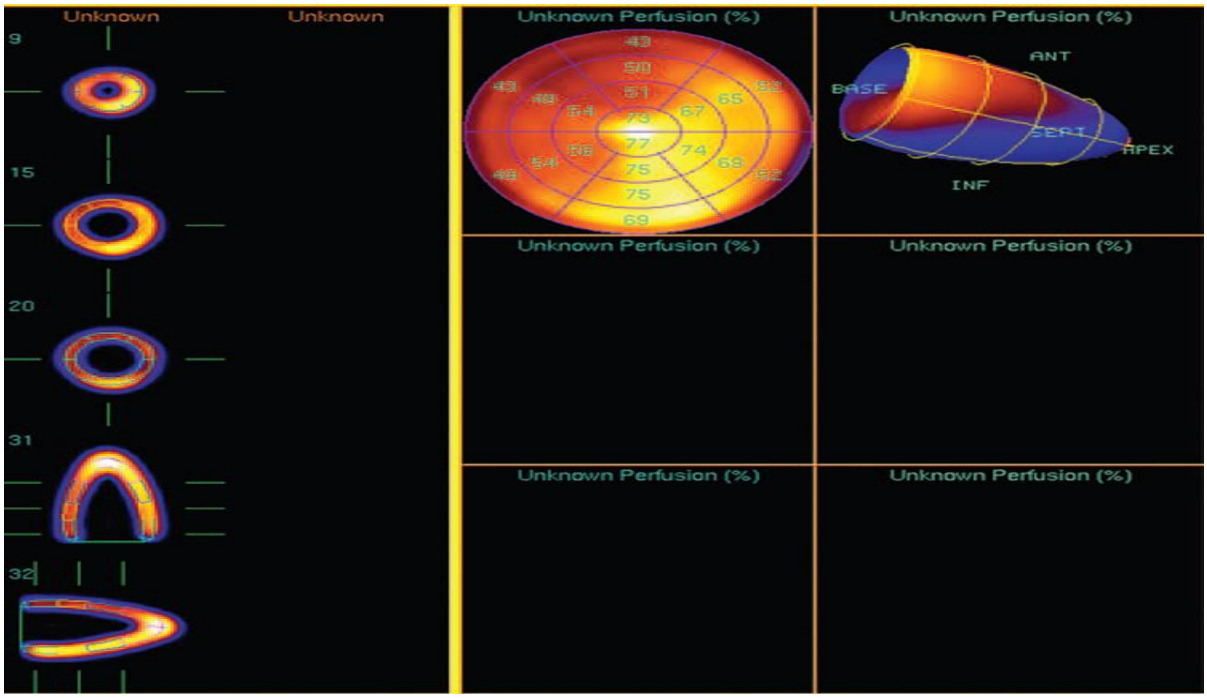

(B)

Figure 4.5. Rest cardiac SPECT imaging of normal myocardium. (A) is short and long axis view of the left ventricular myocardium, while (B) refers to the 20-segment polar map views.

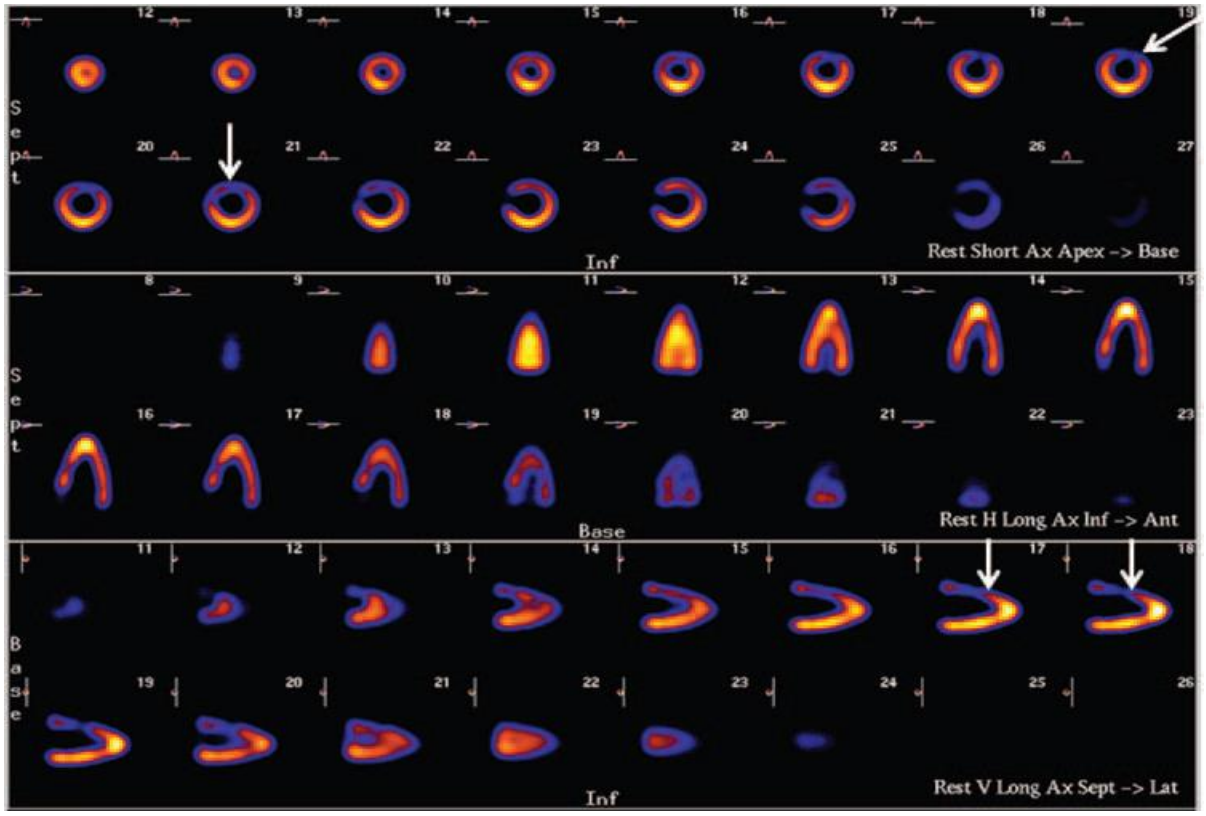

(A)

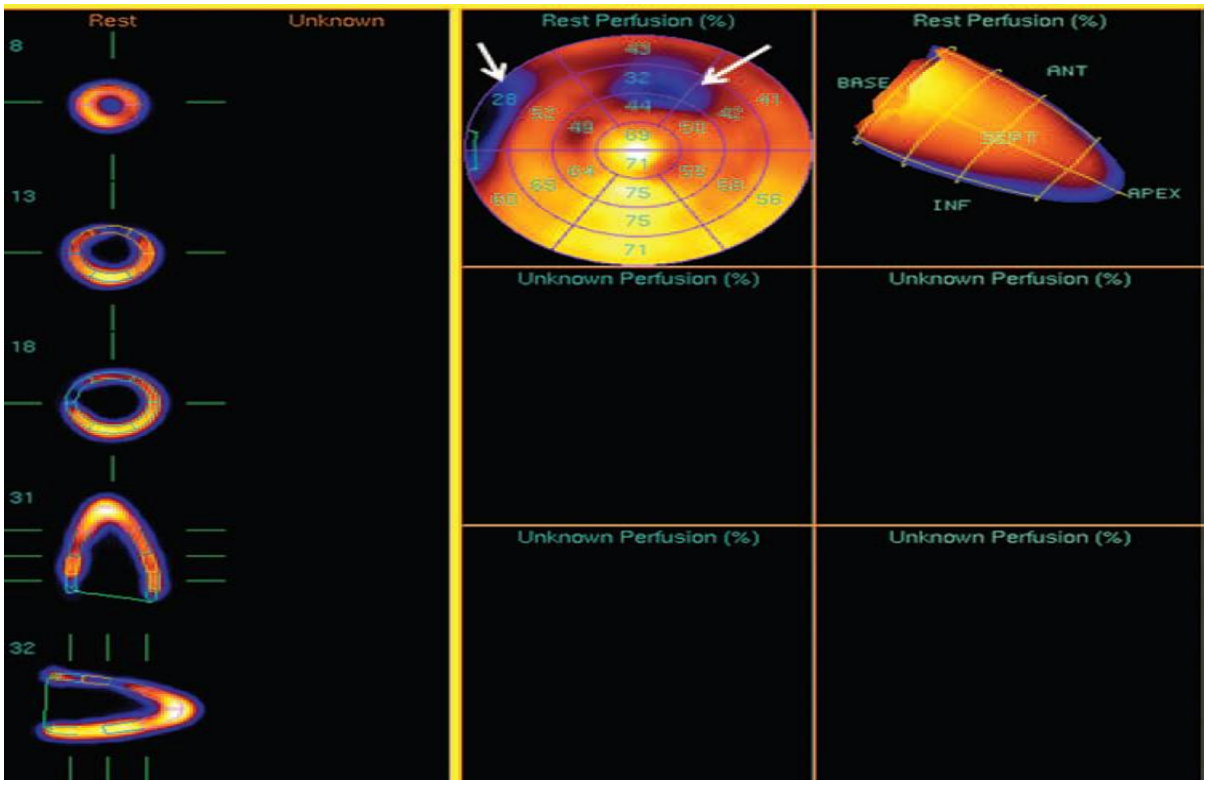

(B)

Figure 4.6. Rest cardiac SPECT imaging of abnormal myocardium. (A) shows the ischemic changes in the left ventricular myocardium visualised on the short and long axis, while (B) refers to the 20-segment polar map views of the corresponding infarcted areas. Arrows point to the infarcted areas.

4.4 Discussion

This study shows our preliminary experience of testing myocardial perfusion SPECT imaging on a cardiac phantom during normal myocardium and simulated infarction. Results show the feasibility of demonstrating cold lesions created by the inserts. Over the last two decades, SPECT myocardial perfusion imaging has become an imaging modality in the routine management of patients with suspected or known coronary artery disease.[11]

Thallium-201 (^{201}T1) SPECT is the oldest and most common method of assessing myocardial ischemia. It is also a well-established means of measuring myocardial viability. Nonetheless, ^{99m}Tc-based radiopharmaceuticals (sestamibi and tetrofosmin) have become the dominant perfusion tracers of SPECT myocardial perfusion imaging in daily clinical practice, due in part to the higher count rates of the ^{99m}Tc agents.[17,18]

This is confirmed in this study as simulated infarcted lesions are reliably detected on SPECT images using the radioisotope of sestamibi. Although advances in cardiac imaging procedures have improved the ability to assess and treat cardiovascular disease, radiation dose is becoming a major issue since cumulative radiation exposure from general medical imaging is substantial in many individuals.

Myocardial perfusion imaging has been reported to account for more than 22% of total effective dose of radiation received by the study population consisting of 655, 613 subjects who underwent at least one imaging procedure associated with radiation dose.[19] CT and nuclear imaging accounted for 21% of the total number of procedures and 75.4% of the total effective dose, according to Fazel et al.'s study.[19]

Extensive research has been performed in cardiac CT imaging with successful dose reduction being achieved by incorporating optimal techniques,[20-22] however, there is a lack of patient-level data on radiation exposure from cardiac nuclear imaging procedures despite a rapid increase in their use. We believe the cardiac phantom developed in this study can be used to investigate optimal SPECT and PET protocols with the aim of reducing radiation exposure to patients.

The effective doses for most of the radiopharmaceuticals used in myocardial imaging are between 2–15 mSv per study, with the highest dose being reported in SPECT using ^{201}T1 which may reach up to 20–30 mSv, and the lowest values being noted for ^{13}N–NH3 and ^{15}O studies.[23]

The doses per study for ^{99m}Tc and ^{201}T1-labeled radionuclides differed significantly by about a factor of 2, and this difference must be evaluated in the context of the numeric uncertainty in individual values. The average amount of radiopharmaceutical used in a resting ^{99m}Tc-MIBI study is 20 mCi, with an effective dose of 6.7 mSv.[24] In this study, only 0.6 mCi was used in the SPECT imaging, which is equivalent to 0.2 mSv.

Further studies based on different volumes of radiopharmaceuticals should be conducted to confirm the diagnostic image quality of SPECT myocardial perfusion imaging with resultant low radiation dose.

There are some limitations in this study that should be acknowledged. First, although the phantom represents normal anatomic structures, it does not have the movable function of heart beats; thus, stress SPECT imaging could not be conducted.

Second, this experimental study only tested the feasibility of SPECT imaging on the cardiac phantom, without measuring the image quality, such as contrast values on both normal myocardium and infarction areas or diagnostic value in terms of sensitivity and specificity. This can be explained by the reason that this preliminary study only focused on testing of the phantom design and clinical applicability.

Further experiments are needed to investigate the quantitative assessment of image quality and qualitative analysis of the detection of inserts. Third, although CT images were used for attenuation correction, the cardiac phantom was not tested inside the thoracic cavity, therefore, no attenuation from chest wall such as breast tissue or thick chest wall was available in the experiments. Further studies with cardiac phantom placed in the realistic chest wall are needed as this is especially important because the experiments were used to test low-dose protocol, while low-dose protocol will suffer from chest wall attenuation to a greater extent which could potentially lead to false positive results.

Finally, this study was performed on a SPECT camera, while PET has been recently reported to be superior to SPECT in myocardial perfusion imaging due to its high spatial and temporal resolution.[13-15, 24,25] Comparison of myocardial perfusion imaging with SPECT and PET is suggested in further experiments with the aim of determining the diagnostic value of SPECT compared to PET.

In conclusion, we have developed a cardiac phantom with insertion of infarcted areas in the left ventricular wall, and tested SPECT myocardial perfusion imaging. Both normal myocardium and simulated infarcted areas are clearly visualised on SPECT images. The phantom can be used to conduct further experiments, including comparison of SPECT with PET using different isotopes, and investigation of optimal cardiac protocols for radiation dose reduction while achieving diagnostic images.

4.5 References

1. He J, He L, Ogden L, Bazzano S, Vupputuri C, Loria P, et al. Risk Factors for Congestive Heart Failure in US Men and Women. Arch Intern Med. 2001;161(7):996-1002.
2. Ghosh N, Ghosh OE, Rimoldi RSB, Beanlands PG, Camici. Assessment of myocardial ischaemia and viability: role of positron emission tomography. Eur Heart J. 2010;31(24):2984-95.
3. Sabarudin A, Sun Z, Md Yusof AK. A Survey Exploring Specialists and Radiographers' Perceptions of the Benefits and Challenges in Relation to Prospectively ECG-Triggered Coronary CT Angiography. J Med Imag Heal Inf. 2013; 3: 388-392.
4. Faust O, Yi LM, Hua LM. Heart Rate Variability Analysis for Different Age and Gender. J Med Imag Heal Inf. 2013; 3: 395-400.
5. Wong KKL, Wong Z, Sun J, Tu S, Worthley J, Mazumdar D, et al. Medical image diagnostics based on computer-aided flow analysis using magnetic resonance images. Comput Med Imaging Graph. 2012;36(7):527-41.
6. Wong KKL, Sun Z, Tu J. Medical imaging and computer-aided flow analysis of a heart with atrial septal defect. J Mech Med Biol. 2012; 12 (5): 1-28.
7. Wong KKL, Kelso RM, Worthley SG, Sanders P, Mazumdar J, Abbott D. Medical imaging and processing methods for cardiac flow reconstruction. J Mech Med Biol. 2009; 9(1) 1-20.
8. Klocke F, Baird M, Lorell B, Bateman T, Messer J, Berman D, et al. ACC/AHA/ASNC Guidelines for the Clinical Use of Cardiac Radionuclide Imaging—Executive Summary. J Am Coll Cardiol. 2003;42(7):1318-33.
9. Iskander S, Iskandrian AE. Risk assessment using single-photon emission computed tomographic technetium-99m sestamibi imaging. J Am Coll Cardiol. 1998; 32: 57-62.
10. Shaw LJ, Iskandrian AE. Prognostic value of gated myocardial perfusion SPECT. J Nucl Cardiol. 2004; 11: 171-178.
11. Almoudi M, Sun Z. A head-to-head comparison of the coronary calcium score by computed tomography with myocardial perfusion imaging in predicting coronary artery disease. J Geriatr Cardiol. 2012; 9:349-357.
12. Gaemperli O, Bengel FM, Kaufmann PA. Cardiac hybrid imaging. Eur Heart J. 2011; 32: 2100-2106.
13. Bengel FM, Higuchi T, Javadi MS, Lautamaki R. Cardiac positron emission tomography. J Am Coll Cardiol. 2009; 54:1-12.
14. Lertsburapa K, Ahlberg AW, Bateman TM, Katten D, Volker L, Cullom SJ, Heller GV. Independent and incremental prognostic value of left ventricular ejection fraction determined by stress gated rubidium 82 PET imaging in patients with known or suspected coronary artery disease. J Nucl Cardiol. 2008; 15: 745-751.
15. Gimelli A, Bottai M, Genovesi D, A. Giorgetti, A. Di Martino F, Marzullo F. High diagnostic accuracy of low-dose gated-SPECT with solid-state ultrafast detectors: Preliminary clinical results. Eur J Nucl Med Mol Imaging. 2012; 39: 83-87.
16. Berman DS, Hachamovitch R, Shaw LJ, Hayes SW, Germano G. Nuclear cardiology, Hurst's the Heart, 12th edn., edited by V. Fuster, R. A. O'Rourke, R. A. Walsh, P.

Poole-Wilson, S. B. King III, R. Roberts, I. S. Nash, and E. N. Prystowsky, McGraw-Hill Companies, Inc., NY, New York. 2008; p. 544.
17. Berman DS, Kang XP, Tamarappoo B, Wolak A, Hayes SW, Nakazato R, et al. Stress Thallium-201/rest technetium-99m sequential dual isotope high-speed myocardial perfusion imaging. JACC Cardiovasc Imaging. 2009; 2, 273-282.
18. Fazel R, Krumholz HM, Wang Y, Ross JS, Chen J, Ting HH, et al. Exposure to low-dose ionizing radiation from medical imaging procedures. N Engl J Med. 2009; 361, 849-857.
19. Sun Z, Choo GH, Ng KH. Coronary CT angiography: Current status and continuing challenges. Br J Radiol. 2012; 85, 495-510.
20. Sun Z, Ng KH. Multislice CT angiography in cardiac imaging, Part III: Radiation risk and dose reduction. Singapore Med J. 2010; 51, 374-380.
21. Xu L, Zhang Z. Coronary CT angiography with low radiation dose. Int. J. Cardiovasc. Imaging. 2010; Suppl 1: 17-25.
22. Gaemperli O, Kaufmann PA. PET and PET/CT in cardiovascular disease. Ann N Y Acad Sci. 2011; 1228: 109-136.
23. Machac J. Cardiac positron emission tomography imaging. Semin Nucl Med. 2005; 35: 17-36.
24. Stabin MG. Radiopharmaceuticals for nuclear cardiology: Radiation dosimetry, uncertainties, and risk. J Nucl Med. 2008; 49: 1555-163.

Chapter 5 Diagnostic value of ^{18}FDG PET in myocardial viability in comparison with ^{99m}Tc SPECT and echocardiography

5.1 Introduction

Coronary artery disease (CAD) is the most common cause of cardiovascular disease responsible for inducing heart attack. Assessment of myocardial viability is an important approach to determine the myocardial function therefore, assisting effective patient management to reduce the mortality. Assessment of myocardial viability is regarded as an appropriate diagnostic technique after revascularisation in patients with damaged left ventricle (LV) function and indication of myocardial viability.[1-5]

The viability can be described as living myocardium. The clinician is concerned about determining whether dysfunctional myocardium is alive or deceased. Viable myocardium refers to areas that can be stunned or hibernated. LV dysfunction may be permanent if a myocardial scar is found, or it may be reversible after revascularization. Reversible LV dysfunction occurs when the myocardium is viable but dysfunction. Since only patients with dysfunctional but viable myocardium benefit from revascularization, the identification and quantification of the extent of myocardial viability is an important part of the work-up of patients with CAD or heart failure when determining the most appropriate treatment strategy. Metabolically depressed ruling of myocardium in response to a concentrated state of myocardial perfusion refers to hibernation. [6,7]

There are a number of diagnostic techniques used to classify myocardial viability such as single photon emission computed tomography (SPECT), positron emission tomography (PET), cardiac magnetic resonance imaging (MRI). Myocardial SPECT technique is widely used with different radioisotopes, such as thallium-201 (^{201}TI) and technetium-99m (^{99m}Tc). Myocardial PET has been also used with fluorine-18-fluorodexy glucose (^{18}F-FDG) as a routine procedure in clinical centres. Presently, ^{18}F-FDG PET imaging is considered as the gold standard for the diagnosis of myocardial viability. [8-10]

Studies have shown that cardiac SPECT and PET have high diagnostic performance in the assessment of myocardial viability [11-13] with high sensitivity, specificity and accuracy in patients after revascularisation.

Also, it has been suggested that the use of nuclear medicine techniques for myocardial viability prediction improved survival after coronary artery bypass grafting. [14-25]

Despite these promising results, there is still a lack of scientific data with regard to the diagnostic value of cardiac PET in the evaluation of myocardial perfusion when compared to SPECT or other functional imaging modalities. Thus, the purpose of this study is to investigate the diagnostic value of ^{18}F-FDG PET in the assessment of myocardial viability patients with known coronary artery disease when compares to the routinely performed ^{99m}Tc-tetrofosmin SPECT and echocardiography by using invasive coronary angiography as the gold standard. We hypothesized that ^{18}F-FDG PET has the ability to demonstrate high diagnostic accuracy in the detection of myocardial viability.

5.2 Materials and Methods

5.2.1 Study population

This prospective study involved consecutive recruitment of patients with known or proved coronary artery disease who underwent invasive coronary angiography and echocardiography in National Heart Institute, Malaysia and Universiti Kebangsaan Malaysia Medical Centre. All patients had previous history of myocardial infarction and LV dysfunction. Exclusion criteria included patients with suspected CAD but clinically confirmed or non-ischemic LV dysfunction, patients refused to participate in the study and patients with pregnancy. Thirty patients met the selection criteria, however, only ten patients (9 men; mean age 59.5 ± 10.5 years) agreed to participate in the study and eventually underwent all of these imaging procedures consisting of invasive angiography, echocardiography, SPECT and PET. All patients signed consent forms, and ethical approval was obtained from each institutional review board.

5.2.2 Imaging protocols-invasive coronary angiography

Coronary angiography was carried out using the standard Seldinger's technique on an angiographic machine by femoral approach which was performed by cardiologists at the National Heart Institute. Cardiologists who had no prior knowledge of SPECT or PET findings quantitatively analyzed the severity of coronary stenosis. The minimal lumen diameter was measured in projections showing the most severe narrowing.

5.2.3 Echocardiography protocol

Dobutamine echocardiography was performed using a standard protocol. First, resting echocardiography was achieved with the patient placed in the left lateral leaning position. Echocardiographic imaging was then completed through an intravenous infusion of dobutamine, first at a dose of 5 μg/kg/min, then it was increased at every 3 min to 7.5, 10, 20, 30, and 40 μg/kg/min, respectively. Images were acquired in the normal parasternal long-axis and short-axis views, with particular attention paid to determining the regional cardiac function. Through dobutamine infusion, the 12-lead ECG and blood pressure were observed every minute. The test was completed early if the heart rate extended 85% of the predicted maximum.

5.2.4 Cardiac SPECT protocol

All patients underwent a gated-SPECT ^{99m}Tc tetrofosmin (GE VENTRI). After a minimum of 4 hours of fasting, nitrates were stopped for 12 hours prior to the study. After intravenous cannulation, ^{99m} Tc tetrofosmin 450 MBq (12 mCi) was administered intravenously under resting conditions. About 45-60 minutes after radiotracer injection, a resting SPECT study was performed under double-headed gamma camera equipped with high-resolution collimators. Data were acquired in 64x64 matrix, with 32 projections, and 8 frames per cardiac cycle, and were used in association with a 20% window centred on the 140-keV photon peak of ^{99m}Tc.

All data from the ^{99m}Tc-tetrofosmin SPECT studies were reoriented into short-axis and horizontal and vertical long-axis sections. Quantitative analysis was performed using a commercially available gated-cardiac software package (4D-MSPECT; University of Michigan Medical Center) for assessing LV regional wall motion. [7] The LV wall motion was classified visually into 4 categories (0= normal, 1 =mild hypokinesis, 2= hypokinesis moderate sever 3 = akinesia or dyskinesia) using a 17-segment model (4 basal and distal segments [anterior, lateral, septal, and inferior] and 1 apical segment).

5.2.5 Cardiac PET protocol

All the patients were informed to fast for at least 6 hours before the scan and baseline blood sugar was checked. About 45-60 minutes after the 50-75 g of injected glucose loading, blood sugar was checked. If it was <140 mg/dL, 444 MBq (12 mCi) of ^{18}F-FDG was injected intravenously. If it was >140 mg/dL, regular insulin was injected intravenously according to blood glucose level (2, 3, and 5 U of regular insulin for 140-160, 160-180, and 180-200 mg/dL of blood glucose, respectively). About 45–60 minutes after FDG injection myocardial FDG PET study was performed in a PET scanner in a 3D mode (Siemens Medical Systems, Erlangen, Germany). PET acquisition parameters were as follows: myocardium was covered in one bed position (5 minute per bed position) with ECG gating (8 frames/RR cycle).

5.2.6 Image analysis

5.2.6.1 Analysis of echocardiographic images

Calculations of the regional wall motion were assumed off line using 16- segment model according to the American Society of Echocardiography.[26-29] These 16 segments were classified as 0, normal; 1, hypokinetic; 2, akinetic; and 3, dyskinetic. Only segments within the infarction-related coronary segment were analysed for wall motion. From this territory, the regional wall motion score was calculated.

5.2.6.2 Analysis of angiographic images

The degree of stenosis was classified into four categories: (1) no stenosis, (2) minimal or mild stenosis (≤50%), (3) moderate stenosis (50%–70%), and (4) severe stenosis (>70%). CAD was defined when lumen diameter reduction was greater than 50% (moderate or severe stenosis).

5.2.6.3 Analysis of SPECT and PET images

A 17-segment model was used for SPECT and PET image analysis. Each segment in both ^{99m}Tc tetrofosmin SPECT and ^{18}F-FDG PET was analysed by an automatic method for percentage of maximum tracer uptake. Segment performance with 50% of the maximum amount was measured as viable as well as for the post-nitrate ^{99m}Tc tetrofosmin study.

In addition to the qualitative assessment, the ACC/AHA/ASNC guidelines recommend a semi-quantitative analysis of PET studies based on a validated segmental scoring system. [29,30] A 17-segment model analysis is proposed using a 5-point scale system in direct proportion to the observed count density of the segment: normal perfusion=0, mild defect=1, moderate defect=2, severe defect=3 and absent uptake=4. Calculations of the summed scores can also be performed incorporating the total extent and severity of a perfusion abnormality.

5.2.6.4 Qualitative SPECT, PET and Echocardiography assessment

The data were analysed by two radiologists blindly and independently. Both radiologists used a 17-segment model to analyse myocardial viability as observed on SPECT and PET images and analysis was recommended using a 5-point scale system in through quantity to the experimental total density of the segment of left anterior descending (LAD), right coronary artery (RCA) and left circumflex (LCX): normal perfusion=0, mild defect=1, moderate defect=2, severe defect=3 and absent uptake=4. For echocardiography, the assessment used was according to the 16-segments model of the American Society of Echocardiography.

5.2.7 Statistical analysis

All data were entered into SPSS V 20.0 for statistical analysis (SPSS, Chicago, ILL). Continuous variables were expressed as mean ± standard deviation (SD), while categorical variables were presented as percentage. A p value of less than <0.05 was considered statistically significant difference.

Agreement in qualitative measurements between radiologists (both intra- and inter-observer variability) and between different methods was compared using kappa statistics (κ) and classified as follows: poor (κ=0.20); fair (κ=0.21–0.40); moderate (κ=0.41–0.60); good (κ=0.61–0.80) and excellent agreement (κ=0.81–1.00). Echocardiography, ^{99m}Tc tetrofosmin SPECT, ^{18}FDG PET and echocardiography were calculated for diagnostic value when compared to invasive angiography which was regarded as the gold standard.

5.3 Results

A total of 10 patients were included in this study and patient's characteristics are shown in Table 5.1. The mean age of the patients were 59.5 (± 10.5) years and the most of patients (90%) were males All the patients had proven CAD but the principal diagnosis in 30% of the patients had triple vessel disease involving LAD, LCx and RCA with more than ≥50% stenosis.

Table 5.1. Patient characteristics.

All patients	N= 10
Age (years)	59.5 ± 10.5
Men/women	9/1
Principal Diagnosis (%)	
Ischaemic Heart Disease	10%
Ischemic Dilated Cardiomyopathy	20%
Inferior STEMI Thrombolysed	20%
Triple vessel	30 %
Non-ST segment elevation myocardial infarction	10%
Double vessel	10%
Cardiac risk factors	
Diabetes	40%
Hypertension	80%
Smoker	20%
Dyslipidaemia	30%
Obesity	10%
Patient management	
Control risk factors	50%
Referral for CABG	50%
Percutaneous Coronary Intervention	20%
Implantable Cardioverter Defibrillator	10%
Medical Therapy	10%
International Normalised Ratio	20%

STEMI-ST elevated myocardial infarction, CABG-coronary artery bypass grafts

5.3.1 Comparison of diagnostic value between SPECT, PET and Echocardiography

A total of 340 segments in 10 patients were analysed for SPECT and PET imaging examinations, while for echocardiography there were 160 segments that were analysed in comparison with SPECT and PET. The diagnostic sensitivity of PET, SPECT and echocardiography was 100%, 90%, and 80% respectively, as shown in Figure 5.1 Since all patients had coronary artery disease, no sensitivity was analysed (true negative value was zero).

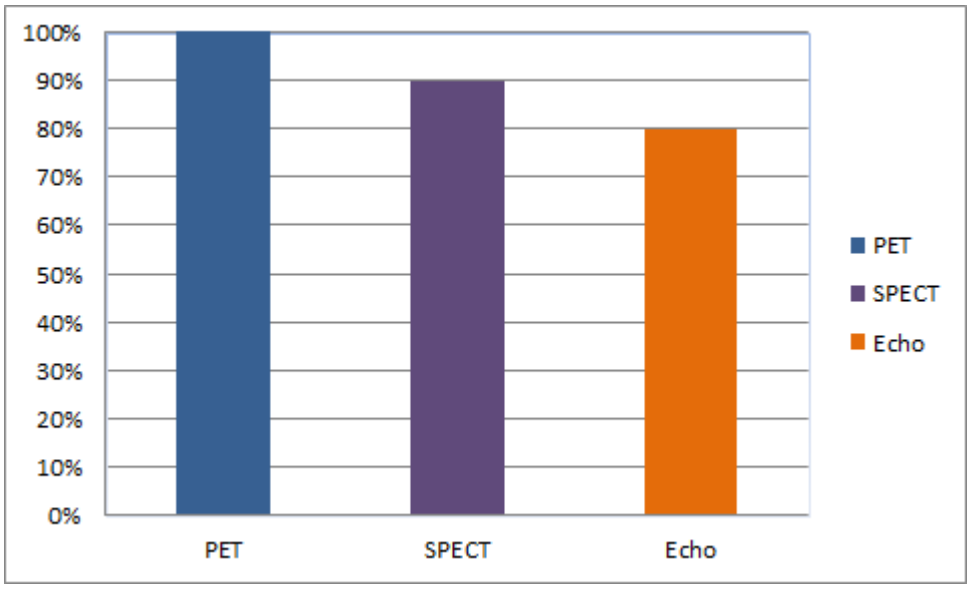

Figure 5.1. Diagnostic sensitivity among PET, SPECT and Echocardiography in comparison with invasive coronary angiography.

5.3.2 Comparison between SPECT and PET for assessment of LAD, LCx, RCA

Comparison was also performed between PET and SPECT in the assessment of three main coronary artery branches, as shown in Figure 5.2. Results showed that PET has the highest diagnostic value in the assessment of all of the three main coronary arteries, while SPECT has moderate diagnostic value in LAD, but low diagnostic performance in the other two arteries, RCA and LCx.

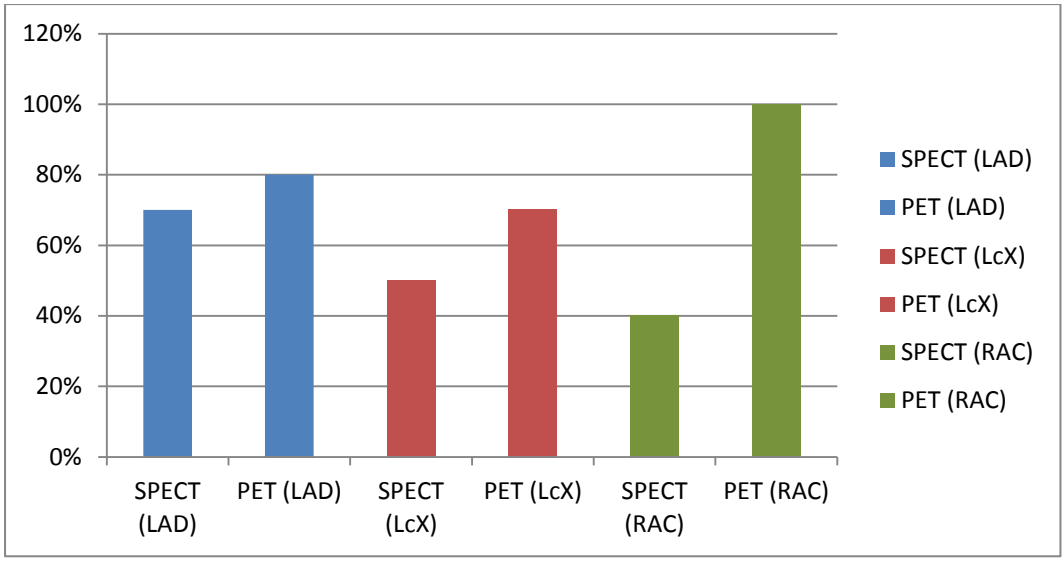

Figure 5.2. Comparison between SPECT LAD, LCx, RCA and, PET LAD, LCx and RCA.

5.3.3 Qualitative assessment of SPECT and PET between observers

Table 5.2 shows the results of inter-observer assessment, namely $SPECT_{observer\ 1}$, $SPECT_{observer\ 2}$, $PET_{observer1}$ and $PET_{observer\ 2}$ in the diagnostic evaluation of myocardial viability. As shown in the table, $PET_{observer1}$ has high diagnostic value, while the diagnostic performance of $PET_{observer\ 2}$ is the same as $SPECT_{observer\ 1}$, $SPECT_{observer\ 2}$, although this did not reach significant difference. Results showed excellent agreement on sensitivity of $PET_{observer\ 1}$ and $PET_{observer2}$ with kappa value of 0.9, $SPECT_{observer\ 1}$ and $SPECT_{observer\ 2}$ with kappa value of 0.9.

Table 5.2. Inter-observer assessment between these imaging modalities

PET/SPECT observer agreement	Sensitivity
$PET_{observer1}$	100%
$PET_{observer\ 2}$	90%
$SPECT_{observer\ 1}$	90%
$SPECT_{observer\ 2}$	90%

Figure 5.3 is an example of SPECT imaging in a patient diagnosed with significant CAD, while Figure 5.4 is another example of PET imaging in the same patient with CAD. Both

SPECT and PET detected myocardial abnormal changes, although PET is superior to SPECT in terms of image quality and accurate assessment of overall all segments.

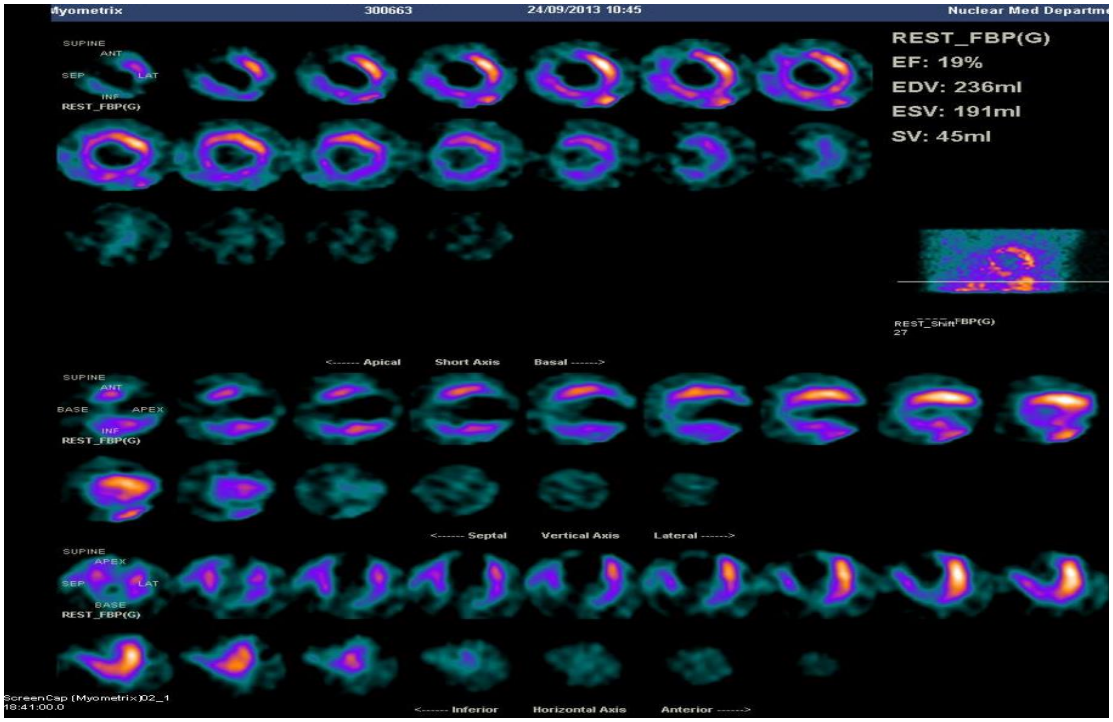

Figure 5.3. The gated SPECT ^{99m}T-tetrofosmin viability study images show marked reduced myocardial thickening and akinetic wall motion at the apex, anterior apical, anteroseptal mid and inferior mid segments.

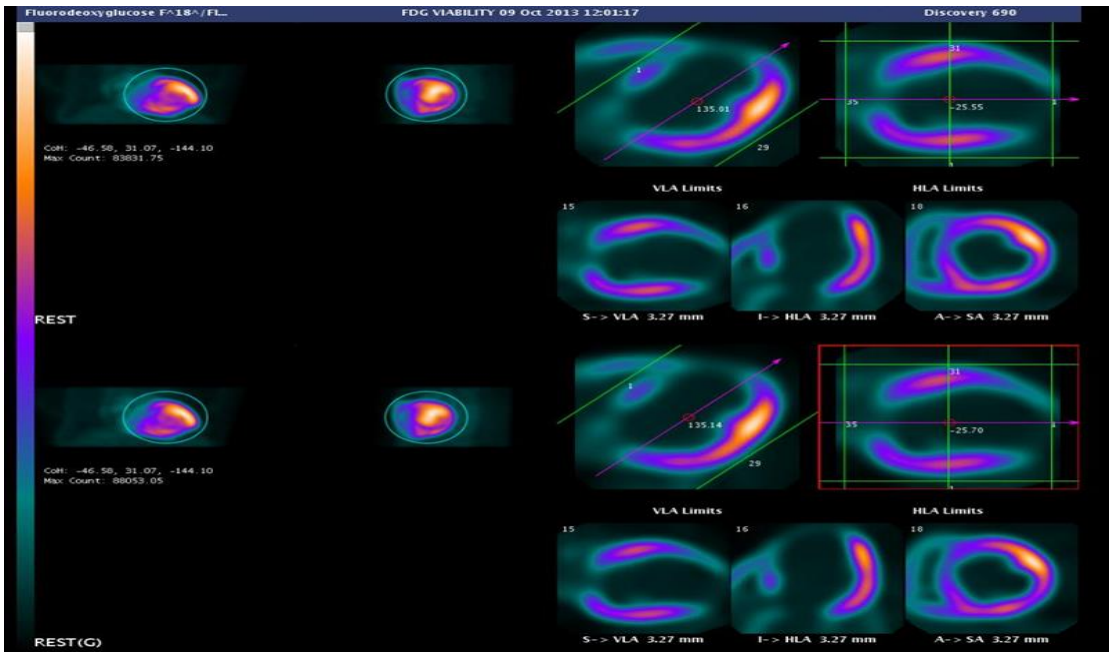

Figure 5.4. The gated PET ^{18}FDG viability study images show severely reduced ^{18}FDG uptake in the inferior apical, inferior mid and inferior basal segments.

5.4 Discussion

This prospective study investigates the diagnostic value of non-invasive cardiac modalities through comparing ^{18}F-FDG PET with ^{99m}Tc tetrofosmin SPECT and echocardiography with the aim of determining myocardial viability in patients with known CAD with invasive coronary angiography as the gold standard. Our results showed that cardiac PET has a sensitivity of 100% and 90% in patients with CAD, which is higher than that of SPECT or echocardiography. The assessment of myocardial viability with ^{18}F-FDG PET is based on its ability to distinguish the two main pathogenic mechanisms for chronic myocardial dysfunction in ischemic cardiomyopathy:

i. Irreversible loss of myocardium due to prior myocardial infarction (scar)
ii. At least partially reversible loss of contractility owing to chronic or repetitive ischemia (hibernating myocardium) .[31]

The distinctive feature of these two mechanisms is that revascularisation has the potential to restore contractile function of the hibernating myocardium but not scar. [29]

This distinction may be of paramount importance in clinical decision-making because of the upfront morbidity and mortality associated with revascularisation procedures in patients with severe left ventricular dysfunction.

Cardiac PET utilizing ^{18}F-FDG is considered the most sensitive modality for detecting hibernating viable myocardium and predicting left ventricular functional recovery post-coronary revascularization. [32-35] ^{18}F-FDG PET imaging showed incremental benefit over ^{201}T1 stress-redistribution/reinjection or ^{99m}Tc-sestamibi SPECT in predicting functional recovery in the patients with very impaired left ventricular function, while in patients with relatively preserved left ventricular function, the predictive value was similar. [36, 37] Tillisch et al [29] in their first landmark trial reported the value of ^{18}F-FDG PET to predict reversibility of cardiac wall motion abnormalities in 17 patients with ischemic cardiomyopathy.

The overall sensitivity and specificity of ^{18}F-FDG PET to demonstrate functional recovery after surgery was 95% and 80%, respectively. A meta-analysis summarizing 24 studies has reported a weighted sensitivity and specificity of 92% and 63%, respectively, with a positive

and negative predictive value of 74% and 87%, respectively, for the diagnosis of hibernating myocardium and prediction of patient outcomes. [36] Our results are consistent with these findings as the diagnostic accuracy of ^{18}F-FDG PET compares well with other established techniques SPECT and echocardiography for viability assessment. ^{18}F-FDG PET was found to have the highest diagnostic sensitivity when compared to SPECT and echocardiography in the assessment of myocardial viability. [44]

Despite these promising results, the use of ^{18}FDG PET in the assessment of left ventricular dyssynchrony is dependent on the severity of CAD. Wang et al [44] in their recent study consisting of 100 CAD patients indicated that ^{18}FDG PET should be carefully used in assessing LV dyssnchrony in patients with severe LV dysfunction. [37-39] In contrast, Pazhenkottil et al [45] reported an excellent agreement between SPECT ^{99m}Tc tetrofosmin and ^{8}FDG PET in the LV dysfunctional assessment, [40-46] and this is again in line with our reports.

There are some limitations in this study that need to be acknowledged. First, the sample size is too small. This is either due to the number of patients who refused to participate in the study or due to the disease severity of CAD or unstable condition, which they decided to undergo revascularization treatment. Second, only patients with known or proven CAD were included in this study, thus, our results should be interpreted with caution. Lastly, assessment of myocardial contour cannot be eliminated completely, thus further investigation on how to delineate the myocardial boundaries more accurately are needed. [45]

In conclusion, ^{18}F-FDG PET has high diagnostic value in the assessment of myocardial viability in patients with known CAD when compared to SPECT and echocardiography. Further studies based on a large cohort are needed to enable a robust conclusion to be drawn.

5.5 References

1. Jones R, Jones E, Velazquez R, Michler G, Sopko J, Oh C, et al. Coronary Bypass Surgery with or without Surgical Ventricular Reconstruction. N Engl J Med 2009;360(17):1705-17.
2. D'Egidio G, Nichol K, Williams A, Guo L, Garrard R, deKemp T, et al. Increasing Benefit From Revascularization Is Associated With Increasing Amounts of Myocardial Hibernation. JACC Cardiovasc imaging. 2009;2(9):1060-8.
3. Beanlands RSB, Beanlands G, Nichol E, Huszti D, Humen N, Racine M, et al. F-18-Fluorodeoxyglucose Positron Emission Tomography Imaging-Assisted Management of Patients With Severe Left Ventricular Dysfunction and Suspected Coronary Disease. J Am Coll Cardiol. 2007;50(20):2002-12.
4. Zhang X. Clinical outcome of patients with previous myocardial infarction and left ventricular dysfunction assessed with myocardial 99mTc-MIBI SPECT and 18F-FDG PET. J Nuc Med. 2001;42(8):1166-73.
5. Allman K, Allman L, Shaw R, Hachamovitch J, Udelson. Myocardial viability testing and impact of revascularization on prognosis in patients with coronary artery disease and left ventricular dysfunction: a meta-analysis. J Am Coll Cardiol. 2002;39(7):1151-8.
6. Bonow, R. O, Mann, D. L, Zipes, D. P., Libby, P. Braunwald's Heart Disease: A Textbook of Cardiovascular Medicine, 2-Volume Set. Elsevier Health Sciences 2011.
7. Stirrup J, Stirrup A, Maenhout K, Wechalekar C, Anagnostopoulos. Radionuclide imaging in ischaemic heart failure. Br Med Bull. 2009;92(1):43-59.
8. He W, He. Tc-99m tetrofosmin tomography after nitrate administration in patients with ischemic left ventricular dysfunction: relation to metabolic imaging by PET. J Nucl Cardiol. 2003;10(6):599-606.
9. Yoshinaga K, Yoshinaga C, Katoh K, Noriyasu S, Yamada Y, Ito Y, et al. Low-dose dobutamine stress gated SPET for identification of viable myocardium: comparison with stress-rest perfusion SPET and PET. Eur J Nucl Med. 2002;29(7):882-90.
10. Travin, Mark I., Steven R. Bergmann. Assessment of myocardial viability. Semin Nucl Med. 2005; 35: 2-16.
11. Dilsizian V, Dilsizian S, Bacharach R, Beanlands S, Bergmann D, Delbeke R, et al. PET myocardial perfusion and metabolism clinical imaging. J Nucl Cardiol 2009;16.4: 651-666.
12. Fratz S, Fratz M, Hauser FM, Bengel A, Hager H, Kaemmerer M, et al. Myocardial scars determined by delayed-enhancement magnetic resonance imaging and positron emission tomography are not common in right ventricles with systemic function in long-term follow up. Heart. 2006;92(11):1673-7.
13. Allman K, Allman L, Shaw R, Hachamovitch J, Udelson. Myocardial viability testing and impact of revascularization on prognosis in patients with coronary artery disease and left ventricular dysfunction: a meta-analysis. J Am Coll Cardiol. 2002;39: 1151-1158.
14. Gioia G, Powers J, Heo J, Iskandrian AS. Prognostic value of rest-redistribution tomographic thallium-201 imaging in ischemic cardiomyopathy. Am J Cardiol 1995;75(12):759-62.
15. Giuseppe G, Milan E, Giubbini R, DePace N, Heo J, Iskandrian AS. Prognostic value of tomographic rest-redistribution thallium 201 imaging in medically treated patients

with coronary artery disease and left ventricular dysfunction. J Nucl Cardiol 1996; 3 (2): 150-156.
16. Shapira I, Heller I, Pines A, Topilsky M, Isakov A. The impact of myocardial viability as determined by rest-redistribution 201Tl single photon emission CT imaging and the choice of therapy on prognosis in patients with left ventricular dysfunction. J Med. 2000; 31: 205-214.
17. Sciagrà R, Pellegri M, Pupi A, Bolognese L, Bisi G, Carnovale V, et al. Prognostic implications of Tc-99m sestamibi viability imaging and subsequent therapeutic strategy in patients with chronic coronary artery disease and left ventricular dysfunction. J Am Coll Cardiol. 2000; 36.3: 739-745.
18. Sicari RA, Ripoli E, Picano AC, Borges A, Varga W, Mathias L, et al. The prognostic value of myocardial viability recognized by low dose dipyridamole echocardiography in patients with chronic ischaemic left ventricular dysfunction. Eur heart J. 2011; 22.10: 837-844.
19. Al Jaroudi W, Al Jaroudi F, Iqbal J, Heo A, Iskandrian. Relation between Heart Rate and Left Ventricular Mechanical Dyssynchrony in Patients with End-Stage Renal Disease. J Nucl Cardiol. 2010; 17.6: 1058-1064.
20. Bonow R, Bonow G, Maurer K, Lee T, Holly P, Binkley P, et al. Myocardial Viability and Survival in Ischemic Left Ventricular Dysfunction. N Engl J Med. 2011;364.17: 1617-1625.
21. Sawada S, Dasgupta J, Nguyen K, Lane I, Gradus Pizlo J, Mahenthiran H, et al. Effect of Revascularization on Long-Term Survival in Patients With Ischemic Left Ventricular Dysfunction and a Wide Range of Viability. Am J Cardiol. 2010;106(2):187-92.
22. He Z-X, He M-F, Yang X-J, Liu R-F, Shi R-L, Gao S-S, et al. Association of myocardial viability on nitrate-augmented technetium-99m hexakis-2-methoxylisobutyl isonitrile myocardial tomography and intermediate-term outcome in patients with prior myocardial infarction and left ventricular dysfunction. Am J Cardio. 2003;92(6):696-9.
23. Underwood, S. Richard, Jeroen J. Bax, Jürgen vom Dahl, Michael Y. Henein, Albert C. van Rossum, Ernst R. Schwarz, Jean-Louis Vanoverschelde, Ernst E. van der Wall, and William Wijns. "Imaging techniques for the assessment of myocardial hibernation Report of a Study Group of the European Society of Cardiology. Eur Heart J. 2004;25:815-36.
24. Schiller NB, Shah PM, Crawford M, et al. Recommendations for quantitation of the left ventricle by two-dimensional echocardiography. J Am Soc Echocardiogr. 1989; 2: 358–367.
25. Bellenger NG, Pennell DJ. Ventricular Function. In: Manning WJ, Pennell DJ, eds. Cardiovascular Magnetic Resonance. New York, NY: Churchill Livingstone; 2001: 99–111.
26. Feigenbaum H. Echocardiography. 5th ed. Philadelphia, Pa: Lea & Febiger; 1994.
27. Henry WL, DeMaria A, Gramiak R, et al. Report of the American society of echocardiography committee on nomenclature and standards in two-dimensional echocardiography. Circulation. 1980; 62: 212–215.

28. Ghosh N, Rimoldi OE, Beanlands RS, Camici PG. Assessment of myocardial ischaemia and viability: role of positron emission tomography. Eur Heart J. 2010; 31: 2984-2995.
29. Tillisch J, Brunken R, Marshall R, et al. Reversibility of cardiac wall motion abnormalities predicted by positron tomography. N Engl J Med. 1986;314: 884–888.
30. Cornel J, Bax A, Elhendy F, Visser E, Boersma D, Poldermans G, et al. Agreement and disagreement between "metabolic viability" and "contractile reserve" in akinetic myocardium. J Nucl Cardiol. 1999;6(4):383-8.
31. Schinkel AF, Bax JJ, Poldermans D, Elhendy A, Ferrari R, Rahimtoola SH. Hibernating myocardium: diagnosis and patient outcomes. Curr Probl Cardiol. 2007; 32: 375–410.
32. Siebelink H-M, Blanksma PK, Crijns H, Bax JJ, van Boven AJ, Kingma T, et al. No difference in cardiac event-free survival between positron emission tomography-guided and single-photon emission computed tomography-guided management. J Am Coll Cardiol. 2001;37:81–88.
33. Srinivasan G, Kitsiou AN, Bacharach SL, Bartlett ML, Miller-Davis C, Dilsizian V. F-18 fluorodeoxyglucose single photon emission computed tomography: Can it replace PET and thallium SPECT for the assessment of myocardial viability? Circulation. 1998; 97:843-850.
34. Arrhighi JA, CK NG, Dey HM, Wackers FJ, Soufer R. Effect of left ventricular function on the assessment of myocardial viability by technetium-99m sestamibi and correlation with positron tomography in patients with healed myocardial infarcts of stable angina pectoris, or both. Am J Cardiol. 1997; 80:1007-1013.
35. Beanlands RS, Nichol G, Huszti E, Humen D, Racine N, Freeman M, et al. F-18-Fluorodeoxyglucose Positron Emission Tomography Imaging-Assisted Management of Patients With Severe Left Ventricular Dysfunction and Suspected Coronary DiseaseA Randomized, Controlled Trial (PARR-2). J Am Coll Cardiol. 2007;50:2002-2012.
36. Ringqvist I, Fisher LD, Mock M, Davis KB, Wedel H, Chaitman BR, et al. Prognostic value of angiographic indices of coronary artery disease from the Coronary Artery Surgery Study (CASS). J Clin Invest. 1983;71:1854–66.
37. Gersh BJ, Kronmal RA, Schaff HV, Frye RL, Ryan TJ, Mock MB, et al. Comparison of coronary artery bypass surgery and medical therapy in patients 65 years of age or older: a nonrandomized study from the Coronary Artery Surgery Study (CASS) registry. N Engl J Med. 1985;313:217–24.
38. Bell MR, Gersh BJ, Schaff HV, Holmes DR Jr, Fisher LD, Alderman EL, et al. Effect of completeness of revascularization on long-term outcome of patients with three-vessel disease undergoing coronary artery bypass surgery. A report from the Coronary Artery Surgery Study (CASS) Registry. Circulation. 1992; 86: 446-457.
39. Tarakji KG, Brunken R, McCarthy PM, Al-Chekakie MO, Abdel-Latif A, Pothier CE, et at. Myocardial viability testing and the effect of early intervention in patients with advanced left ventricular systolic dysfunction. Circulation. 2006; 113:230-237.
40. Siebelin HM, Blanksma PK, Crijns HJ, Bax JJ, van Boven AJ, Kingma T, et al. No difference in cardiac event-free survival between positron emission tomography-guided and single-photon emission computed tomography-guided patient management a prospective, randomized comparison of patients with suspicion of jeopardized myocardium. J Am Coll Cardiol. 2001;37: 81–8.

41. Gerber BL, Ordoubadi FF, Wijns W, Vanoverschelde JL, Knuuti ML, Janier M, et al. Positron emission tomography using18F-fluoro-deoxyglucose and euglycaemic hyperinsulinaemic glucose clamp: optimal criteria for the prediction of recovery of post-ischaemic left ventricular dysfunction. Results from the European Community Concerted Action Multicenter study on use of18F-fluoro-deoxyglucose Positron Emission Tomography for the Detection of Myocardial Viability. Eur Heart J. 2001;22:1691-701.
42. Pagano D, Townend JN, Littler WA, Horton R, Camici PG, Bonser RS. Coronary artery bypasses surgery as treatment for ischemic heart failure: the predictive value of viability assessment with quantitative positron emission tomography for symptomatic and functional outcome. J Thorac Cardiovasc Surg. 1998;115: 791-9.
43. Beanlands RS. DaSilva TJ, Ruddy T, Maddahi J. Myocardial viability." Principles and practices of positron emission tomography. 2nd ed. Philadelphia: Lippincott Williams and Wilkins 2008.
44. Wang L, Wei HX, Yang MF, Guo J, Wang JF, Fang W, et al. Phase analysis by gated F-18 FDG PET/CT for left ventricular dyssynchrony assessment: a comparison with gated Tc-99m sestamibi SPECT. Ann Nucl Med. 2013; 4:1-10.
45. Pazhenkottil AP, Buechel RR, Nkoulou R, Ghadri JR, Herzog BA, Husmann L, et al. Left ventricular dyssynchrony assessment by phase analysis from gated PET-FDG scans. J Nucl Cardiol. 2011;18:920–5.
46. Souvatzoglou M, Bengel F, Busch R, Kruschke C, Fernolendt H, Lee D, et al. Attenuation correction in cardiac PET/CT with three different CT protocols: a comparison with conventional PET. Eur J Nucl Med Mol Imaging. 2007;34(12):1991–2000.

Chapter 6 Conclusions and Future Directions

6.1 Conclusions

In this thesis, diagnostic value of nuclear cardiology techniques, cardiac SPECT and PET was investigated when compared to invasive coronary angiography for detection of coronary artery disease (CAD). This research project was conducted at several stages consisting of retrospective analysis of cardiac SPECT in comparison with coronary calcium score; experiments on a realistic cardiac phantom to determine the imaging protocols, and prospective study of diagnostic value of cardiac PET in myocardial viability A systematic review of the current literature shows that PET has higher sensitivity, specificity and accuracy for detection of CAD than SPECT and PET/CT. PET can be used as a reliable, less invasive modality for functional analysis of patients suspected of CAD.

A correlation of coronary calcium score (CAC) with myocardial perfusion (MPI) by SPECT in a group of patients with suspected CAD was performed.The study shows the limitations in using CAC scores alone as a predictor of coronary disease outcomes. Coronary calcium score should be combined with myocardial perfusion imaging in low-to-intermediate risk patients to improve the diagnostic performance.

The cardiac phantom experiments showed the feasibility of demonstrating cold lesions created by the inserts in the left ventricle. This study provides opportunities of testing cardiac SPECT and PET with regard to optimization of imaging protocols in the evaluation of coronary artery disease.

The prospective study comprising patients with known CAD shows that cardiac PET has high diagnostic sensitivity in the assessment of myocardial viability when compared to SPECT and echocardiography.

The research outcomes are summarized as follows:

- Cardiac PET is increasingly used in the diagnostic evaluation of coronary artery disease, and its diagnostic value is high compared to other less invasive imaging

modalities. This is confirmed by other systematic review and prospective data analysis.

- Coronary calcium score is regarded as a highly sensitive marker of determining the atherosclerotic disease compared with conventional risk factors. However, in patients with a zero or low calcium scores, myocardial perfusion imaging demonstrates potential value of detecting abnormal changes.
- Cardiac ^{18}FDG PET has high diagnostic value in the assessment of myocardial viability in patients with proven coronary artery disease and it is recommended to be incorporated into clinical patient management with the aim of reducing cardiac events.
- Both cardiac PET and cardiac SPECT need to be further validated based on phantom studies and clinical trials with regard to optimization of imaging protocols and reduction of radiation exposure associated with administration of radiopharmaceuticals.

6.2 Future Directions

This study improves our understanding of the diagnostic value of cardiac PET when compared to SPECT for detection of coronary artery disease. However, there are few suggestions for the future research focus in following aspects:

1) Although cardiac PET will continue to play a key role in the investigation of myocardial viability, more data are needed to confirm its clinical efficacy.

2) Cardiac PET is not yet as widely available as SPECT imaging, thus, more experience is needed in image interpretation and operation as it may vary widely.

3) Diagnostic accuracy of ^{18}FDG PET could be variable from centres to centres, depending on the protocols used and level of confidence in interpretation. Therefore, optimization of PET imaging protocols is necessary.

4) To investigate administration of radioisotopes/radiopharmaceuticals with the aim of reducing radiation dose associated with nuclear cardiology examinations. This is the area where little research has been conducted.